MSU
LIBRARIES

RETURNING MATERIALS:
Place in book drop to remove this checkout from your record. FINES will be charged if book is returned after the date stamped below.

EM PROBING AND HEATING OF BIOLOGICAL BODIES WITH BARE AND INSULATED MICROPROBES

By

Abdolhamid Ghods

A DISSERTATION

Submitted to
Michigan State University
in partial fulfillment of the requirements
for the degree of

DOCTOR OF PHILOSOPHY

Department of Electrical Engineering

1984

ABSTRACT

EM PROBING AND HEATING OF BIOLOGICAL BODIES
WITH BARE AND INSULATED MICROPROBES

By

Abdolhamid Ghods

In the present research the schemes of using a microprobe for determining the electrical properties of biological bodies in vivo and for locally heating biological tissues are investigated, with the application to hyperthermia cancer therapy or other medical purposes. The relationship between the input impedance of the probe and the electrical parameters of the surrounding medium is used to determine the electrical properties of the medium, and the EM waves in the biological bodies maintained by the current on the probe are used to heat biological bodies locally.

A detailed analysis of the bare microprobe in a conducting medium has been conducted and the electric field produced by the probe in the medium derived. Using the method of moments, Hallen's integral equation and electric field integral equation for the probe current are transformed into systems of simultaneous algebraic equations which are then solved on a computer.

A general theory for an insulated microprobe in a conducting medium based on lossy transmission line theory is presented. The current on the probe, the electric field in the medium maintained by the probe, and the heat pattern of the probe are found. Various equivalent terminal impedances for the insulated probe are introduced, and their effects on the current distribution and the heat pattern are investigated.

Experiments have been conducted and the input impedances of bare and insulated microprobes in saline with various normalities are measured. The theoretical and experimental results are found to be in good agreement.

ACKNOWLEDGMENTS

The author wishes to express his sincere gratitude to his major professor, Dr. K.M. Chen, for his guidance and encouragement throughout the course of this research.

I also like to thank a member of my guidance committee, Dr. D.P. Nyquist, for his invaluable suggestions and guidance. I appreciate the help I received from the other members of my guidance committee, Dr. B. Drachman and Dr. D. Reinhard. Special thanks also to Mrs. Carol Cole for her skillful typing.

TABLE OF CONTENTS

CHAPTER

LIST OF TABLES

Table

LIST OF FIGURES

Figure

Figure

Figure

Figure

CHAPTER I

INTRODUCTION

In recent years, electromagnetic radiation and propagation have played an important role in human life. Intercontinental satellite communication, radar detection, microwave technology, and the use of EM energy for medical purposes are only a few examples of the applications using electromagnetic energy these days.

Many medical researchers have investigated the scheme of using EM energy to induce hyperthermia in biological bodies for the purpose of cancer therapy. It is known that when the temperature of a cancerous tumor is raised a few degrees above that of the surrounding tissues, the adjoining chemo or radiotherapy becomes more effective in treating tumors [1]. Therefore, it is the objective of many researchers to find a noninvasive method by which to heat the tumor without overheating the surrounding tissues.

Substantial progress was made in hyperthermia cancer therapy when Leveen et al. [2] used 13.56 MHz EM radiation to eradicate the tumors or to slow the progression of tumors in some cancer patients. Other researchers [3,4] have used EM waves at various frequencies to heat the tumors in animal bodies and reported significant tumor eradication.

A successful analysis of the induced EM field inside an irradiated body with an imbedded tumor, and design of an effective device for focusing EM energy in the tumor will depend on the knowledge of electrical properties of the tumor. Some researchers [5-8] have used an open-ended coaxial cable, or a very short monopole, or a symmetric probe [9] to study the electric field induced in the biological bodies and measure the electrical properties of various biological tissues.

In the present research the techniques for determining the electrical properties of biological bodies in vivo and local heating of an imbedded tumor with an unbalanced monopole, which consists of a thin open-ended microcoaxial line with an extended center conductor, are studied theoretically and experimentally.

In Chapter II a theoretical analysis of a bare microprobe in a conducting medium is presented. The distribution of the current on the probe, and the input impedance of the probe are calculated numerically with different methods for various cases. The driving source is modeled as a delta gap or as a magnetic current ring.

In Chapter III the descriptions of the experimental setup and the electrical properties of the saline are given. The input impedance of the probe was measured by the vector voltmeter. The experimental results are compared with the theoretical results.

Chapter IV contains the applications of the bare microprobe. The heat pattern of the microprobe in the conducting medium and the methods for measuring the conductivity and permittivity of the conducting bodies are presented in this chapter.

In Chapter V a theoretical analysis of an insulated microprobe in a conducting medium is given. The theory of lossy transmission line is used to investigate the current distribution on the probe, the input impedance of the probe, and the electric field produced by the probe in the medium. Various physical geometries of the insulated probes with different equivalent terminal impedances are introduced. The current distributions along and the imput impedances of the probes with various terminal impedances are compared in this chapter. A series of experiments were conducted to measure the input impedances of the insulated probes with various physical geometries. The theoretical results and the experimental results are compared.

In Chapter VI the application of insulated probes for local heating is explained. The theory and the numerical results of the heat pattern produced by the insulated probes with various terminal impedances are given.

A brief description of the computer programs used in this study to obtain numerical results is given in Chapter VII.

CHAPTER II

THEORETICAL STUDY OF A BARE MICROPROBE IN A CONDUCTING MEDIUM

To measure the conductivity and the permittivity of a biological tissue in situe or for local heating of a biological body, a microprobe driven by an EM source can be inserted inside the tissue. The evolutional geometries for a bare coaxial microprobe in a conducting medium are shown in Figure 2.1. A coaxial microprobe consists of a microcoaxial line with an extended inner conductor.

In a coaxial line the current is concentrated inside the line and the current on the inner conductor is equal and in opposite direction with the current on the inner surface of the outer conductor. Assuming no accumulation of charges at the end of the outer conductor, the current at this end is continuous and the direction of the current on the outer surface of the outer conductor is as indicated in Figure 2.1(a). Inside the coaxial line the currents are equal and in opposite directions, therefore, their effects cancel each other. Only the current on the extended inner conductor and that on the outer surface of the outer conductor maintain an electric field in the medium. Hence the probe is equivalent to an asymmetric dipole as shown in Figure 2.1(b). Since the dipole is in a lossy

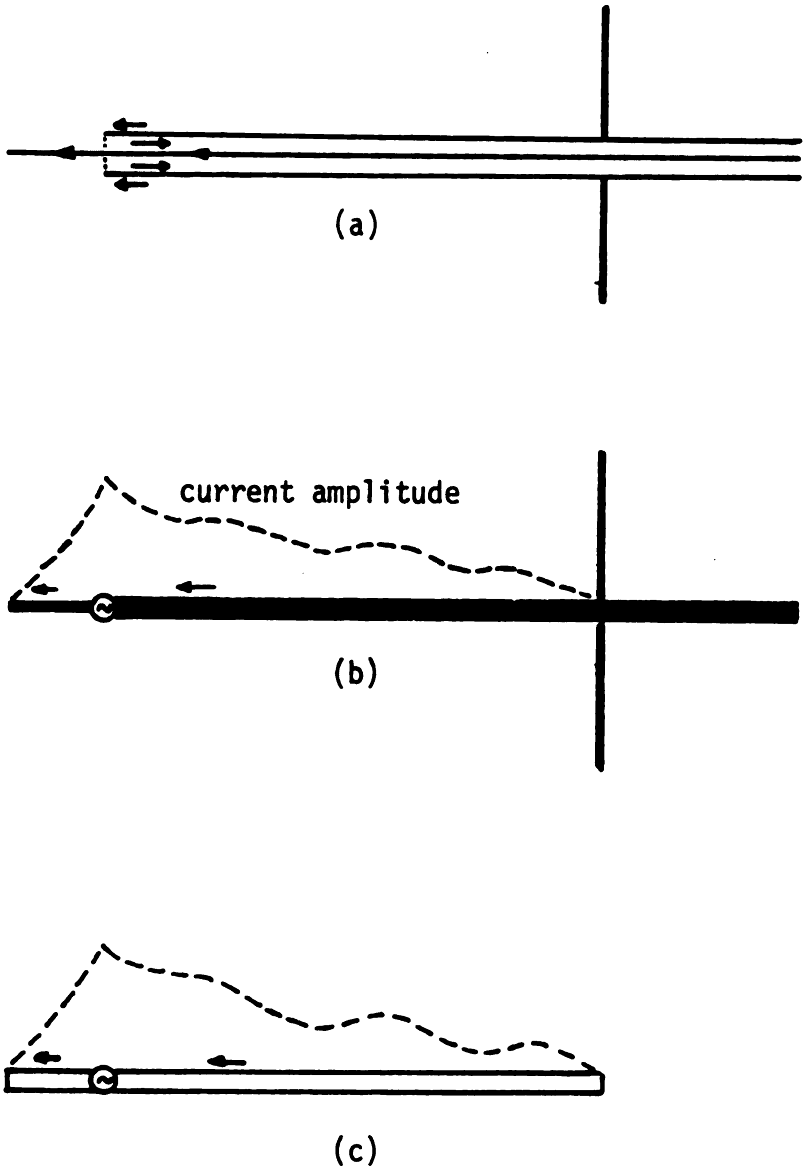

Figure 2.1. Evolution of geometry of a bare microprobe in a conducting medium.

medium, the current decays so rapidly that the probe can be truncated as indicated in Figure 2.1(c) for the analysis.

The probe in a lossy medium is studied first by the well known "Hallen's Integral Equation Method" and then followed by the "Electric Field Integral Equation Method" (Pocklington method).

Modeling the driving source in the probe is very important and it does depend on the physical geometry of the probe. In the electric field integral equation method the driving source is first modeled as a delta gap and later as a magnetic current ring.

2.1. Hallen's Integral Equation for a Microprobe

The vector potential $A_z(z)$ on the surface of the probe maintained by the current $I_z(z)$ on the probe satisfies the following equation:

$$\left(\frac{\partial^2}{\partial z^2} + k^2\right)A_z(z) = \frac{jk^2}{\omega}\left[I_z(z)Z^i(z) - V_0\,\delta(z)\right] \qquad (2.1.1)$$

where $Z^i(z)$ is surface impedance of the probe and in general it is assumed to be non-zero. V_0 is the applied voltage at the gap and $\delta(z)$ is a delta function. The solution to the above differential equation for $A_z(z)$ is given by

$$A_z(z) = A_z^h(z) + A_z^p(z)$$

where the homogeneous solution $A_z^h(z)$ is

$$A_z^h(z) = -\frac{jk}{\omega}[C_1 \cos kz + C_2 \sin kz]$$

and the particular solution $A_z^p(z)$ is

$$A_z^p(z) = -\frac{jk}{\omega}\left[\frac{V_0}{2}\sin k|z| + \int_0^z I_z(z')Z^i(z')\sin k(z' - z)dz'\right]$$

The general solution for $A_z(z)$ is

$$A_z(z) = -\frac{jk}{\omega}\left[C_1 \cos kz + C_2 \sin kz + \frac{V_0}{2}\sin k|z| + \int_0^z I_z(z')Z^i(z')\sin k(z' - z)dz'\right] \quad (2.1.2)$$

On the other hand, the vector potential on the surface of the probe can be expressed as

$$A_z(z) = \frac{\mu}{4\pi}\int_{-h_2}^{h_1} I_z(z')\frac{e^{-jkR}}{R}dz' \quad (2.1.3)$$

With the thin wire approximation, or with the assumption that the surface current on the probe can be approximated by a line current flowing along the axis of the probe, we can approximate R as

$$R = \sqrt{(z - z')^2 + a^2} \quad .$$

After combining equations (2.1.2) and (2.1.3) it gives

$$\int_{-h_2}^{h_1} I_z(z') \frac{e^{-jkR}}{R} dz' = -\frac{jk4\pi}{\omega\mu}\left[C_1 \cos kz + C_2 \sin kz + \frac{V_0}{2} \sin k|z| + \int_0^z I_z(z')Z^i(z')\sin k(z' - z)dz'\right] \qquad (2.1.4)$$

Equation (2.1.4) is called "Hallen's Integral Equation," which cannot be solved in closed form, but it can be done numerically.

2.1.1. Moment Method Solution

In order to solve the integral equation (2.1.4), the moment method is used to convert the integral equation into a system of simultaneous linear algebraic equations with the probe current at different locations of the probe as unknowns [10]. The probe is partitioned into N segments, as shown in Figure 2.2. The unknown current on the probe I(z) can be expressed in terms of a sequence of pulse functions:

$$I(z) = \sum_{n=1}^{N} I_n P_n(z)$$

where

$$P_n(z) = \begin{cases} 1 & z \in (\Delta z)_n \\ 0 & z \notin (\Delta z)_n \end{cases}$$

The boundary conditions (B.C.) state that I(z) = 0 on the tips of the probe, hence $I_1 = I_N = 0$. After the substitution of I(z) in equation (2.1.4) it becomes

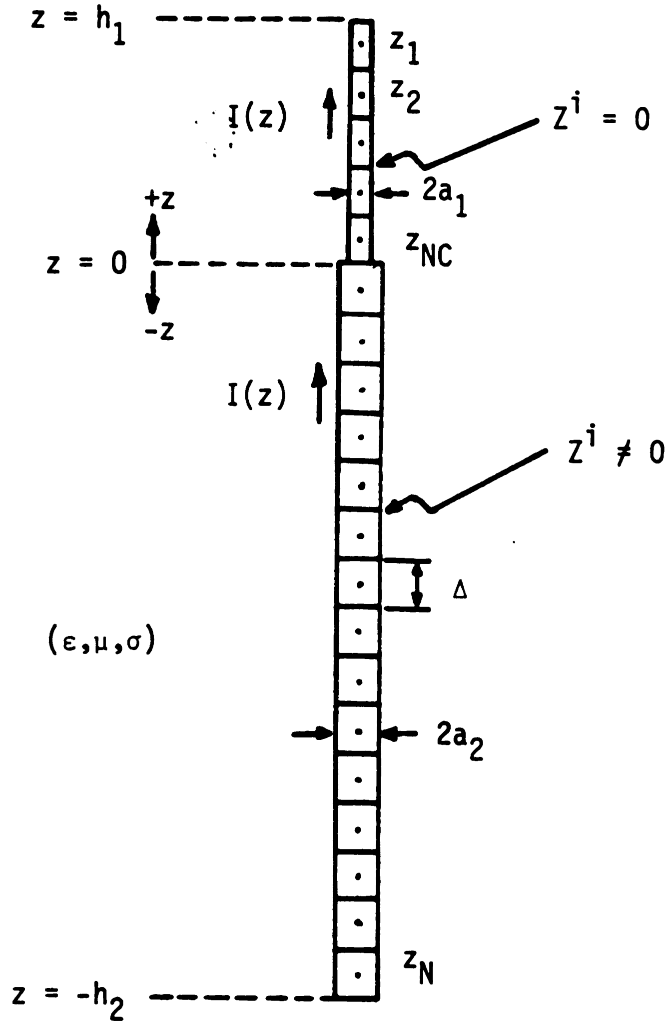

Figure 2.2. Geometry of the bare probe.

$$\sum_{n=2}^{N-1} I_n \int_{-h_2}^{h_1} \psi(z,z')dz' = -\frac{jk4\pi}{\omega\mu}\Bigg[C_1 \cos kz + C_2 \sin kz$$

$$+ \frac{V_0}{2} \sin k|z| + \sum_{N=2}^{N-1} I_n \int_0^z Z^i(z') \sin k(z' - z)dz'\Bigg] \qquad (2.1.5)$$

where $\psi(z,z') = \dfrac{e^{-jkR}}{R}$

Equation (2.1.5) is forced to be satisfied at N midpoints of N segments. Hence there are a system of N simultaneous algebraic equations and N unknowns (C_1, C_2, I_2, I_3, ... I_{N-1}). Let us assume that the short part of the probe (h_1) is made of a very good conducting material so that its surface impedance is approximately zero and the long part of the probe (h_2) is covered with lossy material so that the surface impedance over this part of the probe is finite. We can express $Z^i(z)$ as

$$Z^i(z) = \begin{cases} 0 & 0 \le z \le h_1 \\ Z^i & -h_2 \le z \le 0 \end{cases}$$

The system of equations now becomes

$$C_1 \cos kz_1 + \frac{\omega\mu}{jk4\pi}\sum_{n=2}^{N-1} I_n A_{1n} + C_2 \sin kz_1 = -\frac{V_0}{2}\sin k|z_1|$$

$$C_1 \cos kz_2 + \frac{\omega\mu}{jk4\pi}\sum_{n=2}^{N-1} I_n A_{2n} + C_2 \sin kz_2 = -\frac{V_0}{2}\sin k|z_2|$$

$$\cdot \quad \cdot \quad \cdot$$

$$\cdot \quad \cdot \quad \cdot$$

$$\cdot \quad \cdot \quad \cdot$$

$$C_1 \cos kz_{Nc+1} + \frac{\omega\mu}{jk4\pi}\sum_{n=2}^{N-1} I_n A_{Nc+1\ n} + C_2 \sin kz_{Nc+1}$$

$$+ Z^i I_{Nc+1}\int_0^{z_{Nc+1}} \sin k(z' - z_{Nc+1})dz' = -\frac{V_0}{2}\sin k|z_{Nc+1}|$$

$$C_1 \cos kz_{Nc+2} + \frac{\omega\mu}{jk4\pi}\sum_{n=2}^{N-1} I_n A_{Nc+2\ n} + C_2 \sin kz_{Nc+2}$$

$$+ Z^i\int_0^{z_{Nc+1}+\Delta/2} \sin k(z' - z_{Nc+2})dz'$$

$$+ Z^i\int_{z_{Nc+1}+\Delta/2}^{z_{Nc+2}} \sin k(z' - z_{Nc+2})dz' = -\frac{V_0}{2}\sin k|z_{Nc+2}|$$

$$\cdot \quad \cdot \quad \cdot$$

$$\cdot \quad \cdot \quad \cdot \qquad (2.1.6)$$

$$\cdot \quad \cdot \quad \cdot$$

The surface impedance Z^i of h_2 in these equations is assumed to be constant. Also, the coefficient A_{mn} is defined as

$$A_{mn} = \int_{(\Delta z)_n} \psi(z,z')dz' = \begin{cases} \psi(z,z')\Delta & m \neq n \\ 2Ln\left[\frac{\Delta}{2a} + \sqrt{1 + (\frac{\Delta}{2a})^2}\right] - jk\Delta & m = n \end{cases}$$

$$a = \begin{cases} a_1 & m \leq Nc \\ a_2 & m > Nc \end{cases}$$

Let us define $B_m = -\frac{V_0}{2} \sin k|z_m|$ and $M_{mn} = A_{mn} + D_{mn}$ where $D_{mn} = 0$ for (m and n) $\leq$ Nc and for other values of m and n

$$D_{mn} = \begin{cases} Z^i \displaystyle\int_{z_n-\Delta/2}^{z_n} \sin k(z' - z_m)dz' & m = n \\ Z^i \displaystyle\int_{z_n-\Delta/2}^{z_n+\Delta/2} \sin k(z' - z_m)dz' & m \neq n \\ 0 & m - n < 0 \end{cases}$$

With these definitions equation (2.1.6) can be expressed in the matrix form as

$$\begin{bmatrix} \cos kz_1 & & \sin kz_1 \\ \cos kz_2 & & \sin kz_2 \\ \cdot & & \cdot \\ \cdot & M_{mn} & \cdot \\ \cdot & & \cdot \\ \cos kz_N & & \sin kz_N \end{bmatrix} \begin{bmatrix} C_1 \\ I_2 \\ \cdot \\ \cdot \\ I_{N-1} \\ C_2 \end{bmatrix} = \begin{bmatrix} B_1 \\ B_2 \\ \cdot \\ \cdot \\ \cdot \\ B_N \end{bmatrix} \quad (2.1.7)$$

where various matrix elements have been defined. The inversion of the equation (2.1.7) yields the unknowns: C_1, I_2, I_3, ... I_{N-1}, C_2.

2.2. Electric Field Integral Equation for a Microprobe

Maxwell's equations in a lossy medium are

$$\nabla\cdot\vec{D}(\vec{r}) = \rho(\vec{r})$$

$$\nabla\times\vec{E}(\vec{r}) = -j\omega\mu\vec{H}(\vec{r})$$

$$\nabla\times\vec{H}(\vec{r}) = \vec{J}^e(\vec{r}) + (\sigma + j\omega\varepsilon)\vec{E}(\vec{r})$$

$$\nabla\cdot\vec{B}(\vec{r}) = 0$$

Vector and scalar potentials in a conducting medium are

$$\vec{A}(\vec{r}) = \frac{\mu}{4\pi}\int_V \vec{J}(\vec{r}\,')\,\frac{e^{-jkR}}{R}\,dv' \tag{2.2.1}$$

$$\Phi(\vec{r}) = \frac{1}{4\pi\varepsilon^*}\int_V \rho(\vec{r}\,')\,\frac{e^{-jkR}}{R}\,dv' \tag{2.2.2}$$

where $\varepsilon^* = \varepsilon(1 - \frac{j\sigma}{\omega\varepsilon})$

Electric field can be expressed in terms of scalar and vector potentials as

$$\vec{E}(\vec{r}) = -\nabla\Phi(\vec{r}) - j\omega\vec{A}(\vec{r}) \tag{2.2.3}$$

Using equations (2.2.1) to (2.2.3) and the continuity equation $\nabla\cdot\vec{J}(\vec{r}) + j\omega\rho(\vec{r}) = 0$, which gives the relationship between the current density $\vec{J}(\vec{r})$ and the charge density $\rho(\vec{r})$, the electric field on the surface of the probe can be expressed as

$$E_z(z) = -\frac{j\omega\mu}{4\pi k^2}\int_{z'}\left[\frac{\partial}{\partial z'} I_z(z')\frac{\partial}{\partial z}\psi(z,z') + k^2 I_z(z')\psi(z,z')\right]dz' \quad (2.2.4)$$

The boundary condition on the surface of the probe states that the tangential components of the electric field at the inner surface and outer surface of the probe should be equal:

$$\hat{z}\cdot\vec{E}(r=\bar{a}) = \hat{z}\cdot\vec{E}(r=\overset{+}{a}) \quad (2.2.5)$$

The electric field at the inner surface of the probe maintained by the source and the probe current is

$$\hat{z}\cdot\vec{E}(r=\bar{a}) = Z^i(z)I_z(z) - E_z^e(z) \quad (2.2.6)$$

where $E_z^e(z)$ is the driving electric field maintained by the source. The electric field at the outer surface of the probe maintained by the probe current and charge is given by (2.2.4). By equating (2.2.4) and (2.2.6), we have

$$\int_{-h_2}^{h_1}\left[\frac{\partial}{\partial z'} I_z(z')\frac{\partial}{\partial z}\psi(z,z') + k^2 I_z(z')\psi(z,z')\right]dz' = \frac{j4\pi k^2}{\omega\mu}\left[Z^i(z)I_z(z) - E_z^e(z)\right] \quad (2.2.7)$$

Equation (2.2.7) is called the "Electric Field Integral Equation." In order to be able to solve the above equation, $E_z^e(z)$ should be determined. The driving source should be modeled based on the physical geometry of the probe. First, the probe is studied with a delta gap model and then it is modeled as a magnetic current ring model.

In the case of a delta gap

$$E_z^e(z) = +V_0 f(z) \text{ and } f(z) = \begin{cases} 1/2\delta & z = 0 \\ \\ 0 & z \neq 0 \end{cases}$$

where 2δ is the length of the gap and V_0 is the applied voltage across the gap. After substitution for $E_z^e(z)$ in equation (2.2.7), it is solved by the moment method. The probe is partitioned the same way as it was for solving Hallen's integral equation. The unknown current $I(z)$ is expressed as a sequence of pulse functions and after the substitution of this current in equation (2.2.7), it can be written as follows:

$$\sum_{n=1}^{N} I_n \left[\frac{\partial}{\partial z} \psi(z,z') \Bigg|_{z'=z_{n}^{+}}^{z'=z_{n}^{-}} \right] + \sum_{n=1}^{N} I_n k^2 \int_{(\Delta z)_n} \psi(z,z')dz' =$$

$$\frac{j4\pi k^2}{\omega\mu} [Z^i(z) I_z(z) - V_0 f(z)] \qquad (2.2.8)$$

where

$$z_{\bar{n}} = z_n - \frac{\Delta}{2}$$

$$z_{\overset{+}{n}} = z_n + \frac{\Delta}{2}$$

and

$$\frac{\partial}{\partial z}\,\psi(z,z') = \psi'(z,z') = -\,\frac{(z - z')(1 + jkR)}{R^2}\,\psi(z,z')$$

$$Z^i(z) = \begin{cases} 0 & 0 \le z \le h_1 \\ \\ Z^i & -h_2 \le z \le 0 \end{cases}$$

Equation (2.2.8) can be simplified as

$$\sum_{n=1}^{N} I_n \left\{ \int_{(\Delta z)_n} \psi(z_m,z')dz' + \frac{1}{k^2}\left[\psi'(z_m,z_{\bar{n}}) - \psi'(z_m,z_{\overset{+}{n}})\right] \right\}$$

$$= \frac{j4\pi}{\omega\mu}\left[I_z(z_m)Z^i(z_m) - V_0 f(z_m)\right]$$

$$m = 1, 2, \ldots N \qquad (2.2.9)$$

This system of N simultaneous algebraic equations can be solved numerically. Equation (2.2.9) can be expressed in matrix form as follows:

$$\begin{bmatrix} & & \\ & A_{mn} & \\ & & \end{bmatrix} \begin{bmatrix} I_1 \\ I_2 \\ \cdot \\ \cdot \\ \cdot \\ I_N \end{bmatrix} = \begin{bmatrix} B_1 \\ B_2 \\ \cdot \\ \cdot \\ \cdot \\ B_N \end{bmatrix}$$

Consequently

$$\begin{bmatrix} I_1 \\ I_2 \\ \cdot \\ \cdot \\ \cdot \\ I_N \end{bmatrix} = \begin{bmatrix} & & \\ & A_{mn} & \\ & & \end{bmatrix}^{-1} \begin{bmatrix} B_1 \\ B_2 \\ \cdot \\ \cdot \\ \cdot \\ B_N \end{bmatrix}$$

where matrix [I] gives the current on the surface of the probe, and the matrix [B] is the electric field on the surface of the probe produced by the applied voltage. Matrix [A] is called the impedance matrix. Elements of matrices [A] and [B] are defined as

$$B_m = \begin{cases} 0 & m \neq Nc \\ -\dfrac{j4\pi V_0}{\omega\mu}\left(\dfrac{1}{\Delta}\right) & m = Nc \end{cases}$$

$$A_{mn} = \int_{(\Delta z)_n} \psi(z_m,z')dz' + \frac{1}{k^2}\left[\psi'(z_m,z_{\bar{n}}) - \psi'(z_m,z_{\overset{+}{n}})\right]$$

for $m \leq Nc$, or $m > Nc$ and $m \neq n$.

$$A_{mn} = \int_{(\Delta z)_n} \psi(z_m,z')dz' + \frac{1}{k^2}\left[\psi'(z_m,z_{\bar{n}}) - \psi'(z_m,z_{\overset{+}{n}})\right] - \frac{j4\pi}{\omega\mu} Z^i$$

for $m > Nc$ and $m = n$. (2.2.10)

$$a = \begin{cases} a_1 & m \leq Nc \\ a_2 & m > Nc \end{cases}$$

Some numerical results are shown in Figures 2.3 to 2.5. In Figure 2.3 the current distributions along bare probes of various lengths in a conducting medium, obtained with Hallen's Integral Equation method, are shown. In this case it is assumed that $a_1 = a_2$ and h_2 is variable. Since the probe is in a lossy medium, the current on h_2 is decaying. In Figure 2.4 the current distributions along the same bare probes in the same medium, obtained with the Electric Field Integral Equation method, are given. Again, it is observed that the current on h_2 is decaying. In both Figures 2.3 and 2.4 it was assumed that the surface impedance everywhere on the probe is zero. Figure 2.5 illustrates the current distributions along the bare probes with variable surface impedances on h_2. It is seen that as the surface impedance increases, the current on h_2 decays faster. Therefore, if we make $Z^i \neq 0$, then the length of h_2 has less effect on the input impedance and truncation of h_2 creates less error.

Figures 2.6 and 2.7 illustrate input resistances and input reactances of the bare probes of various lengths in the salines with normalities of 0.0, 0.1, 0.2, 0.3, and 0.4. In all cases $h_1 = 7.5$ mm and a = 0.43 mm, but h_2 is varied from 30 to 75 mm. In the case of $\frac{\sigma}{\omega\varepsilon_0\varepsilon_r} = 0.0$, the input reactance changes rapidly (the input resistance changes moderately) when h_2 is changed. However, for $\frac{\sigma}{\omega\varepsilon_0\varepsilon_r} = 0.43$ the changes on the input resistance and the input reactance are much less than the case of $\frac{\sigma}{\omega\varepsilon_0\varepsilon_r} = 0.0$. For other cases when $\frac{\sigma}{\omega\varepsilon_0\varepsilon_r} > 0.43$, the input impedance of the bare probe

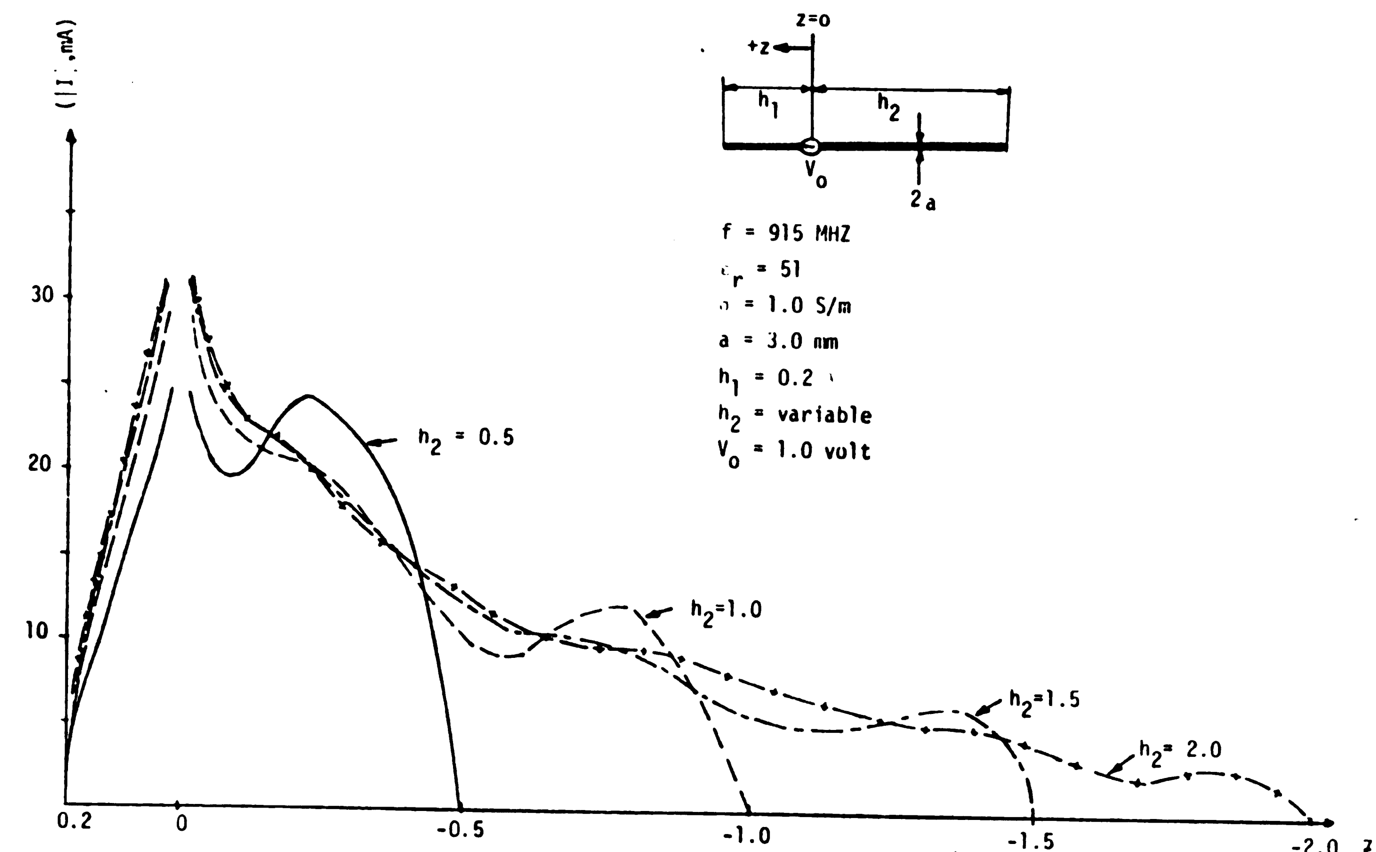

Figure 2.3. Current distributions along bare probes in a conducting medium, obtained with Hallen's Integral Equation method.

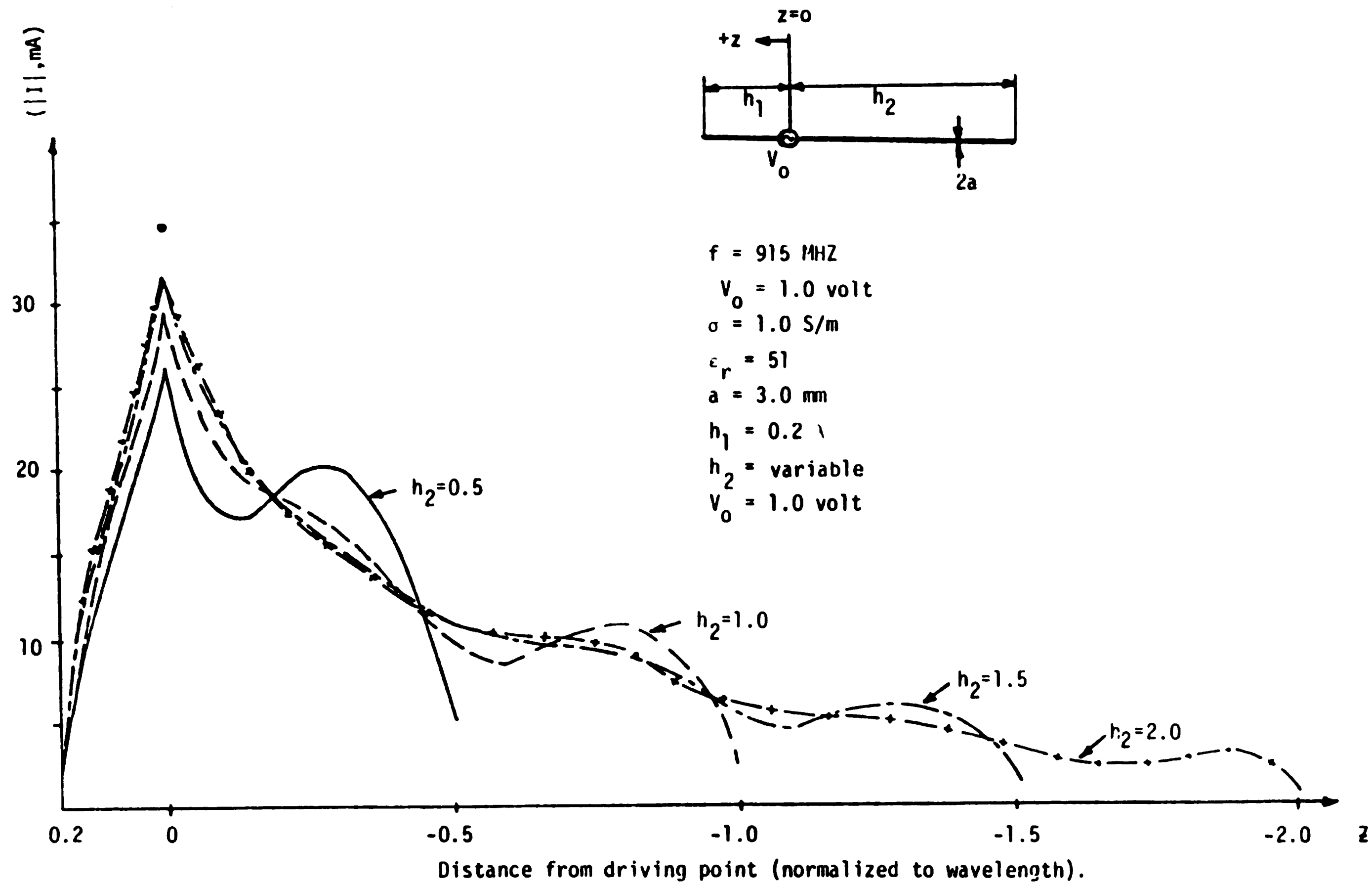

Figure 2.4. Current distributions along bare probes in a conducting medium, obtained with Electric Field Integral Equation method.

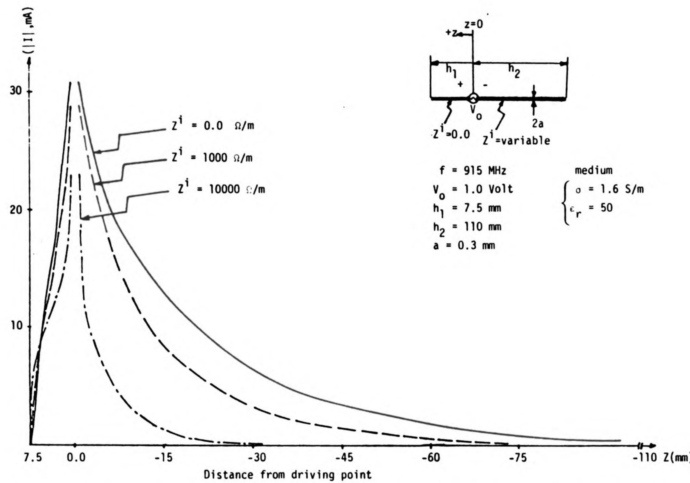

Figure 2.5. Current distribution along a bare probe with various surface impedances when the probe is embedded in a conducting medium, obtained with Electric Field Integral Equation method.

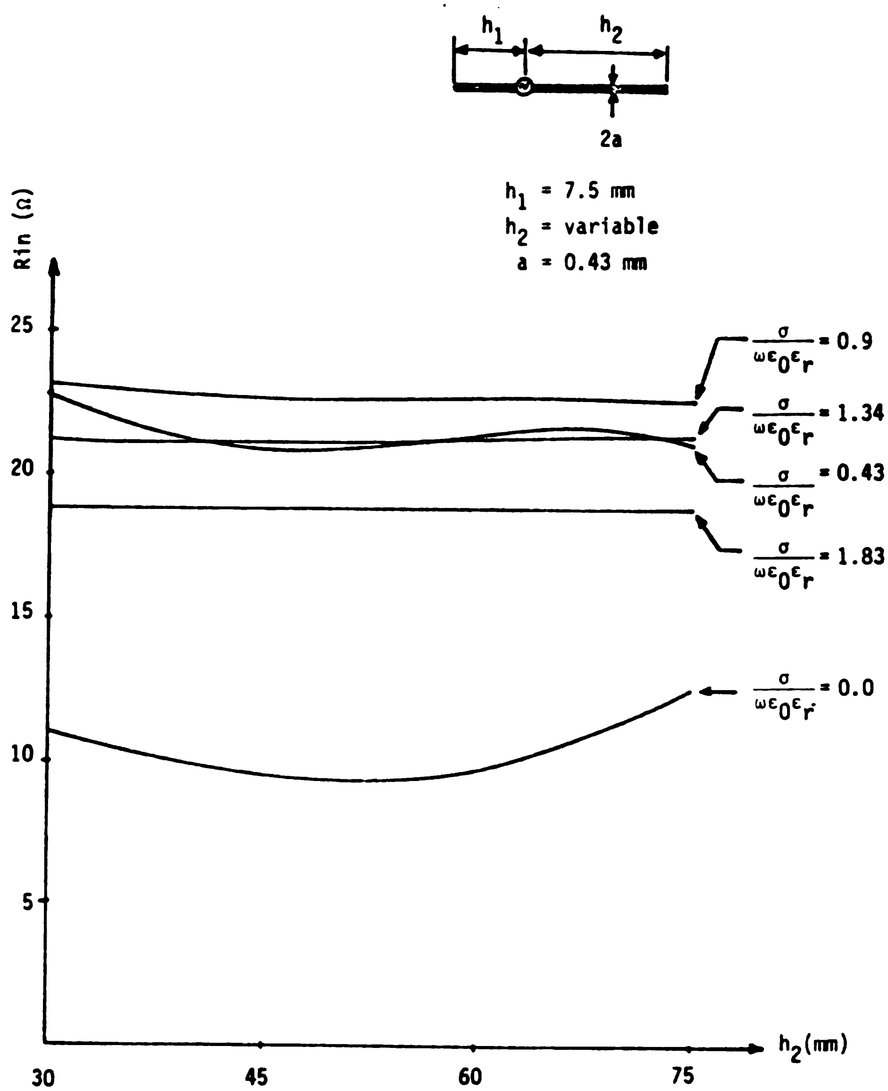

Figure 2.6. Input resistances of bare probes in the salines with different concentrations.

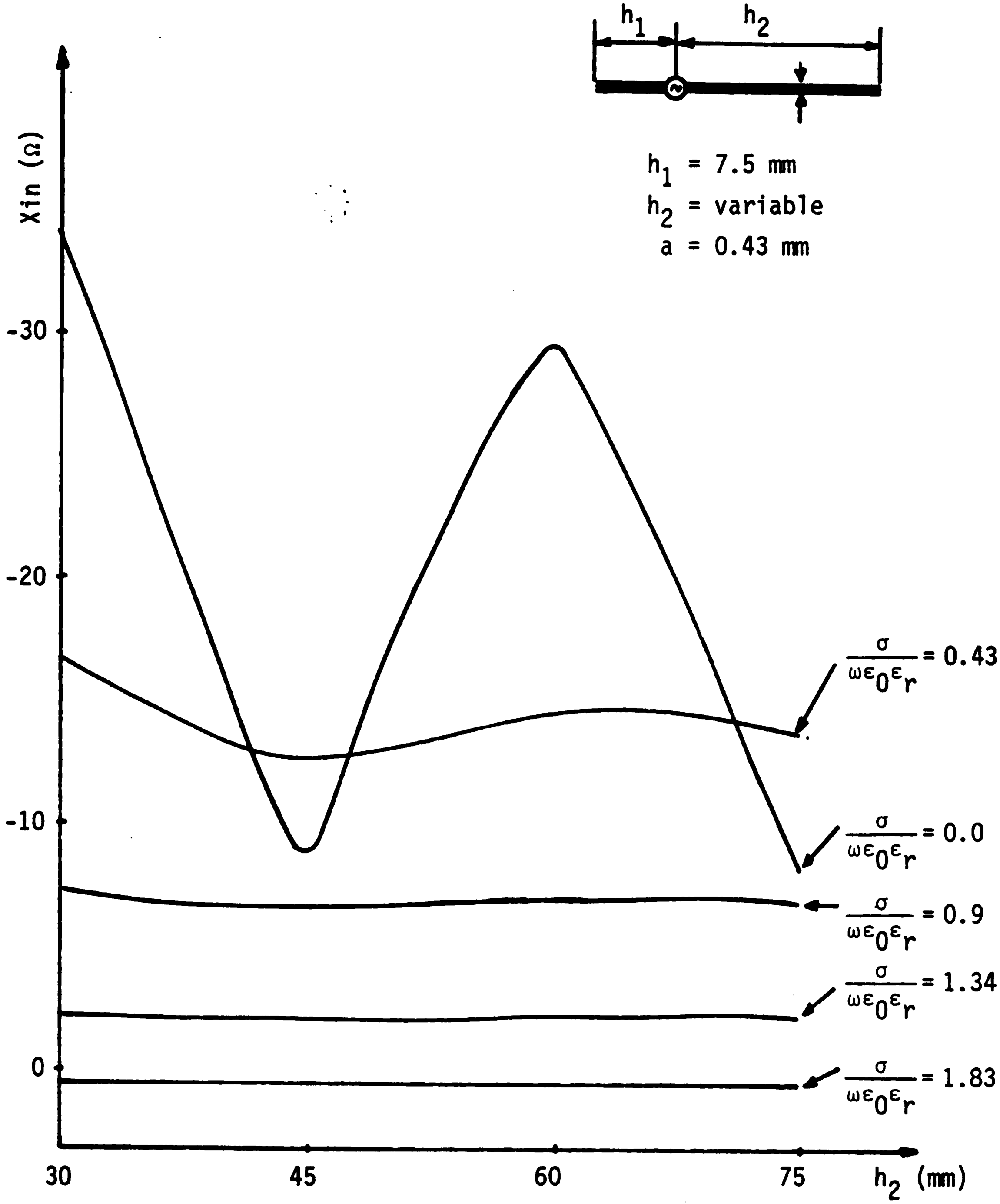

Figure 2.7. Input reactances of bare probes in the salines with different concentrations.

becomes nearly independent of the length of h_2. This phenomenon implies that when the probe is in a lossy medium, with $\frac{\sigma}{\omega\varepsilon_0\varepsilon_r} > 0.43$, the characteristics of the probe mainly depend on the properties of the medium, not on h_2. These characteristics of the bare probe can be used to measure the electrical properties of the lossy medium.

For checking the consistency of the theory let us consider electrically short and thin bare probes. When

$$a \ll h, \ \alpha h \ll 1, \ \beta h \ll 1$$

the current distribution along the probe is approximately triangular. The input admittance Yin of a symmetric bare probe ($h_1 = h_2 = h$) in a lossy medium is known [11] to be

$$\mathrm{Yin} \doteq \mathrm{Gin} + j\omega \mathrm{Cin} = \frac{\pi h}{\mathrm{Ln}(h/a) - 1} (\sigma + j\omega\varepsilon) \tag{2.2.11}$$

Table 2.1 shows the input admittance of the bare probe at different frequencies calculated from equation (2.2.11) and from theory developed in the previous sections, Hallen's Integral Equation method (HIEM) and Electric Field Integral Equation method (EFIE). The physical dimensions of the probe are h = 10 mm and $a_1 = a_2 =$ 0.43 mm. The probe is in a lossy medium with $\sigma = 0.05$ (s/m) and $\varepsilon_r = 7.4\ \varepsilon_0$. The results shown in Table 2.1 confirm the consistency of the theoretical methods developed in this chapter.

Table 2.1. Input admittance of an electrically short and thin bare probe in a conducting medium.

Frequency	HIEM	EFIE	Equation (2.2.11)
10 MHz	0.688 + j0.056	0.715 + j0.059	0.718 + j0.060
100 MHz	0.689 + j0.565	0.717 + j0.588	0.718 + j0.601
600 MHz	0.759 + j3.53	0.789 + j3.67	0.718 + j3.61

2.2.1. Magnetic Current Ring as the Driving Source

In the study of the probe it is very important to properly model the source region at the driving point. In the previous sections the source region at the driving point was modeled as a delta gap and based on that model the current distribution along the probe was found. In this section, the source region is modeled by a magnetic current ring.

As shown in Figure 2.8, the gap is replaced by a circular magnetic current ring with a surface magnetic current, $\vec{K}_m$, flowing around the probe. The relationship between the electric field at the gap produced by the applied voltage and the surface magnetic current is

$$\vec{K}_m = -\hat{n} \times \vec{E} \tag{2.2.12}$$

where $\hat{n}$ is the unit vector in the $\hat{r}$ direction. After substitution for $\hat{n}$ and $\vec{E}$ in the equation (2.2.12). we have

$$\vec{K}_m = -\frac{V}{2\delta}\,\hat{\phi} \tag{2.2.13}$$

The magnetic vector potential produced by the surface magnetic current is

$$\vec{A}_m(\vec{r}) = \frac{\varepsilon}{4\pi}\int_{s'} \vec{K}_m(\vec{r}\,')\psi(\vec{r},\vec{r}\,')ds' \tag{2.2.14}$$

where s' is the area of the source region.

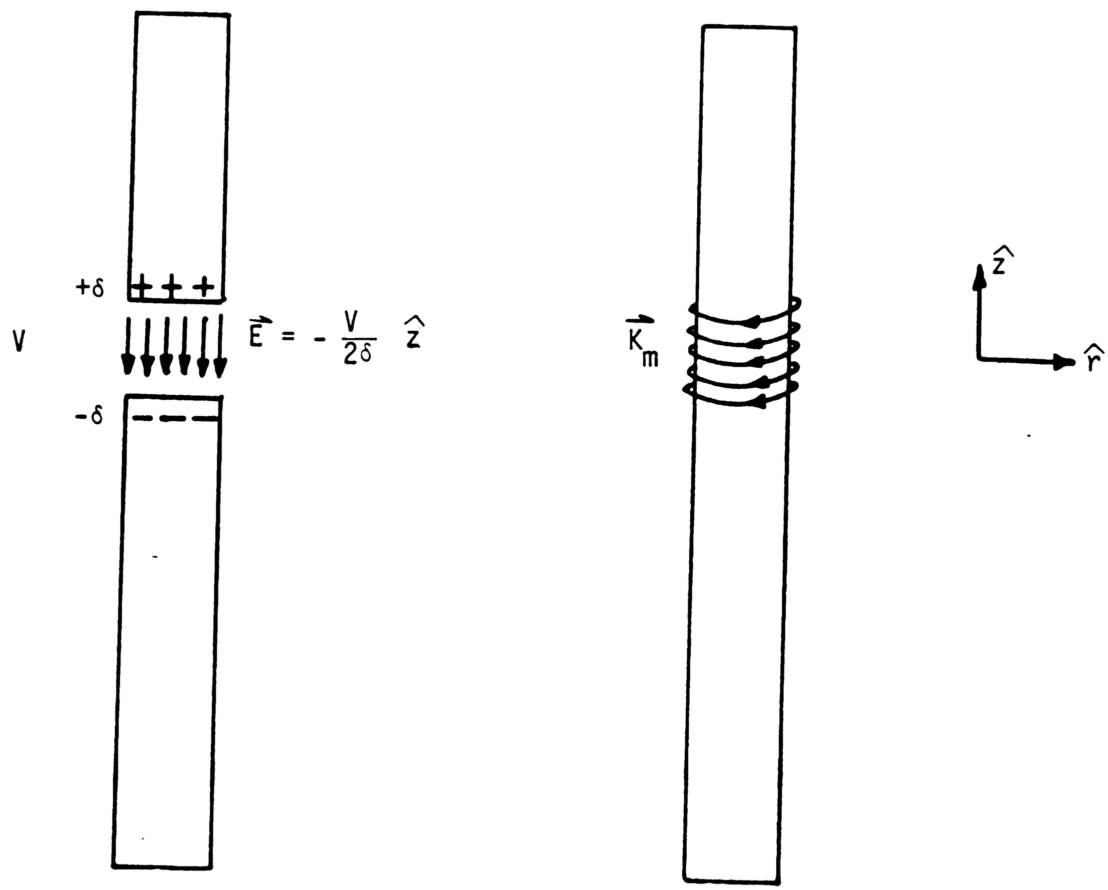

$$\vec{K}_m = - \hat{n} \times \vec{E}$$

$$\vec{K}_m = - \hat{r} \times \left(- \frac{V}{2\delta} \hat{z}\right)$$

$$\vec{K}_m = - \frac{V}{2\delta} \hat{\phi}$$

Figure 2.8. Equivalent magnetic ring model.

Substituting the surface magnetic current from (2.2.13) in (2.2.14), the magnetic vector potential can be written as

$$\vec{A}_m(\vec{r}) = -\frac{V}{2\delta}\frac{\varepsilon}{4\pi}\int_{s'} \hat{\phi}' \frac{e^{-jkR(\vec{r},\vec{r}\,')}}{R(\vec{r},\vec{r}\,')} ds' \quad . \tag{2.2.15}$$

Because of rotational symmetry the observation point is chosen at $\phi = 0$. In a cylindrical coordinate system, $R(\vec{r},\vec{r}\,')$ can be expressed as follows:

$$R = [r^2 + r'^2 - 2rr' \cos \phi' + (z - z')^2]^{\frac{1}{2}}$$

The unit vector $\hat{\phi}'$ in terms of the unit vectors $\hat{x}$ and $\hat{y}$ in the cartesian coordinate system is

$$\hat{\phi}' = -\hat{x} \sin \phi' + \hat{y} \cos \phi' \quad . \tag{2.2.16}$$

With (2.2.16), (2.2.15) becomes

$$\vec{A}_m(\vec{r}) = -\frac{V}{2\delta}\frac{\varepsilon}{4\pi}\left[-\hat{x}\int_{-\delta}^{\delta}\int_0^{2\pi} \sin \phi' \frac{e^{-jkR(\vec{r},\vec{r}\,')}}{R(\vec{r},\vec{r}\,')} d\phi' dz' \right.$$

$$\left. + \hat{y}\int_{-\delta}^{\delta}\int_0^{2\pi} \cos \phi' \frac{e^{-jkR(\vec{r},\vec{r}\,')}}{R(\vec{r},\vec{r}\,')} d\phi' dz' \right] \tag{2.2.17}$$

Since the integrand of the first term on the right hand side is an odd function of ϕ', it integrates to zero. Also, at the plane of $\phi = 0$, $\hat{y} = \hat{\phi}$. The magnetic vector potential $\vec{A}_m(\vec{r})$ is

$$\vec{A}_m(\vec{r}) = -\hat{\phi}\frac{V}{2\delta}\frac{\varepsilon}{4\pi}\int_{s'}\cos\phi'\frac{e^{-jkR(\vec{r},\vec{r}')}}{R(\vec{r},\vec{r}')}ds' \qquad (2.2.18)$$

The electric field is related to the electric vector potential $\vec{A}(\vec{r})$ and the magnetic vector potential $\vec{A}_m(\vec{r})$ by

$$\vec{E}(\vec{r}) = \frac{1}{j\omega\varepsilon}\{\nabla\nabla\cdot + k^2\}\vec{A}(\vec{r}) - \frac{1}{\varepsilon}\nabla\times\vec{A}_m(\vec{r}) \qquad (2.2.19)$$

Since only magnetic current is present, $\vec{A}(\vec{r}) = 0$. Therefore,

$$\begin{aligned}\vec{E}_z(\vec{r}) &= -\frac{1}{\varepsilon}\frac{1}{r}\frac{\partial}{\partial r}(rA_{m\phi}) \\ &= \frac{V}{8\pi\delta}\frac{1}{r}\frac{\partial}{\partial r}\left[r\int_{s'}\cos\phi'\frac{e^{-jkR(\vec{r},\vec{r}')}}{R(\vec{r},\vec{r}')}ds'\right] \qquad (2.2.20)\end{aligned}$$

Let us define the integrand in (2.2.20) as F(r,z):

$$F(r,z) = \int_{s'}\cos\phi'\frac{e^{-jkR(\vec{r},\vec{r}')}}{R(\vec{r},\vec{r}')}ds'$$

The above integral cannot be carried out exactly, therefore, it will be evaluated numerically. When $R \to 0$ the integrand is singular. This happens when the field point is in the source region. In order to evaluate the integral when the field point $P(r, 0, t + \frac{\varepsilon}{2})$ is in the source region (see Figure 2.9), the integral is separated into five integrals as stated below in (2.2.21).

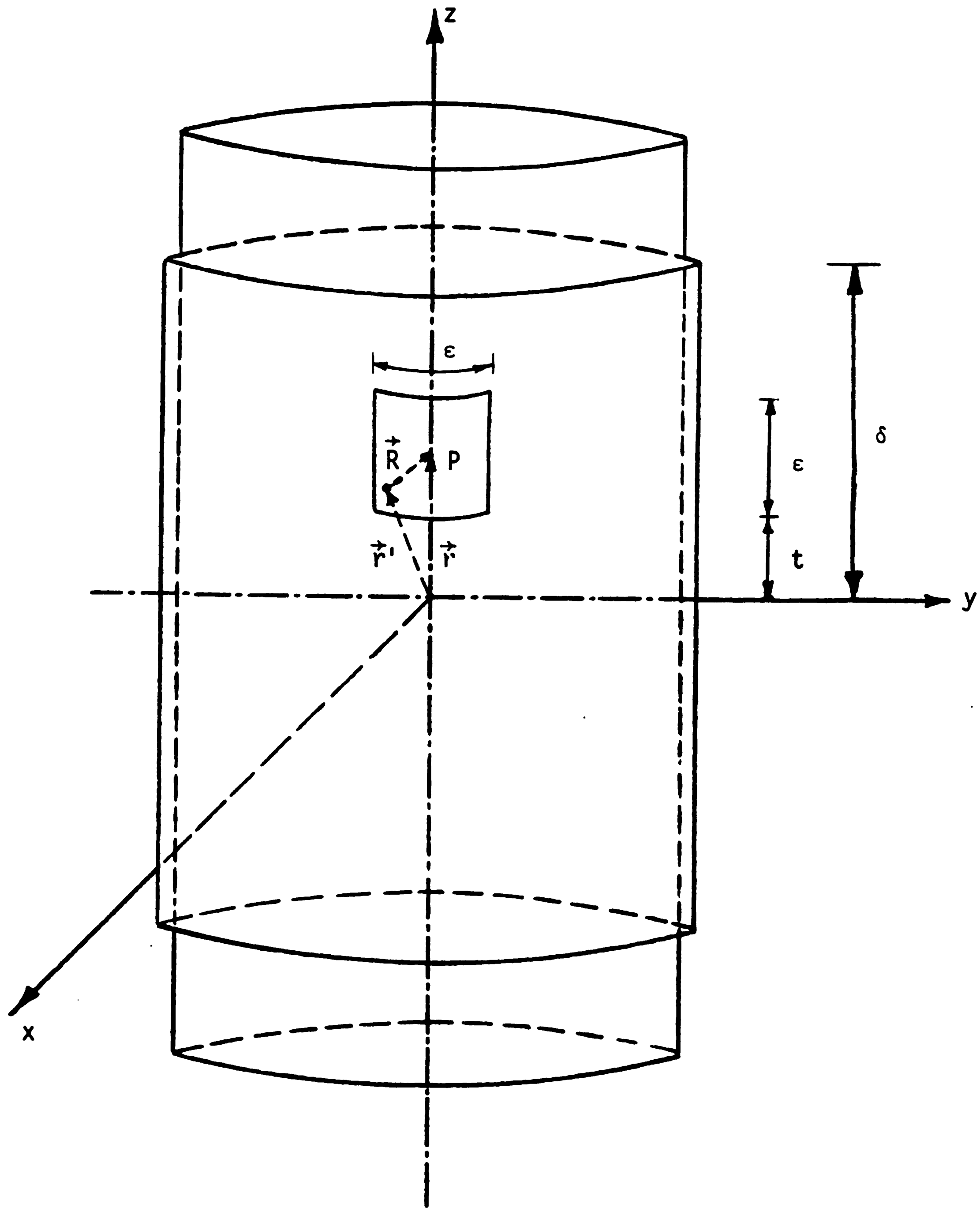

Figure 2.9. Geometry of magnetic current ring when the field point is in the source region.

$$F(r,z) = \int_{-\delta}^{t}\int_{-\pi}^{\pi} \cos\phi' \, \frac{e^{-jkR(\vec{r},\vec{r}')}}{R(\vec{r},\vec{r}')} \, d\phi' dz'$$

$$+\int_{t+\varepsilon}^{\delta}\int_{-\pi}^{\pi} \cos\phi' \, \frac{e^{-jkR(\vec{r},\vec{r}')}}{R(\vec{r},\vec{r}')} \, d\phi' dz'$$

$$+\int_{t}^{t+\varepsilon}\int_{-\pi}^{-\frac{\varepsilon}{2r}} \cos\phi' \, \frac{e^{-jkR(\vec{r},\vec{r}')}}{R(\vec{r},\vec{r}')} \, d\phi' dz'$$

$$+\int_{t}^{t+\varepsilon}\int_{\frac{\varepsilon}{2r}}^{\pi} \cos\phi' \, \frac{e^{-jkR(\vec{r},\vec{r}')}}{R(\vec{r},\vec{r}')} \, d\phi' dz'$$

$$+\int_{t}^{t+\varepsilon}\int_{-\frac{\varepsilon}{2r}}^{\frac{\varepsilon}{2r}} \cos\phi' \, \frac{e^{-jkR(\vec{r},\vec{r}')}}{R(\vec{r},\vec{r}')} \, d\phi' dz' \qquad (2.2.21)$$

The last integral in this equation which has a singular point is carried out analytically. The surface is approximated with the same area [12]. Therefore,

$$\int_{t}^{t+\varepsilon}\int_{-\frac{\varepsilon}{2r}}^{\frac{\varepsilon}{2r}} \cos\phi' \, \frac{e^{-jkR(\vec{r},\vec{r}')}}{R(\vec{r},\vec{r}')} \, d\phi' dz' = \int_{s'} \cos\phi' \, \frac{e^{-jkR(\vec{r},\vec{r}')}}{R(\vec{r},\vec{r}')} \, ds'$$

$$= \int_{s'} \frac{e^{-jkR'}}{R'} R' dR' d\psi = \frac{2\pi}{jk}\left[1 - e^{-jk\frac{\varepsilon}{\sqrt{\pi}}}\right] \qquad (2.2.22)$$

The rest of the terms of F(r,z) can be found numerically and (2.2.22) should be added to it. The derivative of F(r,z) with respect to r, according to the finite difference, is

$$\frac{\partial F(r,z)}{\partial r} \doteq \frac{F(r,z) - F(r - \Delta r,z)}{\Delta r}$$

After taking the derivative of F(r,z) numerically, its value can be substituted in (2.2.20) to determine the electric field $E_z(\vec{r})$ produced by the equivalent magnetic current ring at any point in the medium.

The effect of the length of the magnetic current ring on the electric field produced by it is studied and it is shown in Figure 2.10. In this figure the length of the current ring is assumed to be Δg = 1.0 or Δg = 2.0 mm, on a probe with $a_1 = a_2$ = 0.43 mm, in the medium with σ = 1.1 (s/m) and ϵ_r = 76.7 at 600 MHz frequency. The area under the curve is $\vec{E}\cdot\vec{dl}$. In both cases the area under the curve is approximately equal to one, which is equal to the driving voltage applied to the probe. The distribution of the electric field maintained by the magnetic current ring on the surface of the probe is close to a delta function. For this finding, it is reassumed that the delta gap model for the source region is an accurate model.

The input impedance of the probe has been calculated with the magnetic current ring model for the driving source and using the electric field integral equation method. The effect of the

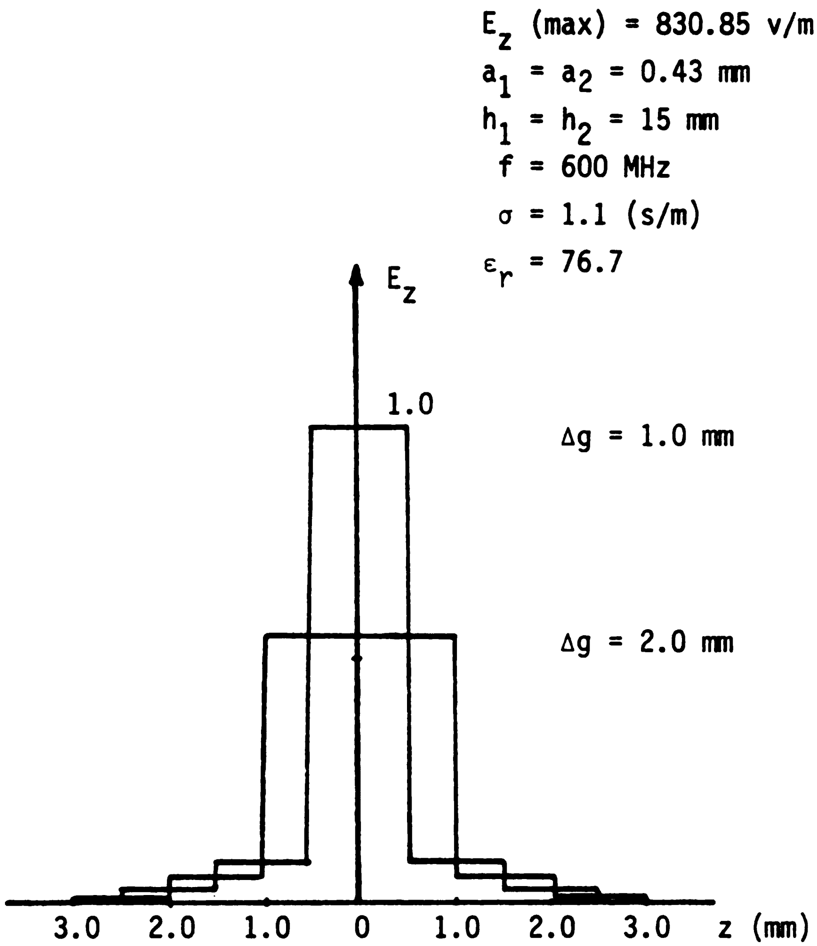

Figure 2.10. Normalized electric field on the surface of the probe maintained by the magnetic current ring model.

length of the magnetic current ring on the input impedance was studied, and the results are shown in Figure 2.11. In this figure the length of the ring is changed from 0.5 mm to 2.0 mm but no significant change in the input resistance or the input reactance is observed for this range of change.

2.3. Comparison of Different Methods

In the previous sections different methods for solving the bare probe in a conducting medium were discussed. The input admittances of the probe with $a_1 = a_2 = 0.43$ mm, $h_1 = 7.5$ mm, and $h_2 = 45$ mm at 600 MHz frequency in saline with 0.1 and 0.2 normalities are shown in Table 2.2. The results in Table 2.2 indicate that the real part of the admittance (conductance) is in good agreement for different methods, but the imaginary part (susceptance) has some variations; this is caused by the size of partitions.

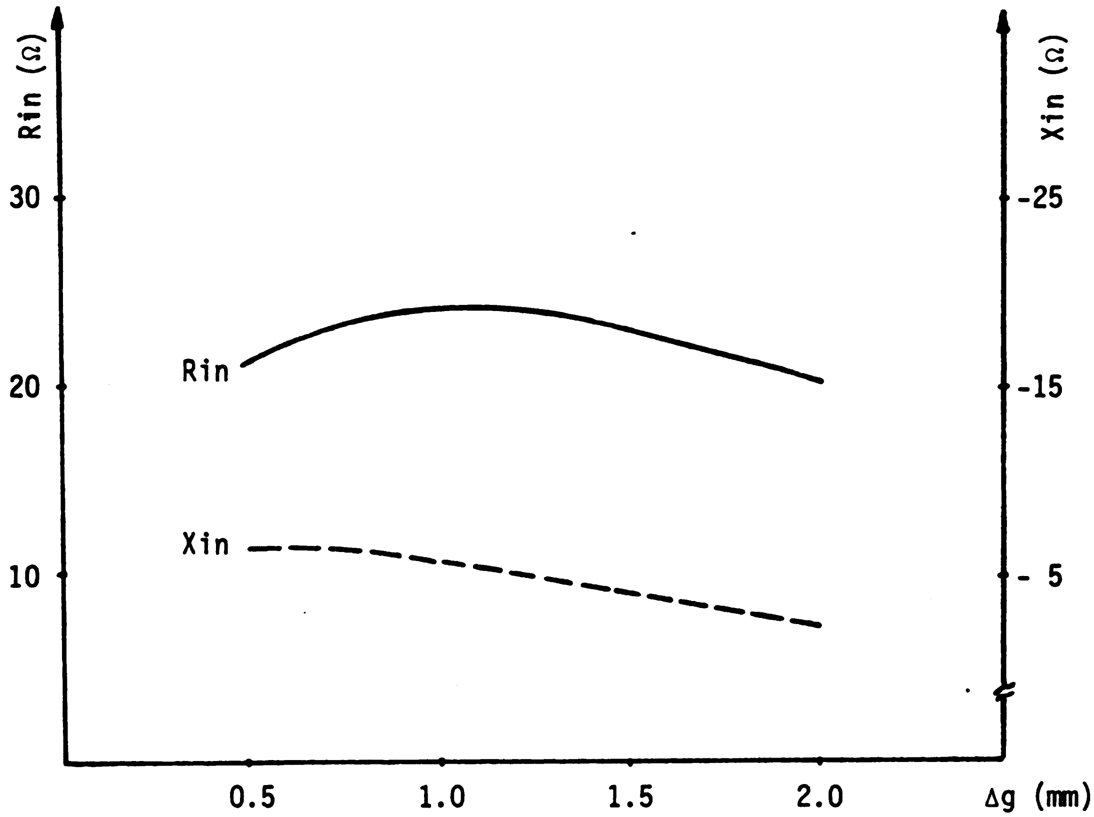

Figure 2.11. Input impedance of the probe varies as the function of the length of the magnetic ring.

Table 2.2. Input admittance of the bare probe in the saline with normalities 0.1 N and 0.2 N.

Method	0.1 N Saline	0.2 N Saline
EFIE with magnetic current ring	36.9 + j17.3	40.3 + j7.8
EFIE with delta gap model	35.1 + j21.2	40.4 + j11.8
HIEM with delta gap model	35.2 + j19.8	39.9 + j10.1

CHAPTER III

EXPERIMENTAL STUDY OF A BARE MICROPROBE IN A CONDUCTING MEDIUM

In order to verify the theory of a bare microprobe in a conducting medium, a series of experiments were conducted. The input impedance of the probe embedded in different lossy media was measured. One way to measure the impedance is to use a slotted line, VSWR meter, and Smith chart. This method has two limitations: first, at a low frequency a long slotted line is needed, and second, with a low resistance in the load the VSWR in the line is very large . and a large VSWR can cause difficulties in using the Smith chart.

Another way to measure the impedance is by a vector voltmeter and a V-I (or E-H) probe, which is explained in more detail in Section 3.2.

To simulate a lossy medium salt water was used, therefore, the electrical properties of saline, permittivity, and the conductivity should be known. These quantities are strongly dependent on the frequency and the temperature. More about electrical properties of saline is explained in references [13-15]. The experimental data in the above references are used in our study.

3.1. Electrical Parameters of Saline

The electrical properties of pure water can be expressed as $\varepsilon = \varepsilon' - j\varepsilon''$, where $\varepsilon' = \varepsilon_0\varepsilon_r'$ and $\varepsilon'' = \varepsilon_0\varepsilon_r''$. The variations in real and imaginary parts of complex permittivity due to the change in frequency are indicated in equations (3.1.1) and (3.1.2).

$$\varepsilon_r' = \frac{\varepsilon_s - 4.9}{1 + (\omega\tau)^2} + 4.9 \tag{3.1.1}$$

$$\varepsilon_r'' = \frac{(\varepsilon_s - 4.9)\omega\tau}{1 + (\omega\tau)^2} \tag{3.1.2}$$

where ω is the angular frequency, ε_s and τ are called the static dielectric constant and the relaxation time, respectively. In these equations ε_s and τ are dependent on the temperature.

After salt is added to pure water, the static dielectric constant (ε_s) and the relaxation time (τ) change with the salt concentration in the solution. ε' varies only due to the changes on τ and ε_s. ε'' varies not only due to the changes on τ and ε_s, but another term needs to be added in the following way:

$$\varepsilon = \varepsilon' - j\varepsilon'' - j\,\frac{\sigma_i}{\omega} \tag{3.1.3}$$

where σ_i is called the inonic conductivity and it is due to Na^+ and Cl^- ions in the solution. The total conductivity is

$$\sigma_t = \sigma_i + \omega\varepsilon''$$

and

$$\varepsilon = \varepsilon' - \frac{j}{\omega}(\sigma_i + \omega\varepsilon'') \tag{3.1.4}$$

In Table 3.1 electrical properties of saline are shown. These results are obtained by interpolation for various normalities of saline. At 600 MHz frequency the dominant terms for conductivity and permittivity are the ionic conductivity and the static dielectric constant, respectively. With the increase in temperature, the conductivity of the saline increases while its permittivity decreases.

3.2. Experimental Setup

The schematic diagram of the experimental setup is shown in Figure 3.1. The microprobe imbedded in a tank of saline is driven by a R.F. generator through an E-H probe. The outputs of the E-H probe are connected to a vector voltmeter for the measurement of the input impedance.

The E-H (V-I) probe consists of a section of transmission line with a short E probe and a small H probe. The E probe is a short monopole that induces a voltage proportional to the E field or voltage in the trnasmission line. The H probe is a small loop that induces a voltage proportional to the H field or the current in the transmission line [16]. The vector voltmeter has two channels, "A" and "B". If two signals are connected to channels "A" and "B", the amplitude of each signal and the phase difference between them can be measured by the vector voltmeter. By definition the impedance at any point in the circuit is the ratio of the voltage to the current at that point. Two signals from E and H probes can be

Table 3.1. Electrical properties of NaCl solution.

Saline Normality	20°C $\tau(10^{-12}$ sec)			30°C $\tau(10^{-12}$ sec)		
	$\tau(10^{-12}$ sec)	ε_s	σ_i(s/m)	$\tau(10^{-12}$ sec)	ε_s	σ_i(s/m)
0	10.1	80	0	7.5	77	0
0.1	9.92	78.2	0.889	7.44	75.2	1.044
0.2	9.74	76.4	1.778	7.38	73.4	2.089
0.3	9.56	74.6	2.667	7.32	71.6	3.113
0.4	9.38	72.8	3.556	7.26	69.8	4.178
0.5	9.2	71.0	4.44	7.2	68	5.22

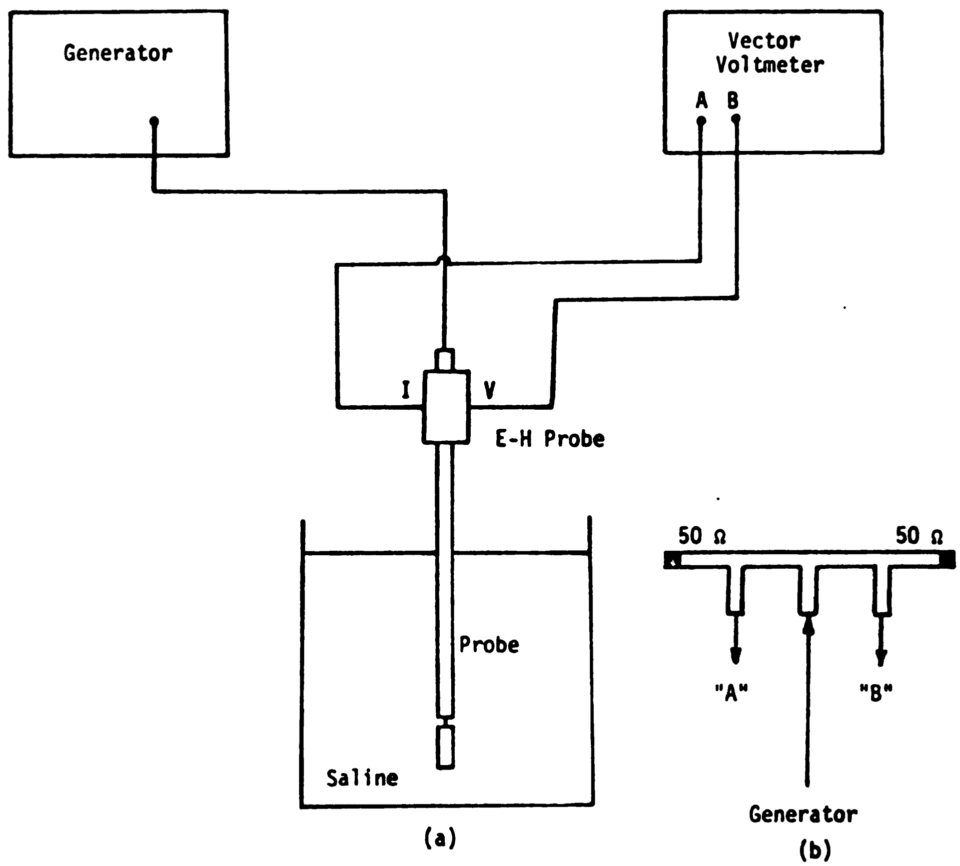

Figure 3.1. (a) Experimental setup for the measurement of the input impedance of a probe with an E-H probe and a vector voltmeter.
(b) Setup for adjusting the phase of a vector voltmeter.

measured by the vector voltmeter and their ratio is the impedance of the line at the V-I probe location. Physical geometry of the bare probe which was used in the experiment is shown in Figure 3.2.

Before measurement several steps should be taken as follows:

(1) The vector voltmeter should be calibrated. For this reason two equal signals are connected to channels "A" and "B" of the vector voltmeter and the phase indicator should be adjusted to show zero (see Figure 3.1(a)). The phase knobs should not be changed during the experiment. The vector voltmeter measures the phase difference between the signal connected to channel "B" with respect to the signal on channel "A". The amplitude of each signal could be measured separately.

(2) The E-H probe should be calibrated. A match load, for this case a 50 Ω load, is connected to the E-H probe and the voltage probe and the current loops on the V-I probe are connected to channels "A" and "B" of the vector voltmeter, respectively. We then let

$$50 = \bar{K} \frac{\bar{V}_B}{\bar{V}_A}$$

where $\bar{V}_A$ and $\bar{V}_B$ are voltages at channels "A" and "B". $\bar{K}$ is called the calibration factor for the E-H probe and it should be evaluated for different frequencies. The bar on V_A and V_B indicates that these parameters are complex.

(3) Connect the unknown load, in this case the probe in saline, to the E-H probe. Read the amplitudes of "A", "B", and the

h_1 = 7.5 mm
h_2 = variable
a_1 = 0.1 mm
a_2 = 0.43 mm
Δg = 1.0 mm

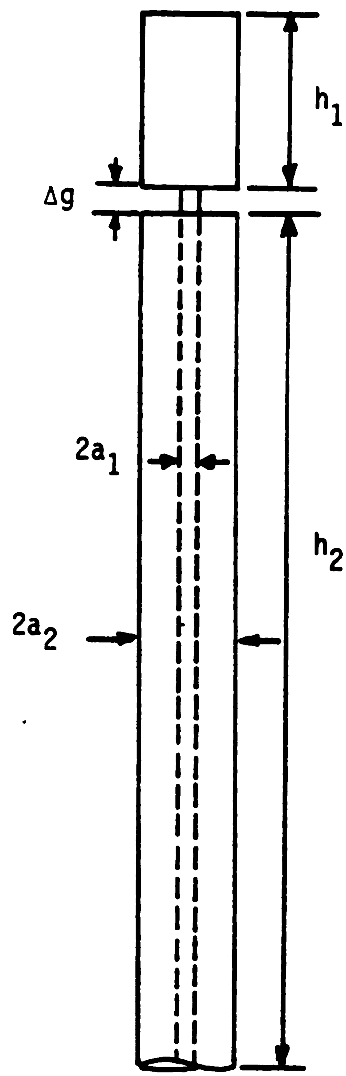

Figure 3.2. Physical geometry of bare probe used in the experiment.

phase difference on the vector voltmeter. The impedance of the probe at the location of the E-H probe is then equal to

$$\bar{Z}_p = \bar{K}\,\frac{\bar{V}_B}{\bar{V}_A} \tag{3.2.1}$$

(4) The value for the input impedance that we found in step (3) should be transformed to the probe location. For this purpose, we need to know the factor of tan γl, where γ is the propagation constant of the transmission line and l is the distance between the probe and the location of the E-H probe. If we short circuit the probe and measure its input impedance we have

$$\bar{Z}_p\ (\text{short}) = -jz_c \tan \gamma l \tag{3.2.2}$$

where Z_c is the characteristic impedance of the line which is 50 Ω in our case.

(5) The impedance of the probe is given by the well-known formula from the transmission line theory [17].

3.3. Comparison of Theoretical and Experimental Results

Experiments were carried out at 600 MHz frequency with the probe imbedded in the saline with various normalities (0.1 N, 0.2 N, 0.3 N, and 0.4 N). The physical dimensions of the probe are: $a = 0.43$ mm, $h_1 = 7.5$ mm, $h_2 = 30$ or 45 mm, and the gap is about 1.0 mm. The tank has the dimensions of 21 cm x 21 cm, 23 cm. The theoretical results are calculated for the same probe in an infinite conducting medium.

In Figures 3.3 to 3.6 theoretical and experimental results on the input resistance and input reactance of the bare probes in the various lossy media are compared. In Figures 3.3 and 3.4, h_2 is 30 mm, and for this case there is a good agreement between theory and experiment on the input resistance, but the agreement is only fair on the input reactance at higher normalities of saline. Figures 3.5 and 3.6 are for h_2 = 45 mm, and for this case the agreement between the theory and experiment is again good for the input resistance and only fair for the input reactance.

In these experiments the sources of errors can be classified as follows:

(1) Small physical dimensions of the probe; since the radius of the probe is very small (0.43 mm), it is very difficult to keep it straight.

(2) The electrical properties of the saline are strongly dependent on the salt concentration and the temperature and any error in the salt concentration and the temperature will produce different conductivity and permittivity.

(3) Another source of error is due to the junctions from the microprobe to a standard GR 50 Ω coaxial transmission line.

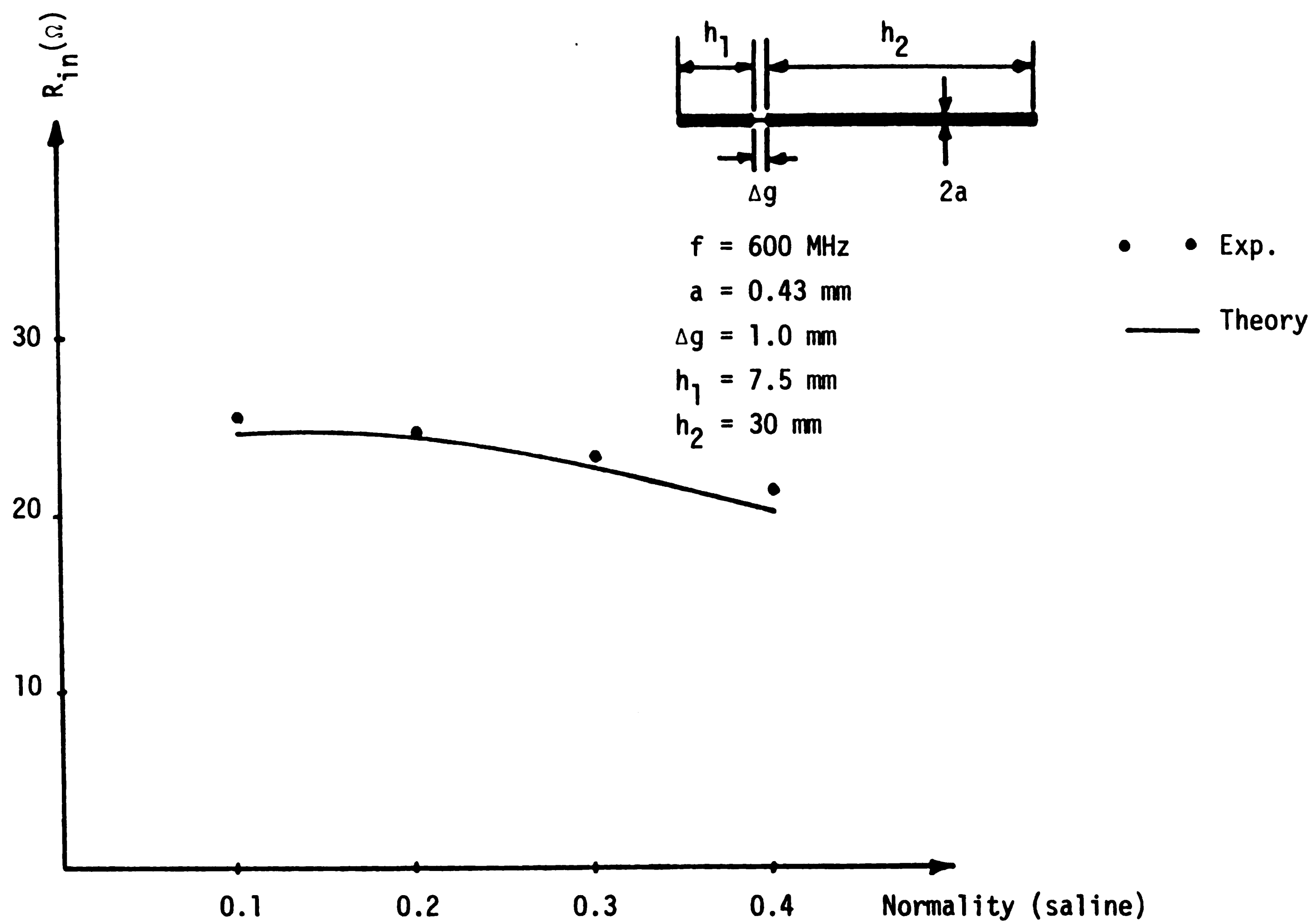

Figure 3.3. Comparison of theoretical and experimental results on the input resistance of a probe in various conducting media.

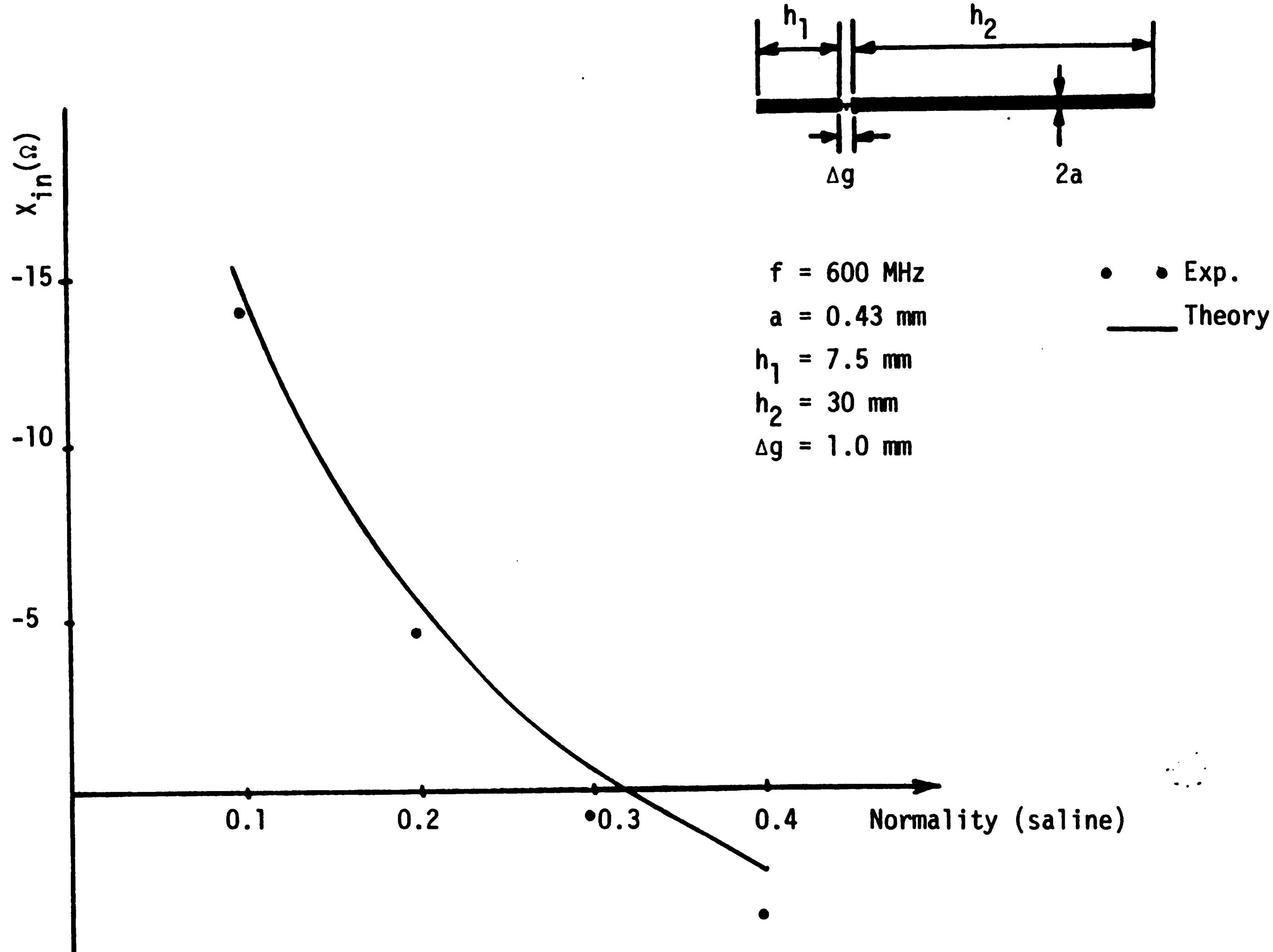

Figure 3.4. Comparison of theoretical and experimental results on the input reactance of a probe in various conducting media.

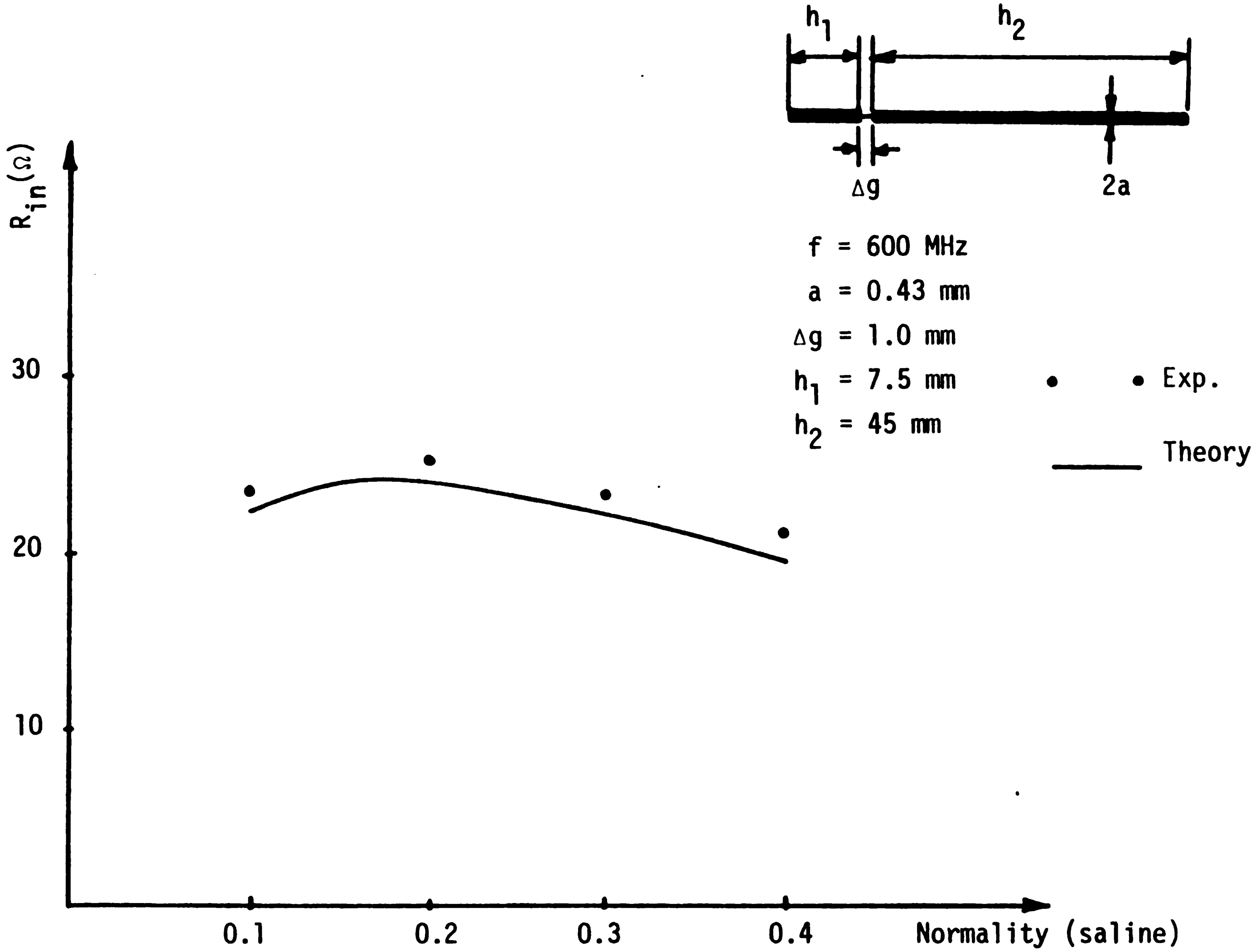

Figure 3.5. Comparison of theoretical and experimental results on the input resistance of a probe in various conducting media.

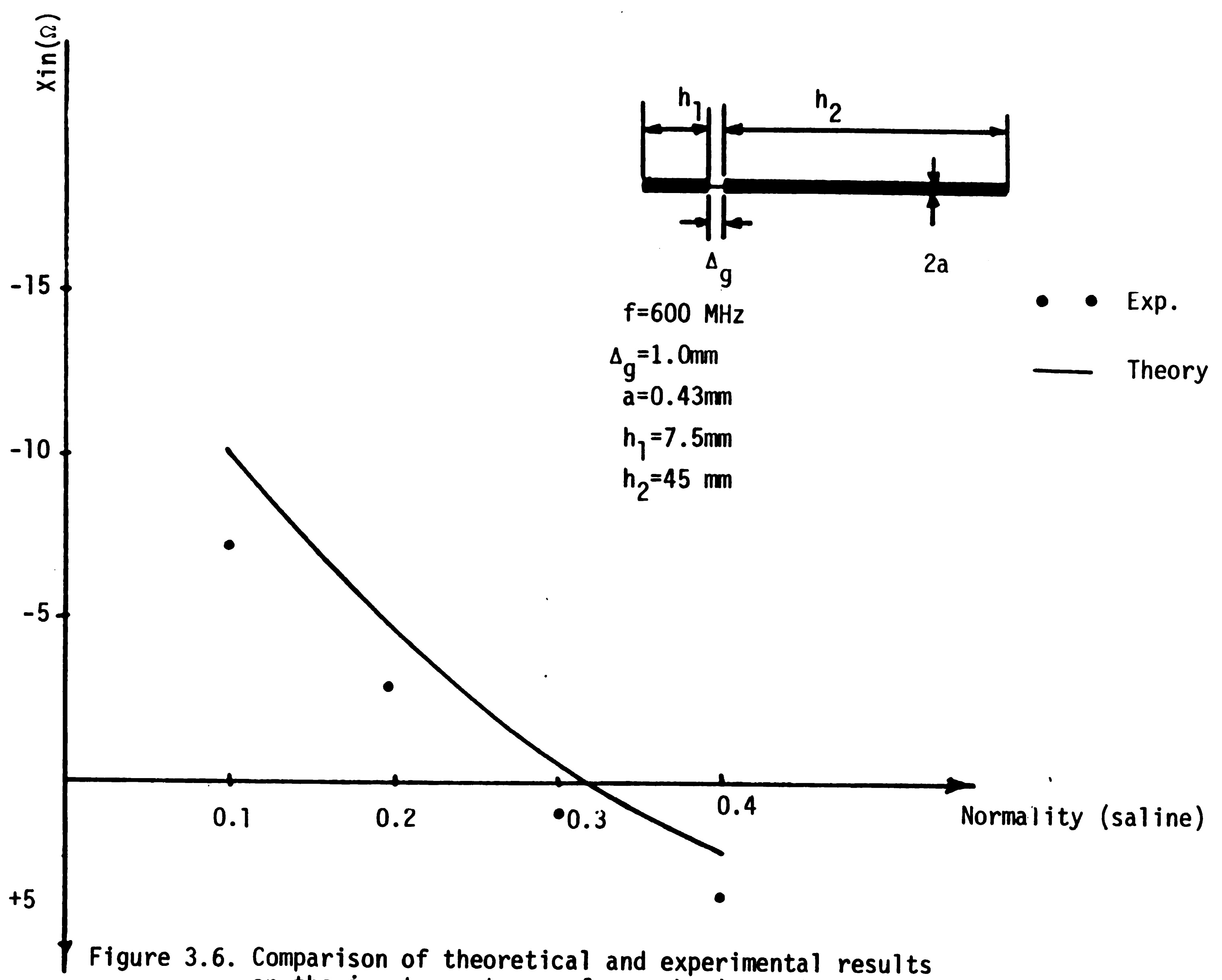

Figure 3.6. Comparison of theoretical and experimental results on the input reactance of a probe in various conducting media.

CHAPTER IV

APPLICATIONS OF THE BARE PROBE

In the study of EM local heating of an imbedded tumor, it is very important to know the conductivity and permittivity of the tumor relative to that of the surrounding tissues. There are reasons to suspect that the electrical properties of the tumor may be different from those of surrounding tissues because the blood flow to and tissue structure of the tumor are different from the normal tissues. A successful analysis of the induced EM field inside an irradiated body with an imbedded tumor and an effective device for focusing EM energy in the tumor will depend on the knowledge of electrical properties of the tumor.

A bare probe can be used to measure the conductivity (σ) and permittivity (ε) of the biological bodies in vivo. A bare probe, when driven by an RF source, can also be used locally to heat the biological tissues. Figure 4.1 shows a bare probe inserted in a tumor.

4.1. Measurement of σ and ε

In Chapter II it was shown that a coaxial probe in a lossy medium is equivalent to an asymmetrical dipole. The input admittance of a dipole is a function of the frequency of operation, physical dimensions of the dipole, and electrical properties of the surrounding medium (i.e. permittivity, permeability, and conductivity of the medium). Permeability is defined as $\mu = \mu_0 \mu_r$, which for a nonmagnetic medium gives $\mu_r = 1$. Therefore, the input admittance of a fixed probe at a certain frequency in a nonmagnetic medium is only a function of σ and ε of the surrounding medium.

The input admittance of a probe, $Yin(\sigma,\varepsilon) = Gin(\sigma,\varepsilon) + jBin(\sigma,\varepsilon)$, has a real part (conductance) $Gin = f_g(\sigma,\varepsilon)$ and an imaginary part (susceptance) $Bin = f_b(\sigma,\varepsilon)$. The input conductance and susceptance are functions of the conductivity and the permittivity of the medium.

For finding σ and ε analytically from the conductance and the susceptance of the probe, the functions f_g and f_b should be known. These functions cannot be expressed in terms of simple functions, but the probe can be calibrated based on the theory developed in Chapter II. Input conductances and input susceptances of the probe are found for various values of σ and ε. There are two ways to use this information about the probe which lead to the determination of the electrical properties of a biological tissue or a lossy medium.

In the first method, two sets of curves are drawn. One set is the conductance and the other set is the susceptance of the probe versus the conductivity, where the permittivity is used as a parameter. These sets of curves for a typical probe are shown in Figures 4.2 and 4.3. The physical dimensions of the probe are given in these figures and the frequency of operation is 600 MHz. The

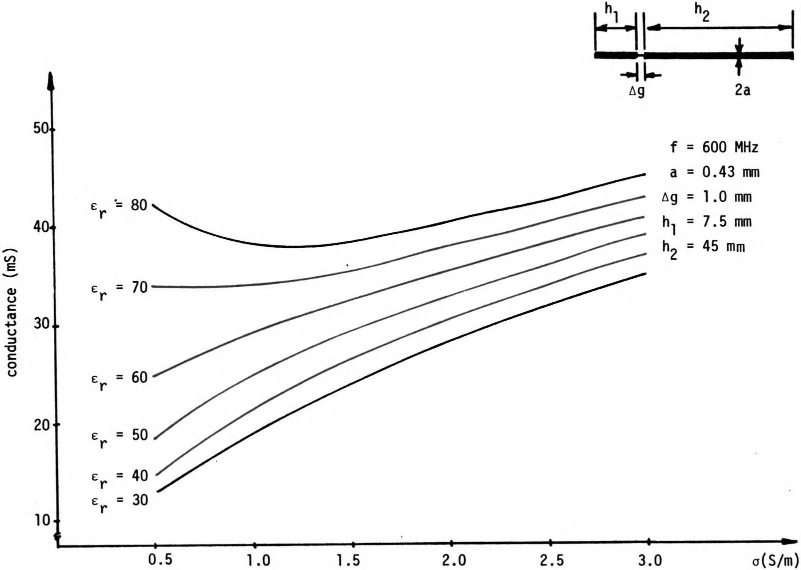

Figure 4.2. Input conductance of a probe in various conducting media, obtained with Electric Field Integral Equation method and the driving point is modeled with a magnetic current ring.

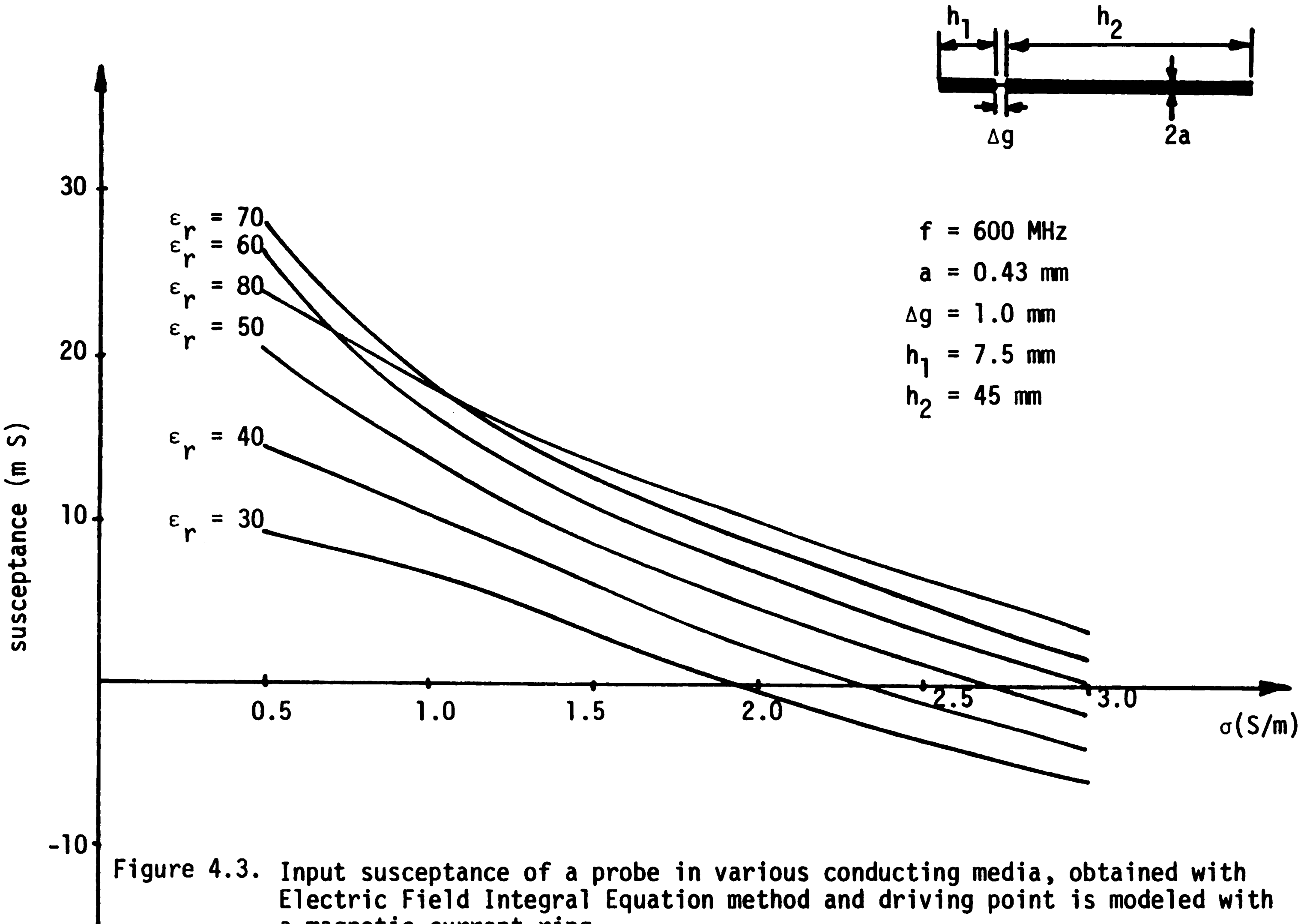

Figure 4.3. Input susceptance of a probe in various conducting media, obtained with Electric Field Integral Equation method and driving point is modeled with a magnetic current ring.

following example shows how electrical properties of a lossy medium can be measured.

An experiment was conducted and the input admittance of a bare probe with the same dimensions as given in Figure 4.2 was measured. The conducting medium was 0.2 normal saline and the temperature was 25°C. The input admittance of the probe was measured to be Yin = 38.98 + j4.97 (m℧). Draw two straight lines for Gin = 38.98 and Bin = 4.97 in Figures 4.2 and 4.3, respectively. From the possible values for ε_r and σ found in these curves intersected by the two straight lines, we can estimate the conductivity to be 2.4 (s/m) and the relative permittivity to be 65. The existing values for 0.2 normal saline at 25°C is about $\sigma = 2.21$ (s/m) and $\varepsilon_r = 74.8$. Thus, the accuracy of this method is considered to be satisfactory.

The second method for finding σ and ε is, after theoretically finding the conductance and susceptance of the probe for various possible values of σ and ε, the information is stored in the computer and then the input admittance of the probe imbedded in a medium with unknown σ and ε is measured. The measured values are fed to the computer and a computer program searches for the closest values for σ and ε of the unknown medium. Using this method the input admittance of the probe measured in the above example gives $\varepsilon_r = 65.5$ and $\sigma = 2.4$ (s/m). The second method seems to give more accurate results.

4.2. Local Heating

Another application of the bare probe is for local heating in cancer therapy by microwave hyperthermia. In this section the heat pattern of a bare probe in a conducting medium is being studied. In the previous chapter the current distribution along the probe has been determined. The electric field produced by the current on the probe at any point in the medium can then be found. The heat created by the electric field in the lossy medium is given by $\frac{1}{2}\sigma|E|^2$.

With the assumption that the current is only in the z direction and with a rotational symmetry in our problem, the vector potential has only one component in the z direction and it is expressed as

$$A_z(r,z) = \frac{\mu}{4\pi}\int_{-h_2}^{h_1} I_z(z')\,\frac{e^{-jkR}}{R}\,dz' \tag{4.2.1}$$

and

$$A_r(r,z) = A_\phi(r,z) = 0 \ .$$

The relationship between the magnetic field and the vector potential is

$$\vec{B} = \nabla \times \vec{A} \ .$$

Therefore,

$$B_r(r,z) = B_z(r,z) = 0$$

and

$$B_\phi(r,z) = -\frac{\partial A_z(r,z)}{\partial r} \quad .$$

Maxwell's equation $\nabla \times \vec{B}(r,z) = \mu(\sigma + j\omega\varepsilon)\vec{E}(r,z)$ implies that

$$E_\phi(r,z) = 0$$

and

$$E_r(r,z) = -\frac{j\omega}{k^2}\frac{\partial^2 A_z(r,z)}{\partial r \partial z} \tag{4.2.2}$$

$$E_z(r,z) = \frac{j\omega}{k^2}\left[\frac{1}{r}\frac{\partial A_z(r,z)}{\partial r} + \frac{\partial^2 A_z(r,z)}{\partial r^2}\right] \quad . \tag{4.2.3}$$

Assuming that $R = [r^2 + (z - z')^2]^{\frac{1}{2}}$ and the current on the probe as

$$I_z(z') = \sum_{n=1}^{N} I_n P_n(z') \quad ,$$

the electric field in the r direction is expressed as

$$E_r(r,z) = -\frac{j\omega\mu}{4\pi k^2}\frac{\partial^2}{\partial r \partial z}\int_{-h_2}^{h_1}\sum_{n=1}^{N} I_n P_n(z')\,\frac{e^{-jkR}}{R}\,dz'$$

or

$$E_r(r,z) = -\frac{j\omega\mu}{4\pi k^2}\sum_{n=1}^{N} I_n \frac{\partial}{\partial r}\int_{-h_2}^{h_1} P_n(z')\,\frac{\partial}{\partial z}\left(\frac{e^{-jkR}}{R}\right) dz'$$

Since $\frac{\partial}{\partial z} = -\frac{\partial}{\partial z'}$, then

$$E_r(r,z) = -\frac{j\omega\mu}{4\pi k^2}\sum_{n=1}^{N} I_n \left[\left(jk\frac{r}{R} + \frac{r}{R^2}\right) \frac{e^{-jkR}}{R} \Bigg|_{z'=z_{\bar{n}}}^{z'=z_{n}^{+}} \right]$$

$$\text{for } -h_2 \le z \le h_1 \qquad (4.2.4)$$

After substitution for the current and the vector potential in (4.2.3), we have

$$E_z(r,z) = \frac{j\omega\mu}{4\pi k^2}\left[\frac{1}{r}\frac{\partial}{\partial r}\int_{-h_2}^{h_1}\sum_{n=1}^{N} I_n P_n(z')\,\frac{e^{-jkR}}{R}\,dz'\right.$$

$$\left. + \frac{\partial^2}{\partial r^2}\int_{-h_2}^{h_1}\sum_{n=1}^{N} I_n P_n(z')\,\frac{e^{-jkR}}{R}\,dz'\right]$$

and then

$$E_z(r,z) = \frac{j\omega\mu}{4\pi k^2}\sum_{n=1}^{N} I_n\left[\frac{1}{r}\frac{\partial}{\partial r}\int_{(\Delta z)_n}\frac{e^{-jkR}}{R}\,dz' + \frac{\partial^2}{\partial r^2}\int_{(\Delta z)_n}\frac{e^{-jkR}}{R}\,dz'\right] \qquad (4.2.5)$$

For large r or small r and $z \notin (\Delta z)_n$ we can write

$$\int_{(\Delta z)_n}\frac{e^{-jkR}}{R}\,dz' = \Delta\,\frac{e^{-jkR}}{R}\,.$$

(4.2.5) then becomes

$$E_z(r,z) = -\frac{j\omega\mu\Delta}{4\pi k^2}\sum_{n=1}^{N} I_n\left[\frac{2jk}{R} + \frac{2+k^2r^2}{R^2} - \frac{3jkr^2}{R^3} - \frac{3r^2}{R^4}\right]\frac{e^{-jkR}}{R} \qquad (4.2.6)$$

For small r and $z \varepsilon (\Delta z)_n$, we have

$$\int_{(\Delta z)_n} \frac{e^{-jkR}}{R} dz' = 2Ln \left\{ \frac{\Delta}{2r} + [1 + (\frac{\Delta}{2r})^2]^{1/2} \right\} - jk\Delta$$

and

$$\frac{\partial}{\partial r} \int_{(\Delta z)_n} \frac{e^{-jkR}}{R} dz' = - \frac{\Delta}{r^2} [1 + (\frac{\Delta}{2r})^2]^{-1/2}$$

$$\frac{\partial^2}{\partial r^2} \int_{(\Delta z)_n} \frac{e^{-jkR}}{R} dz' = \frac{2\Delta}{r^3} [1 + \frac{1}{2} (\frac{\Delta}{2r})^2][1 + (\frac{\Delta}{2r})^2]^{-3/2}$$

Substitute the above approximate expressions in (4.2.5), and we have

$$E_z(r,z) = \frac{j\omega\mu}{4\pi k^2} \sum_{n=1}^{N} I_n(\frac{\Delta}{r^3})[1 + (\frac{\Delta}{2r})^2]^{-3/2}$$

Numerically the r and z components of the electric field can be found in the medium. The heat produced by the field is given by $\frac{1}{2} \sigma |E|^2$, where $|E|^2 = |E_z|^2 + |E_r|^2$.

Figures 4.4 and 4.5 show the equi-power contours for a bare probe in the r-z plane. Electrical properties of the medium and physical dimensions of the probe are also given in these figures. The driving voltages are V_0 = 8.44 volts and V_0 = 7.63 volts in Figures 4.4 and 4.5, respectively. The changes in the driving voltage resulted from keeping the input power equal in both cases (input power = 1 watt). The driving voltage is determined as follows:

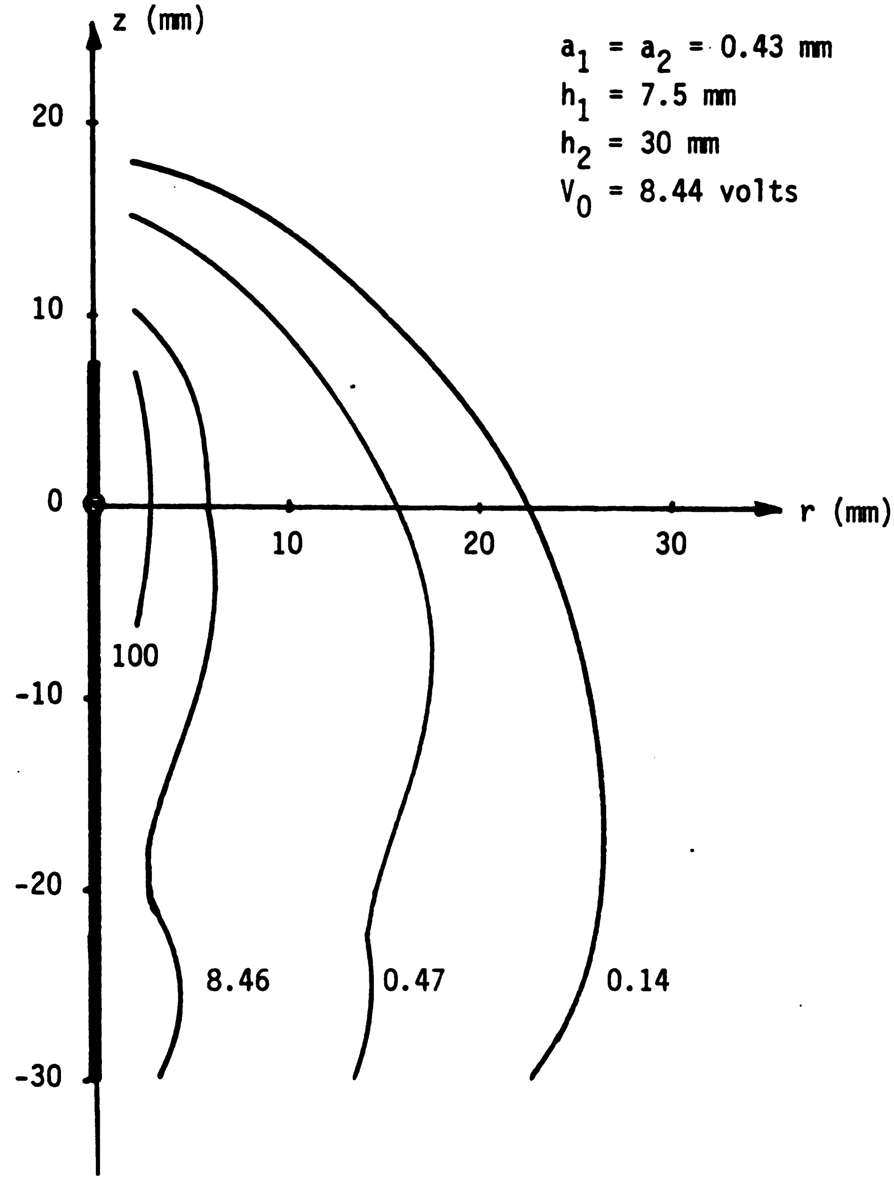

Figure 4.4. Equi-power contours for a bare probe in the r-z plane. The power is normalized and the frequency of operation f = 600 MHz, $\sigma_2 = 1.11$ (s/m), $\varepsilon_{r2} = 76.7$.

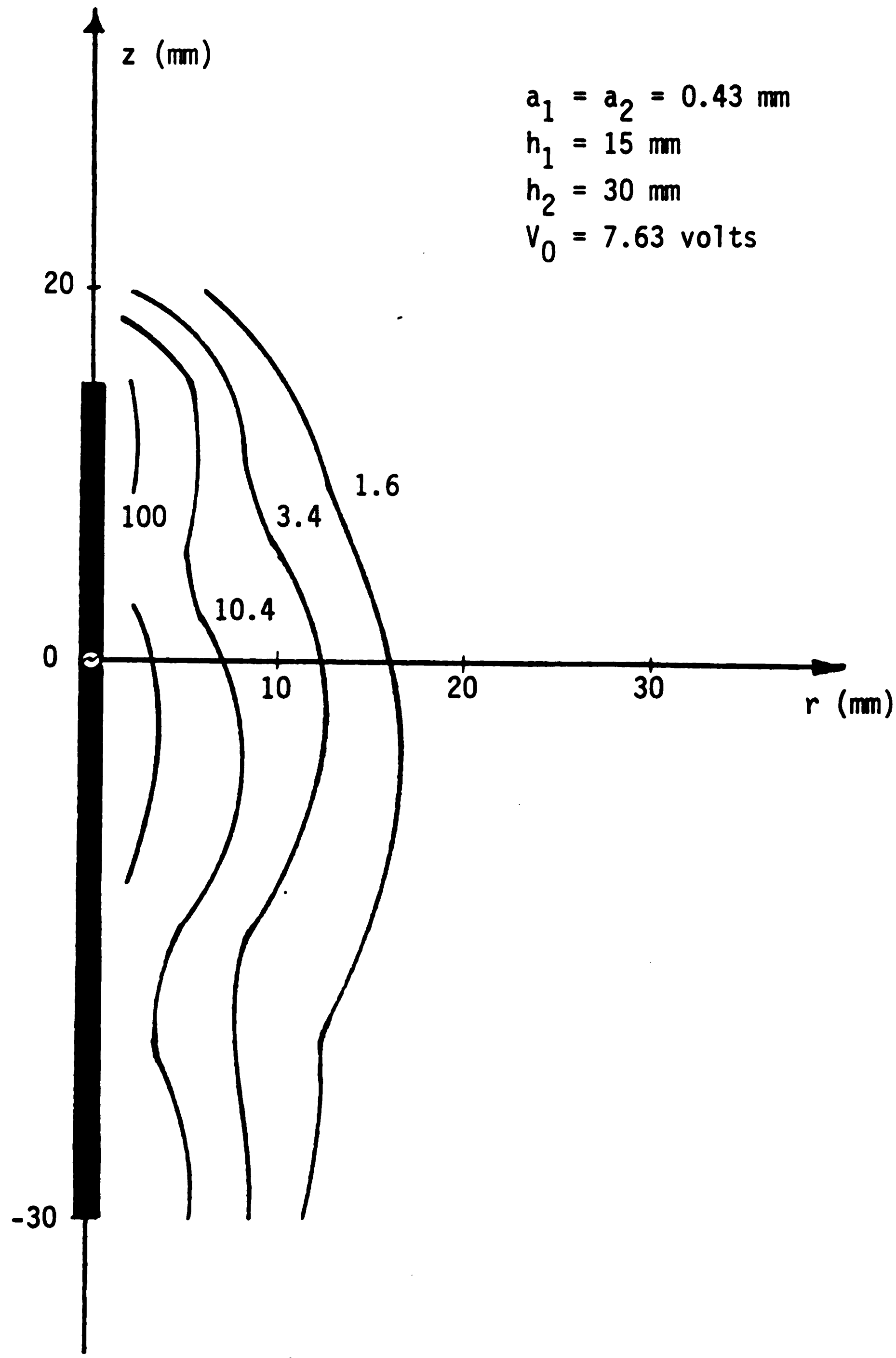

Figure 4.5. Equi-power contours for a bare probe in the r-z plane. The power is normalized and the frequency of operation f = 600 MHz, σ_2 = 1.11 (s/m), ε_{r2} = 76.7.

$$\text{Power (input)} = 1 \text{ watt} = \frac{1}{2}\,\mathrm{Re}V_0 I^*$$

$$= \frac{1}{2}\,\mathrm{Re}\,\frac{V_0^2}{(Rin + jXin)^*}$$

and

$$V_0 = \left(2\ \frac{Rin^2 + Xin^2}{Rin}\right)^{1/2}$$

The power in these figures is normalized. The length of the probe h_1 is 7.5 mm and 15 mm in Figures 4.4 and 4.5, respectively. In both cases most of the power is concentrated near the probe, along the z axis. As we see from these figures the heat pattern can vary with changing the length of the probe.

CHAPTER V

INSULATED PROBES IN A CONDUCTING MEDIUM

In order to transmit energy into the conducting body and to avoid direct contact between the probe and the body tissue, the probe can be covered with insulated material. The insulated probe is used extensively for local heating in biological bodies. For heating applications, the insulated probe has two major advantages in comparison with the bare probe:

(1) The input resistance of the bare probe is less than the input resistance of the insulated probe in a conducting medium, therefore, the insulated probe radiates more EM energy in the conducting medium.

(2) The current on the bare probe decays rapidly along the probe, hence most of the EM energy radiated from the bare probe is concentrated near the driving point. However, in the insulated probe case the current does not decay rapidly along the probe, thus, the EM energy is distributed over a larger volume.

Evolution of geometry of the insulated probe in a conducting medium is shown in Figure 5.1. Since the current flow is as shown in this figure and the surrounding medium is lossy, the probe is treated as a lossy transmission line. In this case the probe cannot

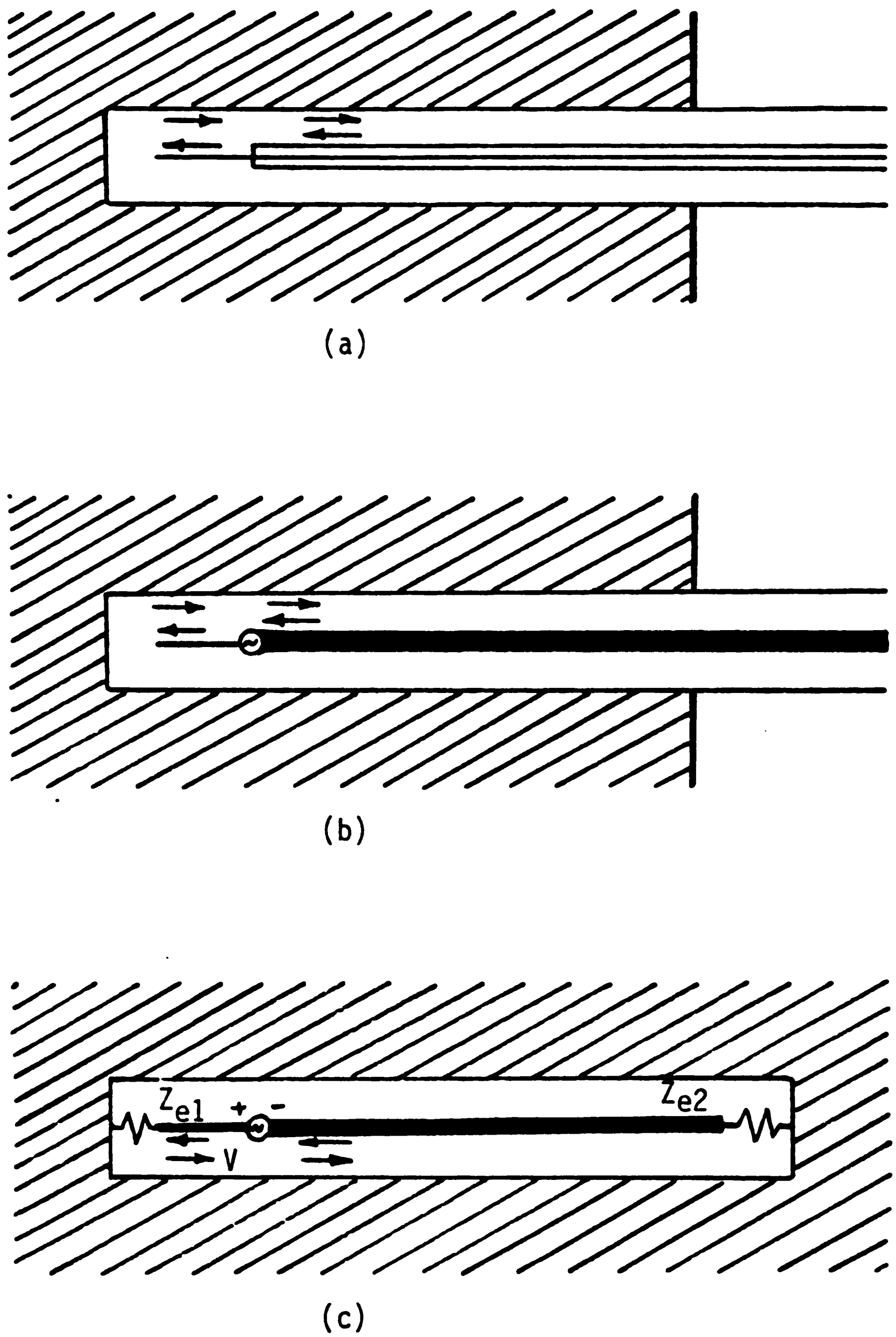

Figure 5.1. Evolution of geometry of an insulated probe in a conducting medium.

be truncated, therefore, equivalent terminal impedances Z_{e1} and Z_{e2} are introduced.

5.1. Theory of the Probe

Since an insulated probe in a conducting medium can be considered as a lossy transmission line, transmission line theory is used to analyze the characteristics of the probe [18]. The equivalent circuits of the insulated probe in a conducting medium in the form of lossy transmission line are shown in Figure 5.2. To start with, the equivalent transmission line of the probe is divided into two sections, where Z_{C1} and Z_{C2} are the characteristic impedances of section (1) and section (2), respectively. The driving voltage V is divided into two voltages, V_1 and V_2. The input impedances of each section are $(Zin)_1$ and $(Zin)_2$, respectively. The input currents of these two sections are I_1 and I_2, but since the current at the junction is continuous, it requires that

$$I_1 = I_2 .$$

This leads to the relation

$$\frac{V_1}{(Zin)_1} = \frac{V_2}{(Zin)_2} . \tag{5.1.1}$$

The other relationship between V_1 and V_2 is

$$V = V_1 + V_2 . \tag{5.1.2}$$

Using (5.1.1) and (5.1.2), V_1 and V_2 can be expressed as follows:

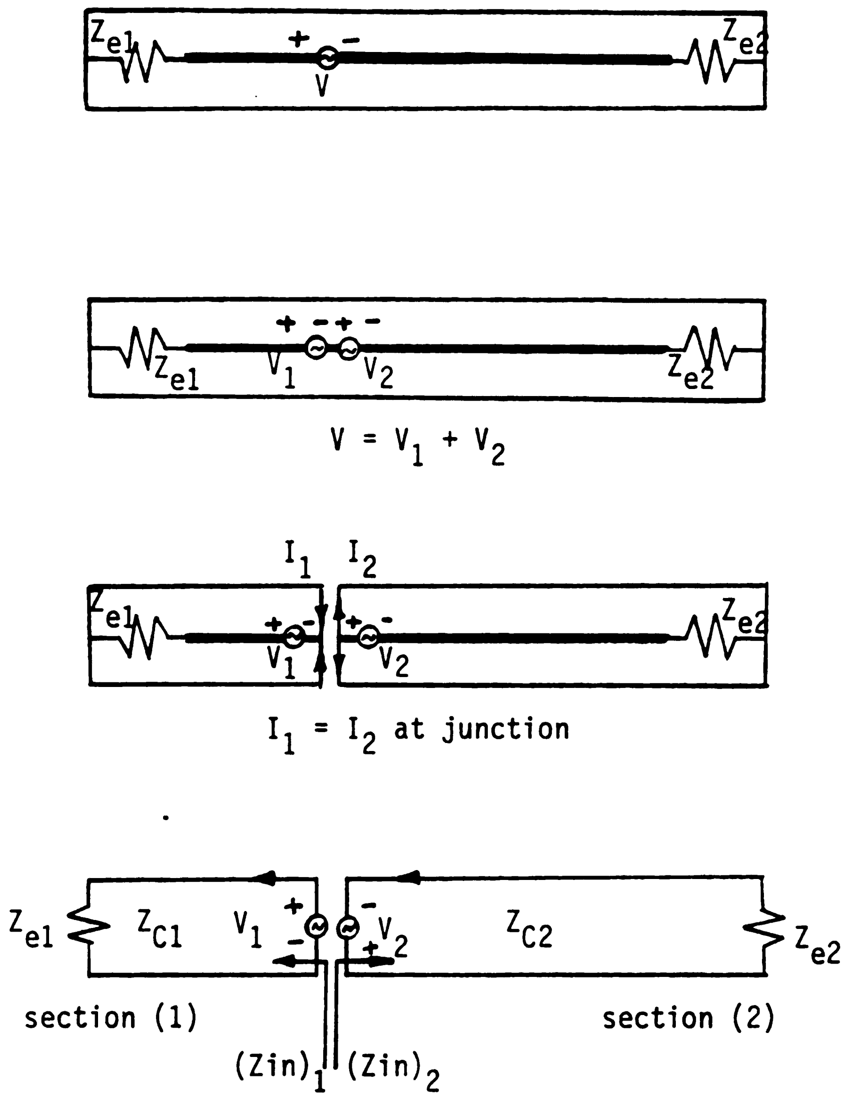

Figure 5.2 Geometries for an insulated probe in a conducting medium.

$$\begin{cases} V_1 = V \dfrac{(Zin)_1}{(Zin)_1 + (Zin)_2} \\ \\ V_2 = V \dfrac{(Zin)_2}{(Zin)_1 + (Zin)_2} \end{cases} \tag{5.1.3}$$

The input impedance of a transmission line is

$$Zin = Z_C \frac{Z_L + Z_C \tanh [\gamma h]}{Z_C + Z_L \tanh [\gamma h]} \tag{5.1.4}$$

where γ is the propagation constant of the line, Z_C and Z_L are the characteristic impedance and load impedance of the line, respectively, and h is the length of the line.

Using the geometry of Figure 5.2 and defining $\tanh \theta_1 = \frac{Z_{C1}}{Z_{e1}}$ and $\tanh \theta_2 = \frac{Z_{C2}}{Z_{e2}}$, where Z_{e1} and Z_{e2} are terminal impedances of two sections, the input impedance for each section of the line can be expressed as

$$\begin{cases} (Zin)_1 = Z_{C1} \coth(\gamma_1 h_1 + \theta_1) \\ \\ (Zin)_2 = Z_{C2} \coth(\gamma_2 h_2 + \theta_2) \end{cases} \tag{5.1.5}$$

Substituting (5.1.5) into (5.1.3), V_1 and V_2 become

$$\begin{cases} V_1 = V \dfrac{Z_{C1} \coth(\gamma_1 h_1 + \theta_1)}{Z_{C1} \coth(\gamma_1 h_1 + \theta_1) + Z_{C2} \coth(\gamma_2 h_2 + \theta_2)} \\ \\ V_2 = V \dfrac{Z_{C2} \coth(\gamma_2 h_2 + \theta_2)}{Z_{C1} \coth(\gamma_1 h_1 + \theta_1) + Z_{C2} \coth(\gamma_2 h_2 + \theta_2)} \end{cases} \tag{5.1.6}$$

The reflection coefficient of each section of the line is

$$\Gamma_1 = \frac{Z_{e1} - Z_{C1}}{Z_{e1} + Z_{C1}}\ , \ \Gamma_2 = \frac{Z_{e2} - Z_{C2}}{Z_{e2} + Z_{C2}}$$

After introducing the above notations, the voltage and current along each section of the probe will be found separately.

A set of coordinate system is introduced for section (1) of the line as indicated in Figure 5.3(a). The voltage along the line can be written as

$$V_1(s) = V^+\left(e^{-\gamma_1 s} + \Gamma_1 e^{\gamma_1 s}\right) \tag{5.1.7}$$

At $s = -h_1$ the voltage $V_1 = V_1(-h_1)$. Substituting for Γ_1 in (5.1.7) we have

$$V^+ = \frac{V_1}{2}\,\frac{\cosh\theta_1 + \sinh\theta_1}{\cosh(\gamma_1 h_1 + \theta_1)} \tag{5.1.8}$$

Using (5.1.7) and (5.1.8), the voltage along section (1) of the line becomes

$$V_1(s) = V_1\,\frac{\cosh(\gamma_1 s - \theta_1)}{\cosh(\gamma_1 h_1 + \theta_1)} \tag{5.1.9}$$

The current distribution along the line is

$$I_1(s) = \frac{V^+}{Z_{C1}}\left(e^{-\gamma_1 s} - \Gamma_1 e^{\gamma_1 s}\right) \tag{5.1.10}$$

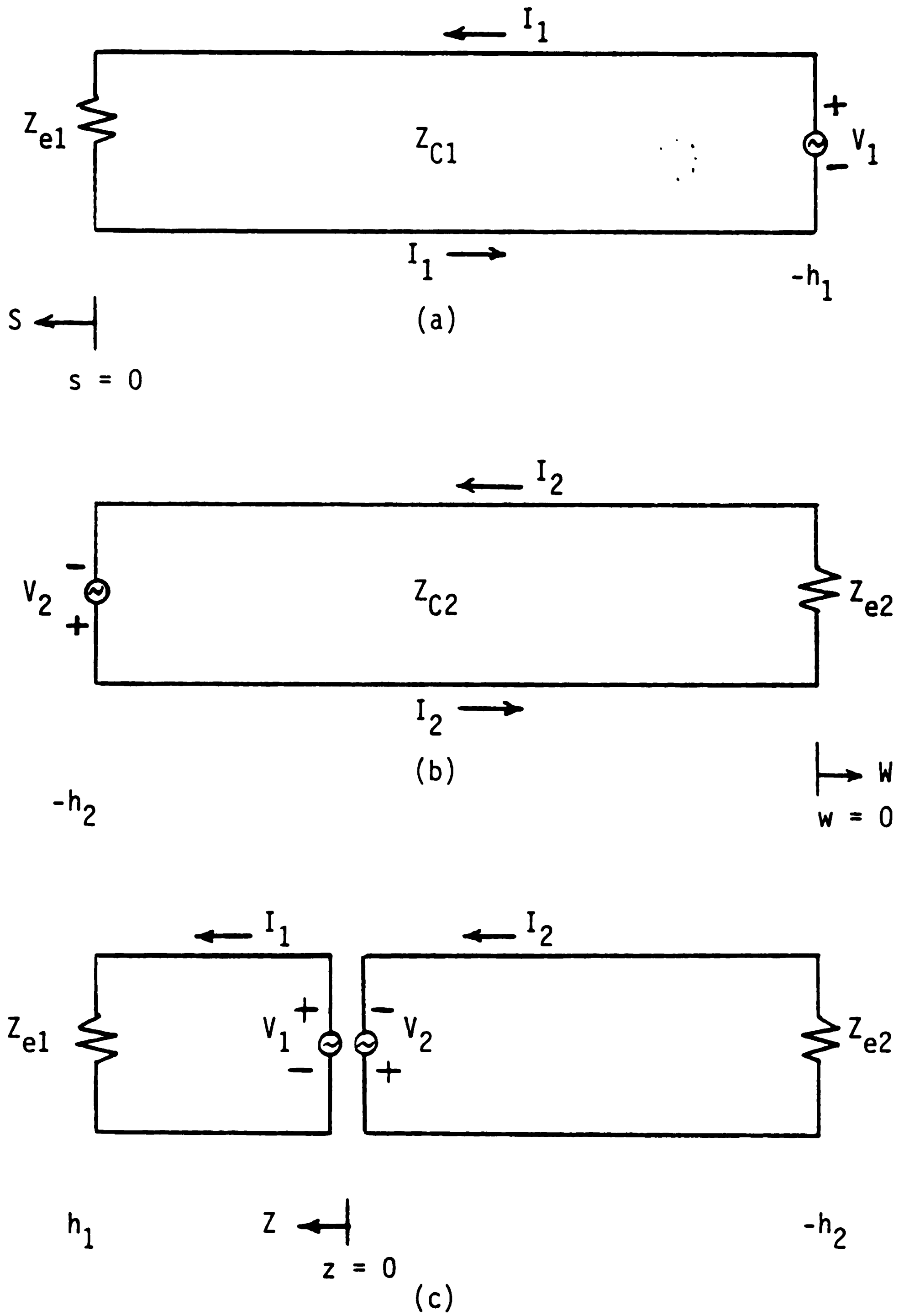

Figure 5.3. (a) Section (1) of the line.
(b) Section (2) of the line.
(c) Common coordinate system for both sections.

After substitution for V^+ and Γ_1 in (5.1.10) the current along section (1) of the line becomes

$$I_1(s) = \frac{V_1}{Z_{C1}} \frac{\sinh(\theta_1 - \gamma_1 s)}{\cosh(\gamma_1 h_1 + \theta_1)} \quad . \tag{5.1.11}$$

In Figure 5.3(b) the coordinate system for section (2) of the line is shown. The voltage and the current along this section of the line are

$$V_2(w) = V_2 \frac{\cosh(\gamma_2 w - \theta_2)}{\cosh(\gamma_2 h_2 + \theta_2)} \tag{5.1.12}$$

$$I_2(w) = \frac{V_2}{Z_{C2}} \frac{\sinh(\theta_2 - \gamma_2 w)}{\cosh(\gamma_2 h_2 + \theta_2)} \quad . \tag{5.1.13}$$

So far there are two different coordinate systems for section (1) and section (2) of the probe. Choose one common coordinate system as indicated in Figure 5.3(c) and transform both coordinate systems to the new coordinate system as

$$Z = s + h_1$$

$$Z = -w - h_2$$

After transformation the voltage and current along the probe are

$$\begin{cases} V_1(z) = V_1 \dfrac{\cosh[\gamma_1(z-h_1) - \theta_1]}{\cosh[\gamma_1 h_1 + \theta_1]} & (5.1.14) \\ & \text{for } 0 \le Z \le h_1 \\ I_1(z) = \dfrac{V_1}{Z_{C1}} \dfrac{\sinh[\theta_1 - \gamma_1(z-h_1)]}{\cosh[\gamma_1 h_1 + \theta_1]} & (5.1.15) \end{cases}$$

and

$$\begin{cases} V_2(z) = V_2 \dfrac{\cosh[\gamma_2(z+h_2) + \theta_2]}{\cosh[\gamma_2 h_2 + \theta_2]} & (5.1.16) \\ & \text{for } 0 \ge z \ge -h_2 \\ I_2(z) = \dfrac{V_2}{Z_{C2}} \dfrac{\sinh[\theta_2 + \gamma_2(z+h_2)]}{\cosh[\gamma_2 h_2 + \theta_2]} & (5.1.17) \end{cases}$$

In these equations V_1 and V_2 are expressed in (5.1.6).

5.2.1. Parameters of the Transmission Line

In Figure 5.4(a) an insulated probe in a conducting medium is shown. Region (1) in this figure is the outer conductor of the microprobe and it is usually made of a material with very high conductivity. Region (2) is the conducting medium with $(\sigma_2, \varepsilon_2)$, and region (3) is the insulating material with $(\sigma_d, \varepsilon_d)$.

The insulated probe in a conducting medium is equivalent to a lossy coaxial cable with a complex propagation constant defined as

$$\gamma = \sqrt{YZ} = \alpha + j\beta$$

where Y is the admittance per unit length and Z is the total impedance per unit length of the line. For a coaxial cable Y is

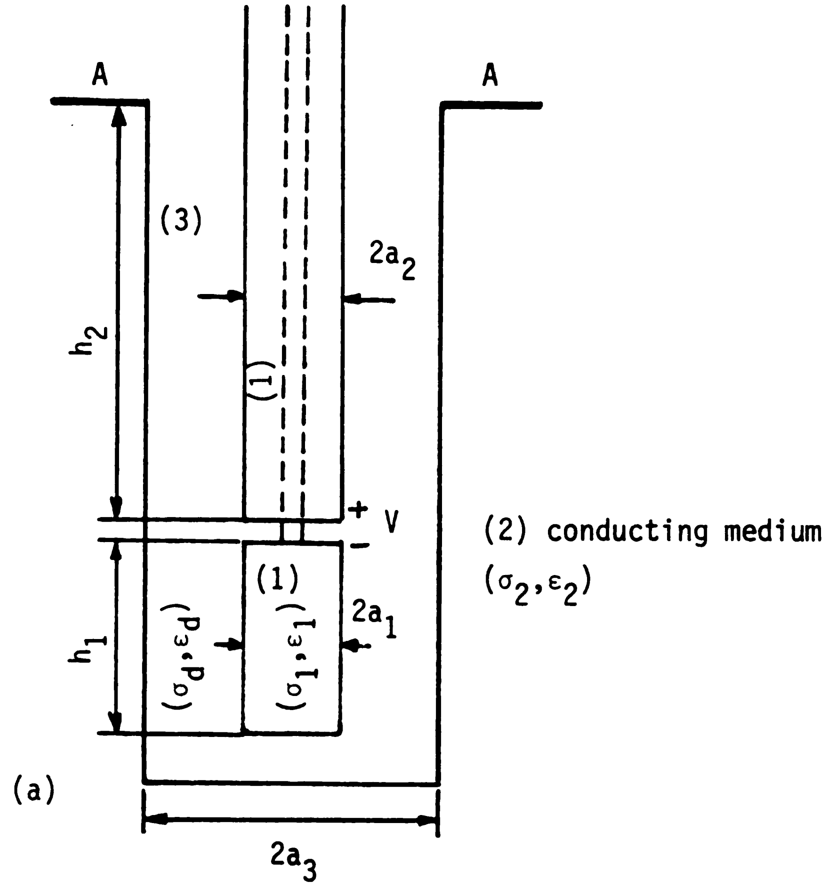

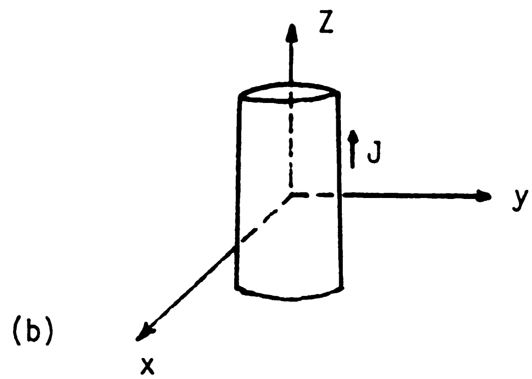

Figure 5.4. (a) Insulated probe in a conducting medium.
(b) Infinite cylinder.

$$Y = g + j\omega C$$

where

$$g = \frac{2\pi\sigma_d}{\ln(a_3/a_1)} \qquad \text{and} \qquad C = \frac{2\pi\varepsilon_d}{\ln(a_3/a_1)}$$

and the total impedance per unit length is

$$Z = Z_1^i + Z_2^i + Z^e$$

where Z_1^i and Z_2^i are the surface impedances of the inner and outer conductors of the transmission line, respectively, and Z^e is called the external impedance of the line.

For finding Z_1^i and Z_2^i we assume the infinite cylinder geometry and that the current on the cylinder flows only in the z direction as indicated in Figure 5.4(b). Start with Maxwell's curl equations:

$$\nabla \times \vec{E}(\vec{r}) = -j\omega\vec{B}(\vec{r})$$

$$\nabla \times \vec{B}(\vec{r}) = \mu(\sigma + j\omega\varepsilon)\vec{E}(\vec{r}) \ .$$

Since the cylinder is assumed to be infinitely long and there is rotational symmetry in the problem, we have

$$\frac{\partial\vec{E}(\vec{r})}{\partial z} = \frac{\partial\vec{H}(\vec{r})}{\partial z} = 0$$

$$\frac{\partial\vec{E}(\vec{r})}{\partial\phi} = \frac{\partial\vec{H}(\vec{r})}{\partial\phi} = 0$$

The electric field has only one component on the $\hat{z}$ direction and it is

$$\vec{E}(\vec{r}) = \hat{z}E_z(r) \quad .$$

Substituting for the electric field in Maxwell's equations, we have

$$\frac{\partial^2 E_z(r)}{\partial r^2} + \frac{1}{r}\frac{\partial E_z(r)}{\partial r} + k^2 E_z(r) = 0$$

where

$$k^2 = \omega^2 \mu\varepsilon - j\omega\mu\sigma \ .$$

The solution of the above differential equation for the inner conductor is

$$E_z(r) = AJ_0(k_1 r) + BN_0(k_1 r)$$

where constants A and B can be determined by the boundary conditions. On the z axis (r = 0) the electric field should be finite; this condition implies that B = 0, therefore,

$$E_z(r) = AJ_0(k_1 r) \quad .$$

On the surface of the cylinder at $r = a_1$ we have

$$E_z(a_1) = AJ_0(k_1 a_1)$$

or

$$A = \frac{E_z(a_1)}{J_0(k_1a_1)}$$

Substituting for A, the electric field inside the cylinder is

$$E_z(r) = E_z(a_1)\,\frac{J_0(k_1r)}{J_0(k_1a_1)} \qquad 0 \le r \le a_1$$

The current density on the cylinder becomes

$$J_z(r) = \sigma_1 E_z(r)$$

The total current in the cylinder is

$$I_z = \int_0^{a_1}\int_0^{2\pi} \sigma_1 E_z(r)\,r\,dr\,d\phi = \frac{2\pi a_1\sigma_1}{k_1}\,E_z(a_1)\,\frac{J_1(k_1a_1)}{J_0(k_1a_1)}$$

The definition of the surface impedance is the ratio of the electric field on the surface to the total current. For good conductors most of the current flows on the surface, therefore,

$$Z_1^i = \frac{E_z(a_1)}{I_z} = \frac{k_1}{2\pi a_1\sigma_1}\,\frac{J_0(k_1a_1)}{J_1(k_1a_1)} \quad .$$

The solution of the differential equation for $E_z(r)$ in the outer conductor is

$$E_z(r) = CH_0^{(1)}(k_2r) + DH_0^{(2)}(k_2r)$$

Boundary conditions for this region are:

(1) Electric field at infinity is $E_z(r \to \infty) \to 0$; this implies that C = 0. Therefore

$$E_z(r) = DH_0^{(2)}(k_2 r) \quad .$$

(2) At $r = a_3$ we have

$$E_z(a_3) = DH_0^{(2)}(k_2 a_3)$$

or

$$D = \frac{E_z(a_3)}{H_0^{(2)}(k_2 a_3)} \quad .$$

The electric field in region (2) is

$$E_z(r) = E_z(a_3) \frac{H_0^{(2)}(k_2 r)}{H_0^{(2)}(k_2 a_3)}$$

The current in this region is

$$I_z = \int_0^{2\pi} \int_{a_3}^{\infty} \sigma_2 E_z(a_3) \frac{H_0^{(2)}(k_2 r)}{H_0^{(2)}(k_2 a_3)} \, r dr d\phi = - \frac{2\pi a_3 \sigma_2}{k_2} E_z(a_3) \frac{H_1^{(2)}(k_2 a_3)}{H_0^{(2)}(k_2 a_3)}$$

The surface impedance for the outer conductor is then

$$Z_2^i = \frac{E_z(a_3)}{I_z} = - \frac{k_2}{2\pi a_3 \sigma_2} \frac{H_0^{(2)}(k_2 a_3)}{H_1^{(2)}(k_2 a_3)}$$

In the transmission line theory the external impedance is due to the interaction between the currents on the conductors of the line. The external impedance Z^e is defined as

$$Z^e = r^e + j\omega l^e .$$

For coaxial cables there is no radiation; therefore, r^e is zero and the external impedance becomes

$$Z^e = j\omega l^e$$

where

$$l^e = \frac{\mu}{2\pi} \ln(a_3/a_1) .$$

It is assumed that the insulated material is nonmagnetic ($\mu = \mu_0$), thus, we have

$$Z^e = j\omega \frac{\mu_0}{2\pi} \ln(a_3/a_1) .$$

The total impedance per unit length and the admittance per unit length of the probe have been defined for a general case. Now we will consider some special cases.

<u>Case (1)</u>. $|k_1 a_1| << 1$, $|k_2 a_3| << 1$

Small argument approximations for the first kind Bessel functions are

$$J_0(x) \doteq 1 - \left(\frac{x}{2}\right)^2$$

$$J_1(x) \doteq \frac{x}{2}\left\{1 - \frac{1}{2}\left(\frac{x}{2}\right)^2\right\}$$

With these approximations the surface impedance of the inner conductor is

$$Z_1^i = \frac{k_1}{2\pi a_1 \sigma_1} \frac{1 - \left(\frac{k_1 a_1}{2}\right)^2}{\frac{k_1 a_1}{2}\left[1 - \frac{1}{2}\left(\frac{k_1 a_1}{2}\right)^2\right]}$$

and $k_1 = \sqrt{-j\omega\mu\sigma_1}$. This leads to

$$Z_1^i = \frac{1}{\pi a_1^2 \sigma_1} + j\frac{\omega\mu}{8\pi}$$

Small argument approximations for Hankle functions are

$$H_0^{(2)}(x) \doteq 1 + j\,\frac{2}{\pi}\,\ln\frac{2}{\gamma x}$$

$$H_1^{(2)}(x) \doteq j\,\frac{2\pi}{x}$$

where $\gamma = 1.781$. The surface impedance of the outer conductor in this case can be written as

$$Z_2^i = -\frac{k_2}{2\pi a_3 \sigma_2} \frac{1 + j\,\frac{2}{\pi}\,\ln\frac{2}{\gamma k_2 a_3}}{j\,\frac{2}{\pi k_2 a_3}}$$

For $k_2 = \sqrt{-j\omega\mu\sigma_2}$, the surface impedance can be expressed as

$$Z_2^i = \frac{\omega\mu}{8} + j\,\frac{\omega\mu}{2\pi}\,\ln\frac{2}{\gamma a_3\,\sqrt{\omega\mu\sigma_2}}$$

<u>Case (2)</u>. $|k_1 a_1| >> 1$, $|k_2 a_3| >> 1$

The argument of Bessel functions are very large for this case and asymptotic approximations can be used. In this case the first kind of Bessel functions are

$$J_n(x) \cong \frac{2}{\pi x} \cos\left(x - \frac{n\pi}{2} + \frac{\pi}{4}\right) \qquad |x| >> 1$$

The surface impedance for the inner conductor then becomes

$$Z_1^i = j\,\frac{k_1}{2\pi a_1 \sigma_1}$$

For $k_1 = \sqrt{-j\omega\mu\sigma_1}$, the surface impedance on the inner conductor is

$$Z_1^i = \frac{1}{2\pi a_1}\sqrt{\frac{\omega\mu}{2\sigma_1}}\,(1 + j)$$

Asymptotic approximations for Hankle functions are

$$H_n^{(2)}(x) \doteq \sqrt{\frac{2}{\pi x}}\, e^{-j\left(x - \frac{n\pi}{2} - \frac{\pi}{4}\right)} \qquad |x| >> 1$$

The surface impedance of the outer conductor for this case can be expressed as

$$Z_2^i = j\,\frac{k_2}{2\pi a_3 \sigma_2}$$

For a good conductor, $k_2 = \sqrt{-j\omega\mu_2\sigma_2}$, and the surface impedance of the outer conductor becomes

$$Z_2^i = \frac{1}{2\pi a_3}\sqrt{\frac{\omega\mu_2}{2\sigma_2}}\,(1 + j)$$

The characteristic impedance of the line by definition is $Z_C = \frac{Z}{\gamma} = \sqrt{\frac{Z}{Y}}$, where

$$Z = r + jx, \quad Y = g + j\omega C .$$

Substituting for Z and Y, the characteristic impedance becomes

$$Z_C = \sqrt{\frac{r + jx}{g + j\omega C}}$$

The propagation constant of the line γ can be written as

$$\gamma = \alpha + j\beta = \sqrt{(r + jx)(g + j\omega C)}$$

Squaring both sides of the above equation and equating the real and imaginary parts of both sides, we have

$$\alpha = \left\{ \frac{1}{2}(rg - \omega xC) + \frac{1}{2}\left\{ (rg - \omega xC)^2 + (gx + \omega rC)^2 \right\}^{1/2} \right\}^{1/2}$$

$$\beta = \left\{ \frac{1}{2}(\omega xC - rg) + \frac{1}{2}\left\{ (rg - \omega xC)^2 + (gx + \omega rC)^2 \right\}^{1/2} \right\}^{1/2}$$

The propagation constant of a lossy coaxial line is tabulated in Table 5.1. The inner conductor of the line is copper and the outer conductor is lossy medium with $\varepsilon_{r2} = 69$ and $\frac{\sigma}{\omega\varepsilon_2} = 8.8$. In this table it is assumed that $\omega = 7.16 \times 10^8 \text{ sec}^{-1}$, $k_2 = 41.6\ (1 - j)$. Since the inner conductor is a very good conductor, the surface impedance of the inner conductor is very small. The surface impedance of the outer conductor and the external impedance of the line for various values of a_1 and a_3 are shown. α_{approx} and β_{approx} are taken from [19], but α_{exact} and β_{exact} are calculated numerically.

5.2.2. Terminal Impedances of the Probe, Z_{e1} and Z_{e2}

In Figure 5.5(a) a configuration of an insulated probe in a conducting medium is shown. In order to investigate the characteristics of the probe it is necessary to know the terminal impedances of the probe at plane AA (Z_{e1}) and at plane BB (Z_{e2}). At plane BB the equivalent terminal impedance is complicated. The current at this plane is not zero, therefore, this terminal impedance is not infinity. An equivalent circuit for the terminal AA is shown in Figure 5.5(b). In this figure when d = 0 the inner conductor is in direct contact with the outer conductor of the transmission line, or the conducting medium, therefore, Z_{e1} is very small.

For $d/(a_2 - a_1) << 1$ and $2\pi d/\lambda << 1$ we have [20]

$$\frac{B}{Y_C} = \frac{2a_1}{\lambda} \ln \frac{a_2}{a_1}\left(\frac{\pi}{4}\frac{a_1}{d} + \ln \frac{a_2 a_1}{d}\right) \qquad (5.2.1)$$

Table 5.1. Parameters of lossy coaxial cable.

a_1(cm)	0.3175	0.3175	0.3175	0.3175	0.635
a_2(cm)	0.3968	1.27	1.905	3.81	2.54
α_{approx}	3.5853	0.399	0.249	0.1137	0.270
β_{approx}	11.2248	3.05	2.758	2.530	2.7613
α_{exact}	1.2198	0.31869	0.21806	0.1078	0.2358
β_{exact}	7.0304	2.99816	2.7460	2.5291	2.7465
Z^e	j31.93	j198.4	j256.5	j355.67	j198.4
Z_2^i	96.1 + j237	66.5 + j111.3	53.7 + j80.2	33.9 + j43.2	45.11 + j62.6

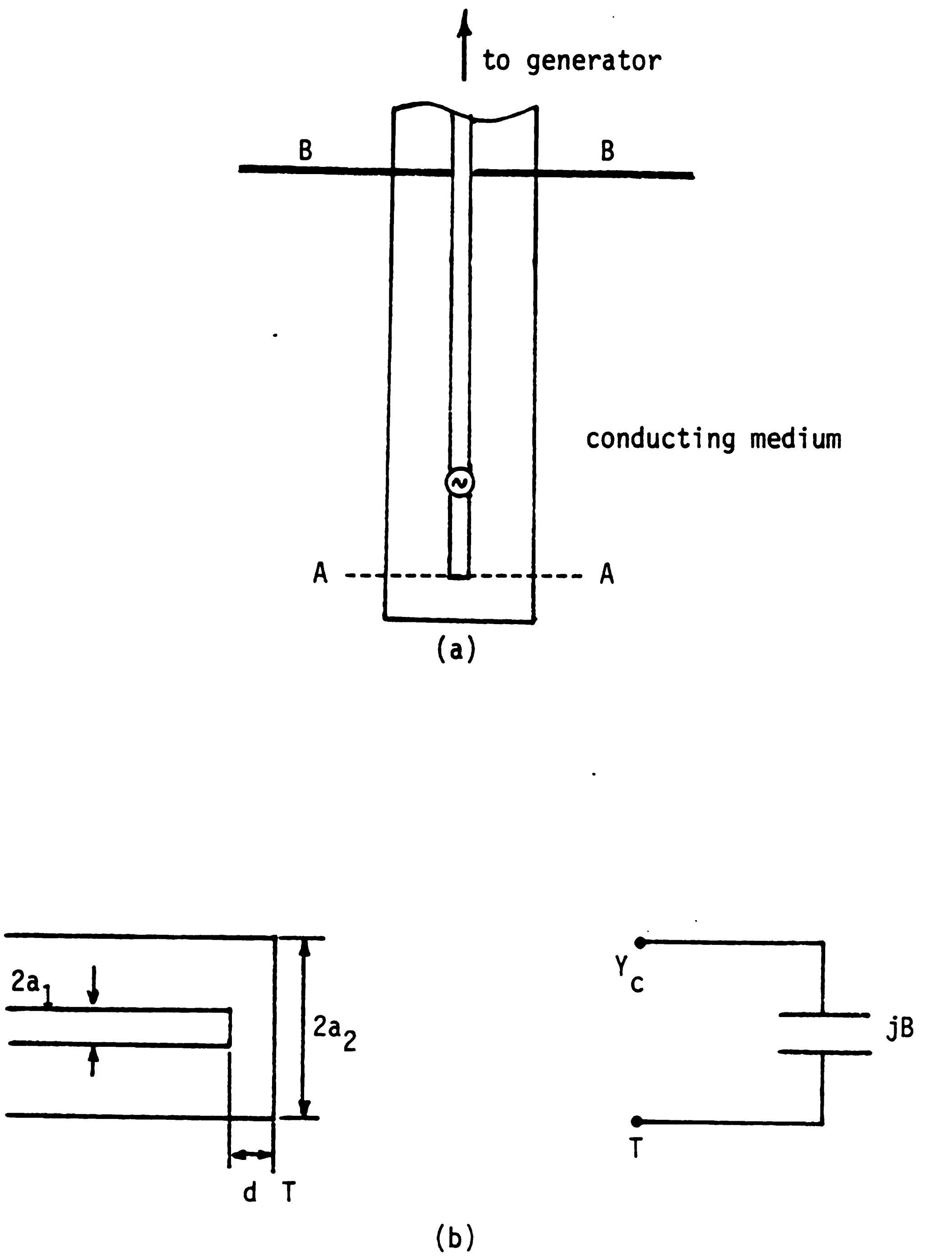

Figure 5.5. (a) Configuration of an insulated probe in a conducting medium.
(b) Equivalent circuit for terminal AA.

In the following example the terminal impedance (Z_{e1}) of an insulated probe is found.

Example: For an insulated probe with dimensions of $a_1 = 0.43$ mm, $a_2 = 0.96$ mm, d = 0.1 mm, and the dielectric material with $\sigma_d = 0$, $\varepsilon_{rd} = 2.45$, the terminal impedance (Z_{e1}) at 600 MHz frequency is

$$B = 0.0065\ Y_C$$

and

$$Z_{e1} = JB = j0.0065\ Y_C\ .$$

In our study the line is lossy, therefore, a conductance should be parallel with the capacitor in the equivalent circuit.

5.3.1. Input Impedance of the Probe

The input impedance of the insulated probe is a function of several parameters. It is a function of physical dimensions of the probe, the electrical properties of the conducting medium and the insulator, the terminal impedances, and the frequency of the operation.

In Figure 5.3(c) the current at the origin is

$$I_1(0) = I_2(0) = I(0)$$

but from equation (5.1.15) the current at Z = 0 is given as

$$I(0) = \frac{V_1}{Z_{C1}} \frac{\sinh\left[\gamma_1 h_1 + \theta_1\right]}{\cosh\left[\gamma_1 h_1 + \theta_1\right]} \tag{5.3.1}$$

Substituting for V_1 using (5.1.6) in (5.3.1), the current at the origin in

$I(0) =$

$$V\frac{\sinh(\gamma_1 h_1 + \theta_1)\sinh(\gamma_2 h_2 + \theta_2)}{Z_{C1}\cosh(\gamma_1 h_1 + \theta_1)\sinh(\gamma_2 h_2 + \theta_2) + Z_{C2}\sinh(\gamma_1 h_1 + \theta_1)\cosh(\gamma_2 h_2 + \theta_2)} \tag{5.3.2}$$

By definition the input impedance is $Zin = \frac{V}{I(0)}$, or

$Zin =$

$$\frac{Z_{C1}\cosh(\gamma_1 h_1 + \theta_1)\sinh(\gamma_2 h_2 + \theta_2) + Z_{C2}\sinh(\gamma_1 h_1 + \theta_1)\cosh(\gamma_2 h_2 + \theta_2)}{\sinh(\gamma_1 h_1 + \theta_1)\sinh(\gamma_2 h_2 + \theta_2)} \tag{5.3.3}$$

In this study it is assumed that both sections of the probe have the same diameters for inner and outer conductors, and the same dielectric material, therefore, the characteristic impedances $Z_{C1} = Z_{C2} = Z_C$ and the propagation constants $\gamma_1 = \gamma_2 = \gamma$. With these assumptions the input impedance can be written as

$$Zin = Z_C\frac{\cosh(\gamma h_1 + \theta_1)\sinh(\gamma h_2 + \theta_2) + \sinh(\gamma h_1 + \theta_1)\cosh(\gamma h_2 + \theta_2)}{\sinh(\gamma h_1 + \theta_1)\sinh(\gamma h_2 + \theta_2)} \tag{5.3.4}$$

The input impedance of the probe for three different cases of terminal impedances are considered as follows.

<u>Case (1)</u>. In this case it is assumed that both terminal impedances of the probe are infinity, $Z_{e1} = Z_{e2} = \infty$; this implies $\theta_1 = \theta_2 = \tanh^{-1} 0 = 0$. Substituting for θ_1 and θ_2 in (5.3.4), the input impedance of the probe becomes

$$Zin = Z_C \frac{\sinh [\gamma(h_1 + h_2)]}{\sinh [\gamma h_1] \sinh [\gamma h_2]} \quad . \tag{5.3.5}$$

For a symmetric probe, $h_1 = h_2 = h$, (5.3.5) becomes

$$Zin = 2Z_C \coth [\gamma h] \tag{5.3.6}$$

or

$$Zin = 2Z_C \frac{\sinh (2\alpha h) - j\sin (2\beta h)}{\cosh (2\alpha h) - \cos (2\beta h)}$$

If Z_C is pure resistive, for $\beta h = n\pi/2$, $n = 1, 2, 3, \ldots$ the input impedance of the probe becomes pure resistive.

In Figure 5.6 the input impedance of the insulated probe in a dissipative medium as a function of the probe length is shown. In this figure it is assumed that $h_1 = h_2$, $a_1 = a_2 = 0.47$ mm, $a_3 = 0.96$ mm, and the frequency of operation is 915 MHz. The electrical properties of the insulator and the conducting medium are $\sigma_d = 0.0$ (s/m), $\epsilon_{rd} = 1.37$ and $\sigma_2 = 0.88$ (s/m), $\epsilon_{r2} = 42.5$, respectively. For short insulated probes the input impedance is mostly capacitive; the same phenomenon is observed in an electrically short bare probe.

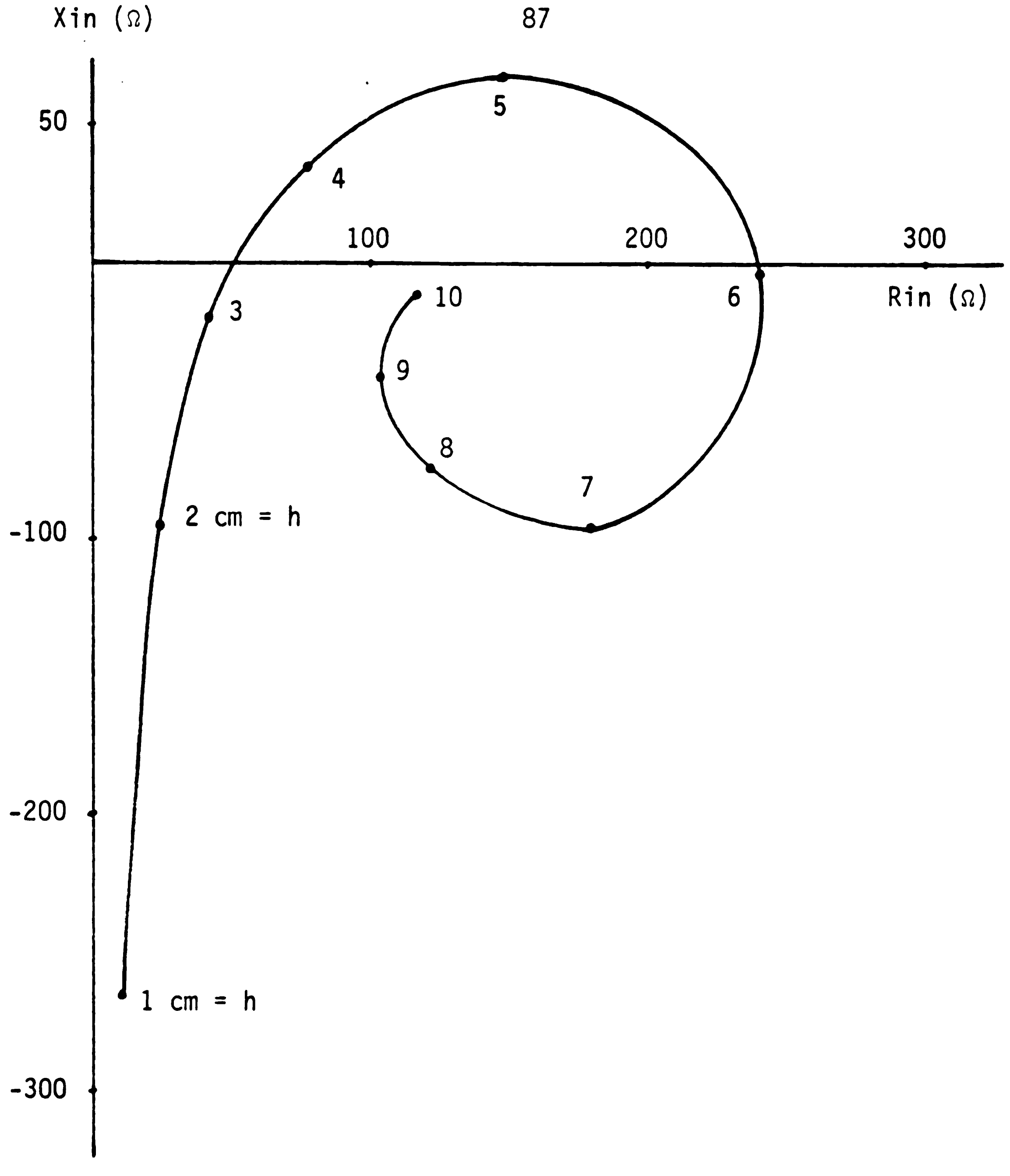

Figure 5.6. Input impedance Zin = Rin + jXin of symmetric insulated probes in a dissipative medium, $\gamma = 10.72 + j49.38$ and $Z_C = 70.77 - j15.36\ \Omega$. Both terminal impedances are assumed to be infinity.

<u>Case (2)</u>. In this case it is assumed that both terminal impedances are zero, $Z_{e1} = Z_{e2} = 0$, $\theta_1 = \theta_2 = \tanh^{-1} \infty = j\pi/2$. Substituting for θ_1 and θ_2 in (5.3.4), the input impedance of the probe becomes

$$Zin = Z_C \frac{\sinh [\gamma(h_1 + h_2]}{\cosh [\gamma h_1] \cosh [\gamma h_2]} \qquad (5.3.7)$$

For a symmetric insulated probe $h_1 = h_2 = h$, the input impedance can be expressed as

$$Zin = 2Z_C \tanh [\gamma h] \qquad (5.3.8)$$

or

$$Zin = 2Z_C \frac{\sinh (2\alpha h) + j\sin (2\beta h)}{\cosh (2\alpha h) + \cos (2\beta h)}$$

With the assumption that Z_C is pure resistive, for $\beta h = n\pi/2$, $n = 1, 2, \ldots$ the input impedance of the insulated probe is pure resistive. Figure 5.7 shows the input impedance of the insulated probe in a lossy medium as a function of the probe length. The terminal impedances of the probe Z_{e1} and Z_{e2} are assumed to be zero. The physical dimensions of the probe and the electrical properties of the insulator and the lossy medium are the same as in case (1).

In this case for an electrically short probe the input impedance is not mostly capacitive, and the input resistance is larger than the input resistance of case (1).

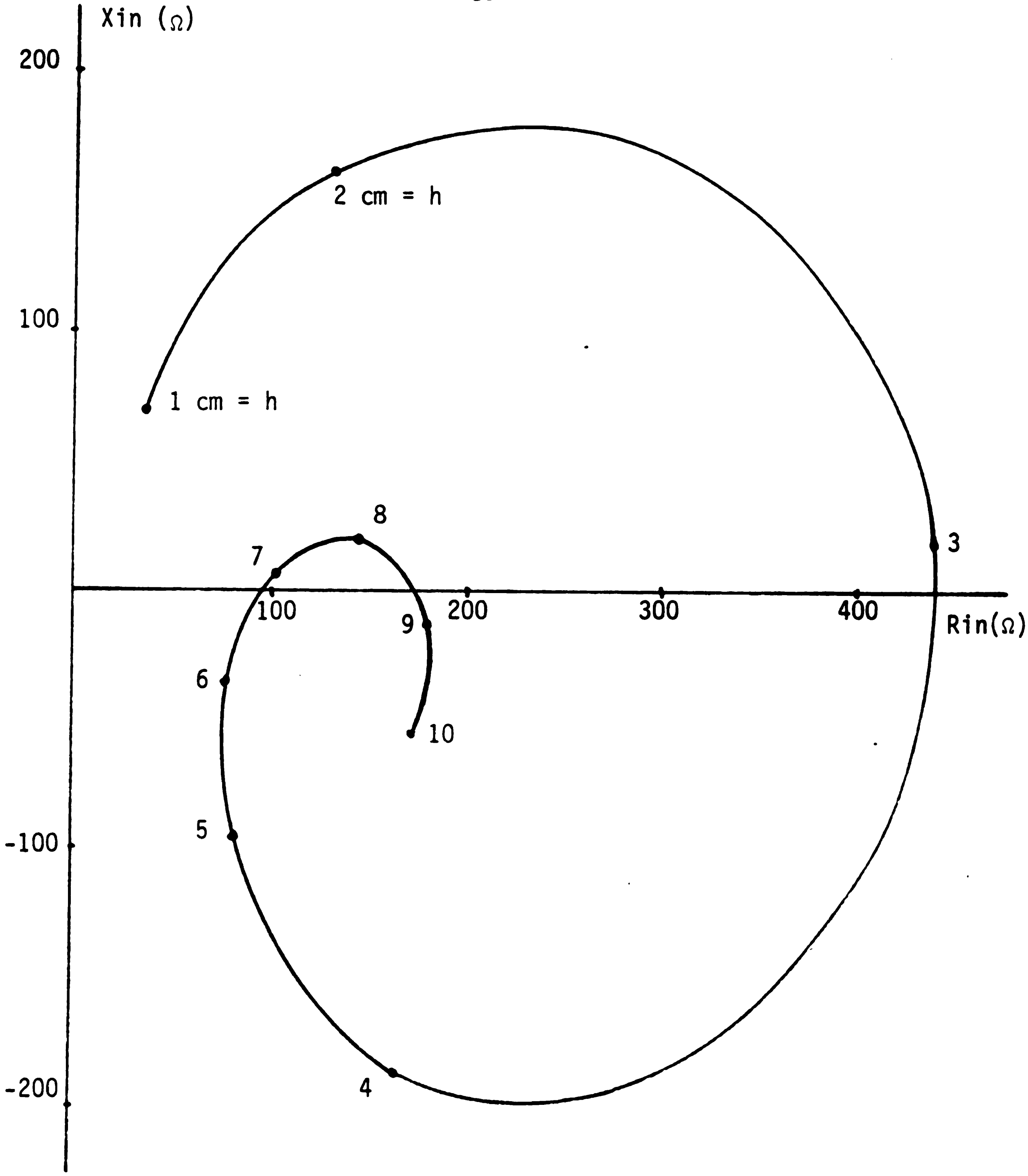

Figure 5.7. Input impedance Zin = Rin + jXin of symmetric insulated probes in a dissipative medium, γ = 10.72 + j49.38 and Z_C = 70.77 - j15.36 Ω. Both terminal impedances are assumed to be zero.

<u>Case (3)</u>. In this case it is assumed that one of the terminal impedances is zero and the other infinity.

(a). The terminal impedances $Z_{e1} = 0$ and $Z_{e2} = \infty$. Substituting for θ_1 and θ_2 in (5.3.4), the input impedance of the probe becomes

$$Zin = Z_C \frac{\cosh [\gamma(h_1 + h_2)]}{\cosh [\gamma h_1] \sinh [\gamma h_2]} \tag{5.3.9}$$

(b). The terminal impedances $Z_{e1} = \infty$ and $Z_{e2} = 0$. The input impedance of the probe is

$$Zin = Z_C \frac{\cosh [\gamma(h_1 + h_2)]}{\sinh [\gamma h_1] \cosh [\gamma h_2]} \tag{5.3.10}$$

Now consider a symmetric probe with $h_1 = h_2 = h$. The input impedance of the probe becomes

$$Zin = 2Z_C \coth [2\gamma h] \tag{5.3.11}$$

or

$$Zin = 2Z_C \frac{\sinh [4\alpha h] - j\sin (4\beta h)}{\cosh [4\alpha h] - \cos (4\beta h)}$$

For $\beta h = n\pi/4$, $n = 1, 2, 3, \ldots$ the impedance of the probe is pure resistive (Z_C is a pure resistance).

In Figure 5.8 the input impedance of the insulated probes with the terminal impedances of one zero and the other infinity are shown. In this figure the dimensions of the probe and the

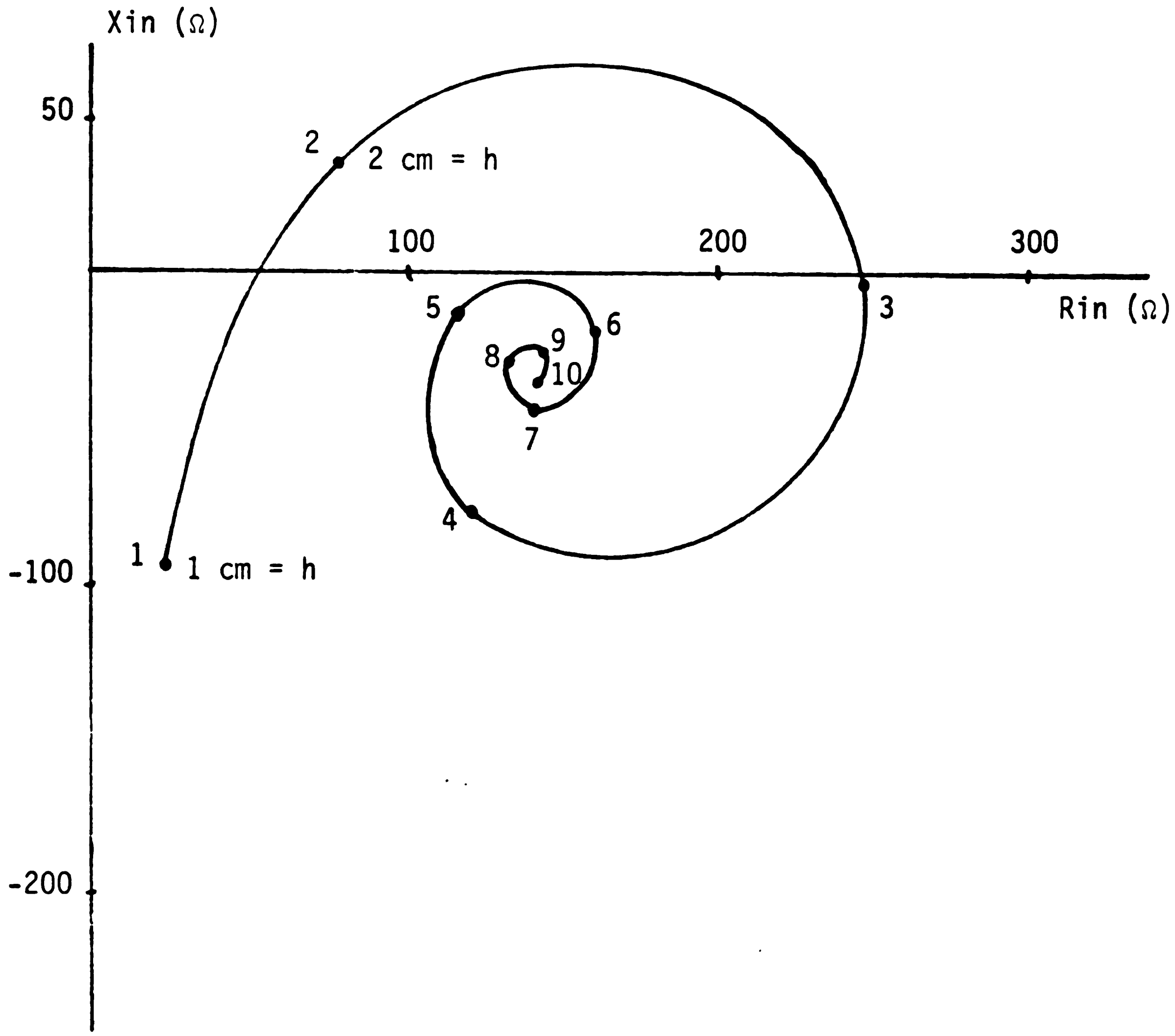

Figure 5.8. Input impedance Zin = Rin + jXin of symmetric insulated probes in a dissipative medium, γ = 10.72 + j49.38 and Z_C = 70.77 - j15.36 Ω. Terminal impedances Z_{e1} = 0 and Z_{e2} = ∞.

electrical properties of the insulator and the conducting medium are kept the same as that in case (1).

The input impedance of the insulated probe is a function of the electrical properties of the insulator. In Figure 5.9 the input impedance of the probe versus the dielectric constant of the insulator is shown. Both terminal impedances of the probe are assumed infinity in this figure. Physical dimensions of the probe are $a_1 = a_2 = 0.43$ mm, $h_1 = 15$ mm, $h_2 = 45$ mm, and the frequency of operation is 600 MHz. The probe is immersed in a conducting medium with $\sigma = 1.86$ (s/m), $\varepsilon_r = 76.3$, and the insulator has $\sigma_d = 0$ and a variable permittitivity. Changes in the input reactance is more significant than the input resistance of the probe.

For an electrically short and thin insulated probe in a dissipative medium we have

$$\alpha h << 1, \ \beta h << 1, \ a_3 << h$$

and the input admittance of the probe has been found [11] to be

$$Yin \doteq G + j\omega C = \frac{\sigma\pi h}{\ln(h/a_3) - 1} \frac{\gamma^2}{p^2 + (1+\gamma)^2}$$
$$+ j\omega \frac{\varepsilon_d \pi h}{\ln(a_3/a_2)} \frac{p^2 + (1+\gamma)}{p^2 + (1+\gamma)^2} \tag{5.3.12}$$

where

$$P = \frac{\sigma}{\omega\varepsilon_0\varepsilon_r} \quad \text{and} \quad \gamma = \frac{\varepsilon_{rd}}{\varepsilon_r} \frac{\ln(h/a_3) - 1}{\ln(a_3/a_2)}$$

The input admittance of the insulated probe obtained from (5.3.12) and that from the theory developed in this study are compared in Table 5.2. The input susceptances are in good agreement, but there are some deviations in the input conductances. Mostly the deviations in the input conductances come from the fact that the theory developed in this study is not accurate for short insulated probes. In this table the probe is symmetric with $h_1 = h_2 = 15$ mm, $a_1 = a_2 = 0.43$ mm. The electrical properties of the insulator are $\sigma_d = 0.0$ (s/m), $\varepsilon_{rd} = 2.25$, and the electrical properties of the conducting medium are variable.

In Figure 5.10 the input impedance of the insulated probe with three different terminal impedances are compared with input impedance of a bare probe. The dimensions of the probes are: $a_1 = a_2 = 0.43$ mm, $h_1 = 15$ mm, $h_2 = 45$ mm, and the frequency of operation is 600 MHz. The electrical properties of the insulator are $\sigma_d = 0$ (s/m), $\varepsilon_{rd} = 2.25$, and the probes are immersed in the saline with various normalities. The input resistances of the bare probe and the insulated probe with terminal impedances $Z_{e1} = Z_{e2} = \infty$ are very close, but their input reactances are different.

So far it is assumed that both sections of the probe have the same radius ($a_1 = a_2$). Now we consider the case with $a_1 \neq a_2$, and find the input impedance of the insulated probe. In Table 5.3 the input impedances of the insulated probes with $a_1 = a_2$ and $a_1 \neq a_2$ are compared. The input resistances are very close in two different cases, but there is a constant shift in the input reactance.

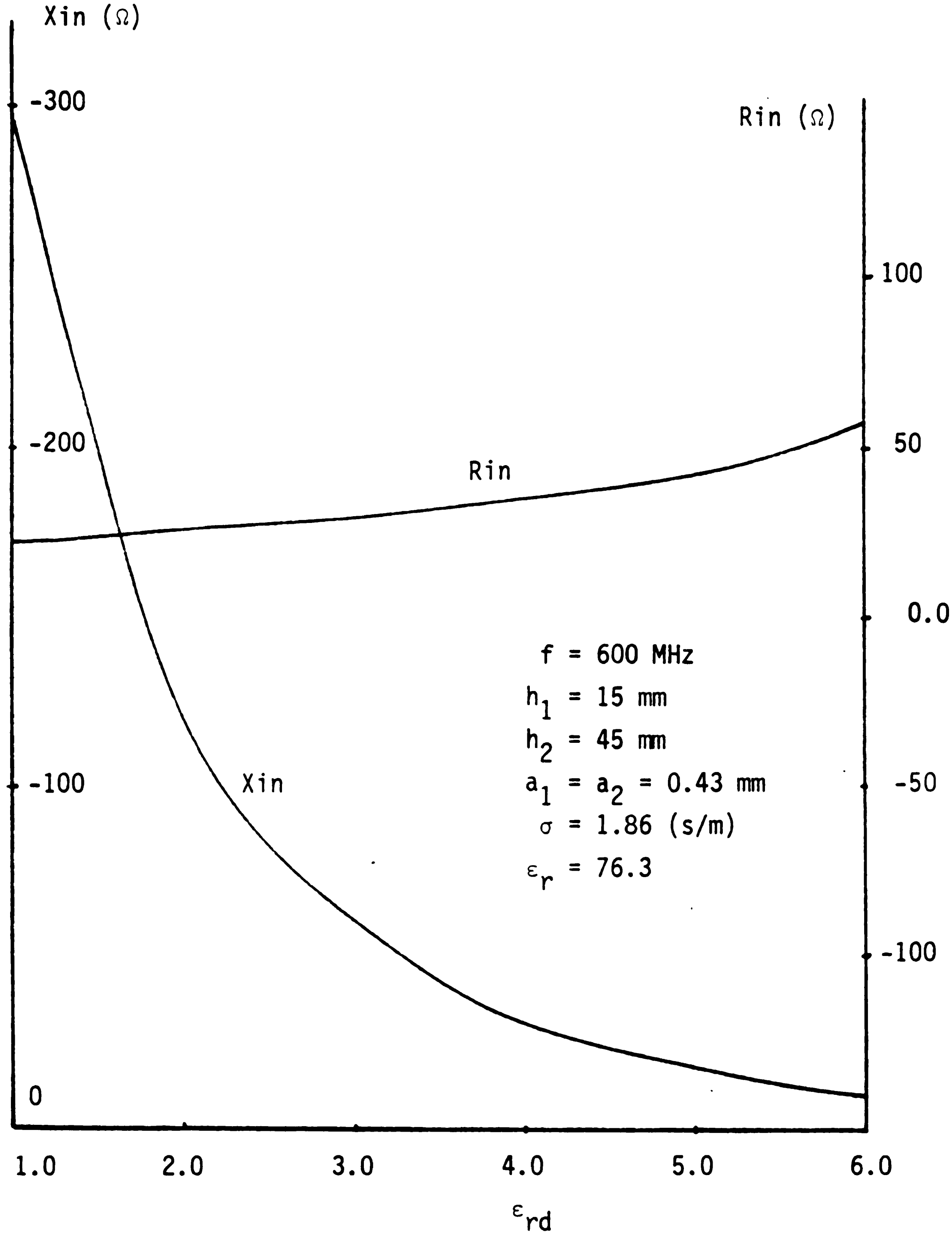

Figure 5.9. Input impedance Zin = Rin + jXin of the insulated probe in a conducting medium versus permittivity of the insulator. Terminal impedances $Z_{e1} = Z_{e2} = \infty$.

Table 5.2. Input admittance of the electrically short and thin insulated probe in a conducting medium.

Frequency	$P = \frac{\sigma}{\omega\varepsilon}$	Yin (Theory) $\times 10^{-6}$	Yin (Formula) $\times 10^{-6}$
10 MHz	25.84	0.0005 + j73.3	0.18 + j73.3
10 MHz	52.94	0.0005 + j73.3	0.091 + j73.3
10 MHz	80.63	0.0005 + j73.3	0.06 + j73.3
10 MHz	109.73	0.0005 + j73.3	0.046 + j73.3
100 MHz	2.85	0.66 + j736.4	15.3 + j726.4
100 MHz	5.32	0.60 + j736.4	8.7 + j731.4
100 MHz	8.06	0.57 + j736.4	6.0 + j732.3
100 MHz	10.97	0.56 + j735.8	4.55 + j732.6

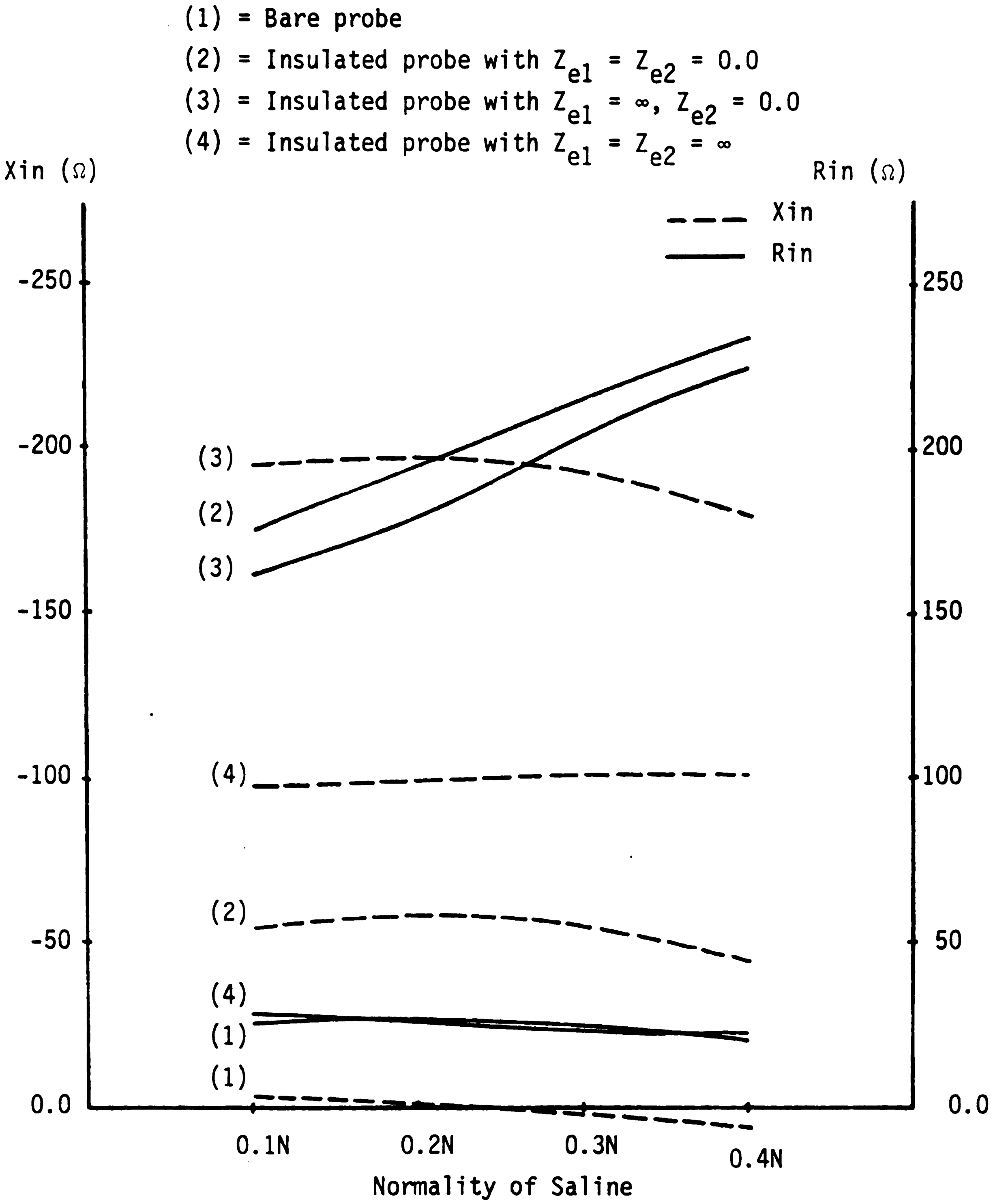

Figure 5.10. Comparison of the input impedance Zin = Rin + jXin of the bare probe with insulated probes with different terminal impedances.

Table 5.3. Input impedance.

$P = \frac{\sigma}{\omega\varepsilon}$	Terminal Impedances	$a_1 = a_2 = 0.43$ mm	$a_1 = 0.1$ mm, $a_2 = 0.43$ mm	Difference (in reactance)
0.73	$Z_{e1} = 0,\ Z_{e2} = 0$	189.8 - j58.7	188.2 - j42.5	-16.2
0.73	$Z_{e1} = \infty,\ Z_{e2} = 0$	177.6 - j198	177.6 - j399.2	201.2
0.73	$Z_{e1} = \infty,\ Z_{e2} = \infty$	25.8 - j99	25.7 - j299.8	200.8
1.91	$Z_{e1} = 0,\ Z_{e2} = 0$	238.3 - j41.9	237.2 - j25.7	-16.2
1.91	$Z_{e1} = \infty,\ Z_{e2} = 0$	228.8 - j179.7	228.8 - j380.5	200.8
1.91	$Z_{e1} = \infty,\ Z_{e2} = \infty$	19.9 - j102.5	19.9 - j303.4	200.9
3.68	$Z_{e1} = 0,\ Z_{e2} = 0$	266.9 + j8.3	266.1 + j26.4	-18.1
3.68	$Z_{e1} = \infty,\ Z_{e2} = 0$	258.9 - j127.6	258.9 - j328.5	200.9
3.68	$Z_{e1} = \infty,\ Z_{e2} = \infty$	16.7 - j106.4	16.7 - j307.2	200.8

The shift in the reactance is due to the change in the admittance per unit length of the transmission line. The admittance per unit length is $Y = g + j\omega C$, where g and C are inversely proportional to the $\ln(a_3/a_2)$. In this case g is zero, since $\sigma_d = 0$, and only C is affected.

5.3.2. Experimental Verification of the Theory

In order to test the theory developed in this study, a series of experiments were conducted to measure the input impedance of the insulated probes with various terminal impedances in different conducting media. To realize the terminal impedance of the probe $Z_{e2} = \infty$ in practice is very difficult, but the terminal impedance Z_{e1} can be made very large. In Figure 5.11(a), since the probe is in direct contact with the conducting medium (the outer conductor) the terminal impedances of the probe, Z_{e1} and Z_{e2}, are very small. On the other hand, in Figure 5.11(b) the terminal impedance Z_{e2} is again small but the terminal impedance Z_{e1} is very large. The experiments were carried out only for these two cases.

The measurement was conducted by the vector voltmeter, and the conducting medium was saline. The experimental procedures have been explained in more detail in Chapter III. In Figures 5.12-5.15 the physical dimensions of the probe are $a_1 = a_2 = 0.43$ mm, $a_3 = 0.96$ mm, $h_1 = 15$ mm, and $h_2 = 45$ mm. In Figures 5.12-5.15 the theoretical values and the experimental results of the input resistances and the input reactances of the insulated probes are compared. The terminal impedances in Figures 5.12 and 5.13 are

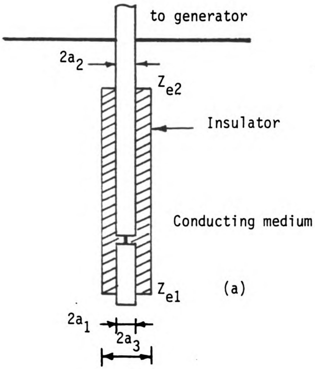

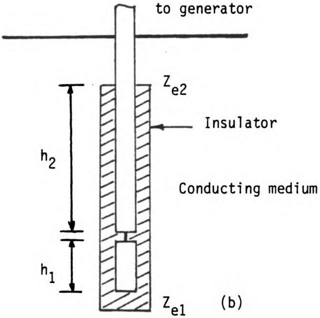

Figure 5.11. Configurations of insulated probes.
(a) Terminal impedances Z_{e1} and Z_{e2} very small.
(b) Z_{e1} very large and Z_{e2} very small.

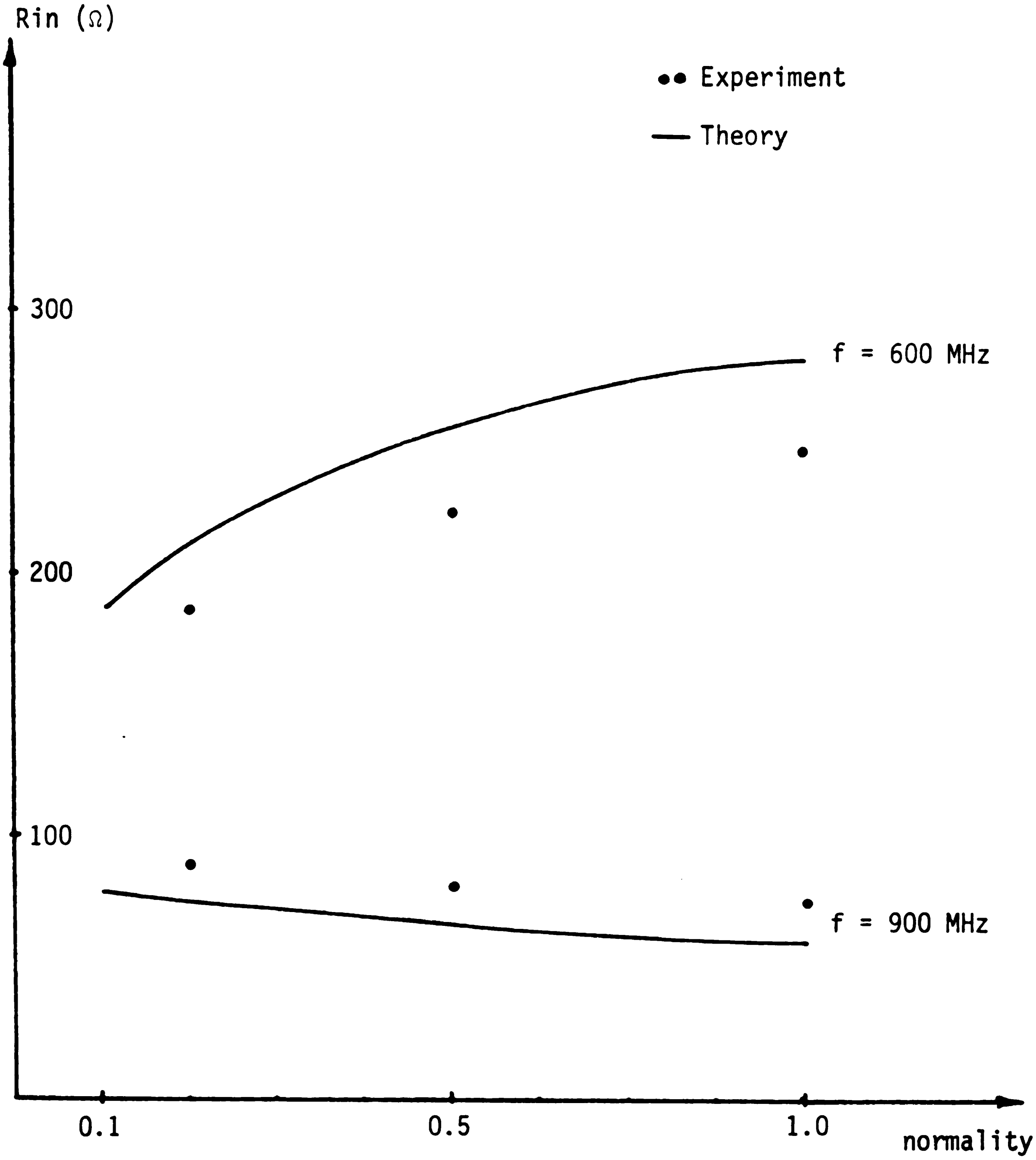

Figure 5.12. Comparison of theoretical and experimental results on the input resistance of an insulated probe with terminal impedances $Z_{e1} = 0.0$, $Z_{e2} = 0.0$ in various conducting media.

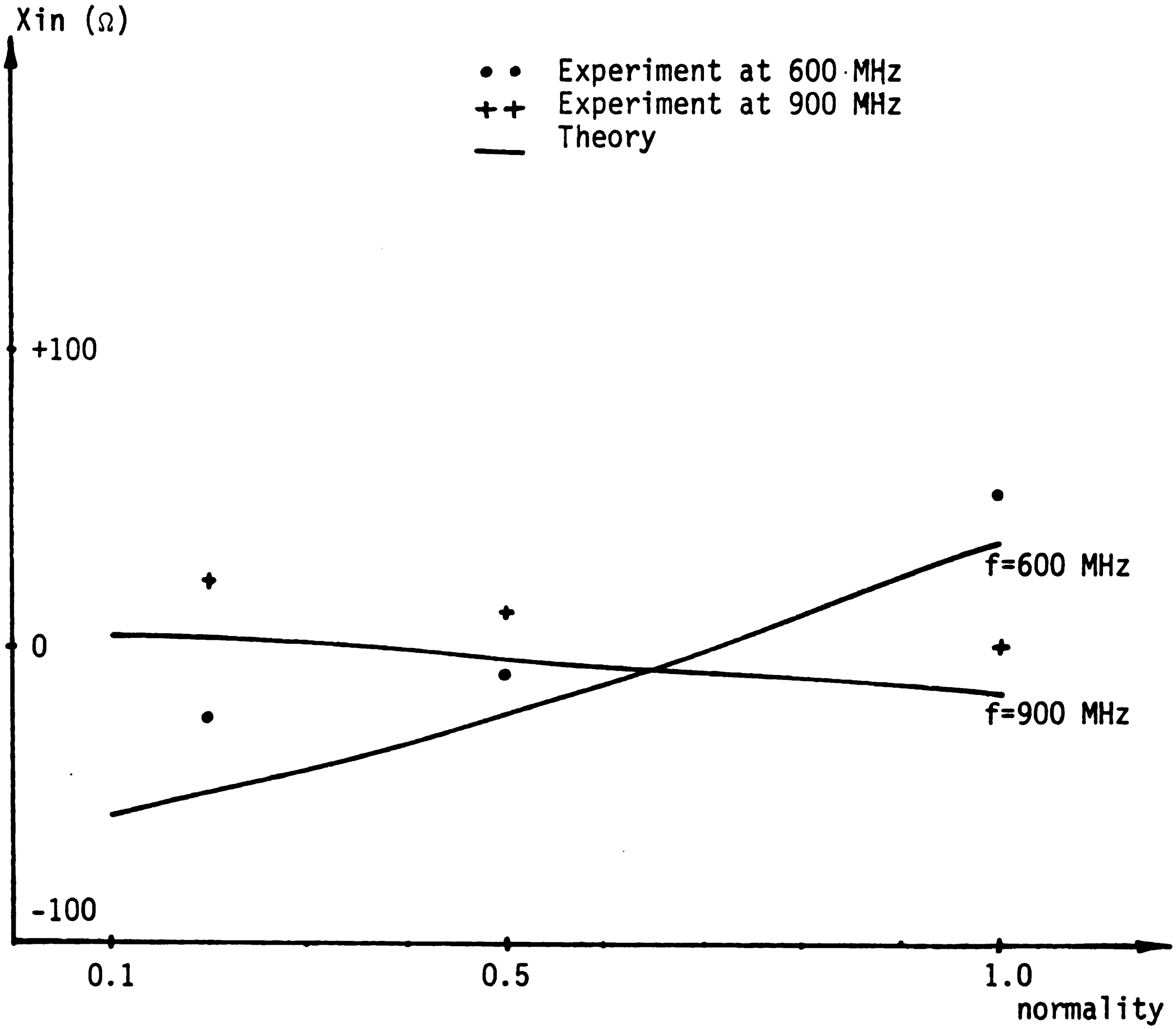

Figure 5.13. Comparison of theoretical and experimental results on the input reactance of an insulated probe with terminal impedances $Z_{e1} = 0.0$, $Z_{e2} = 0.0$ in various conducting media.

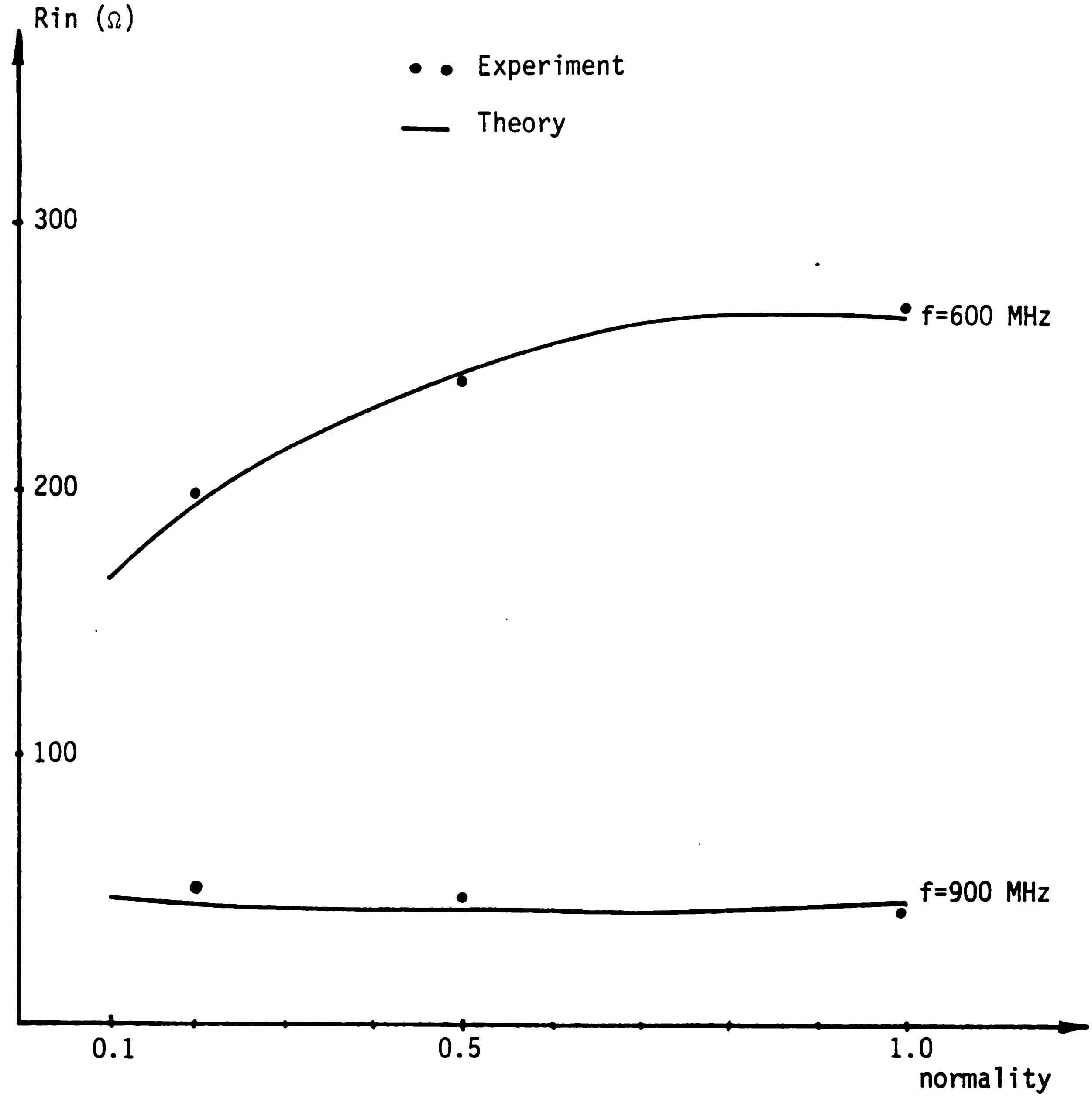

Figure 5.14. Comparison of theoretical and experimental results on the input resistance of an insulated probe with terminal impedances $Z_{e1} = \infty$, $Z_{e2} = 0.0$ in various conducting media.

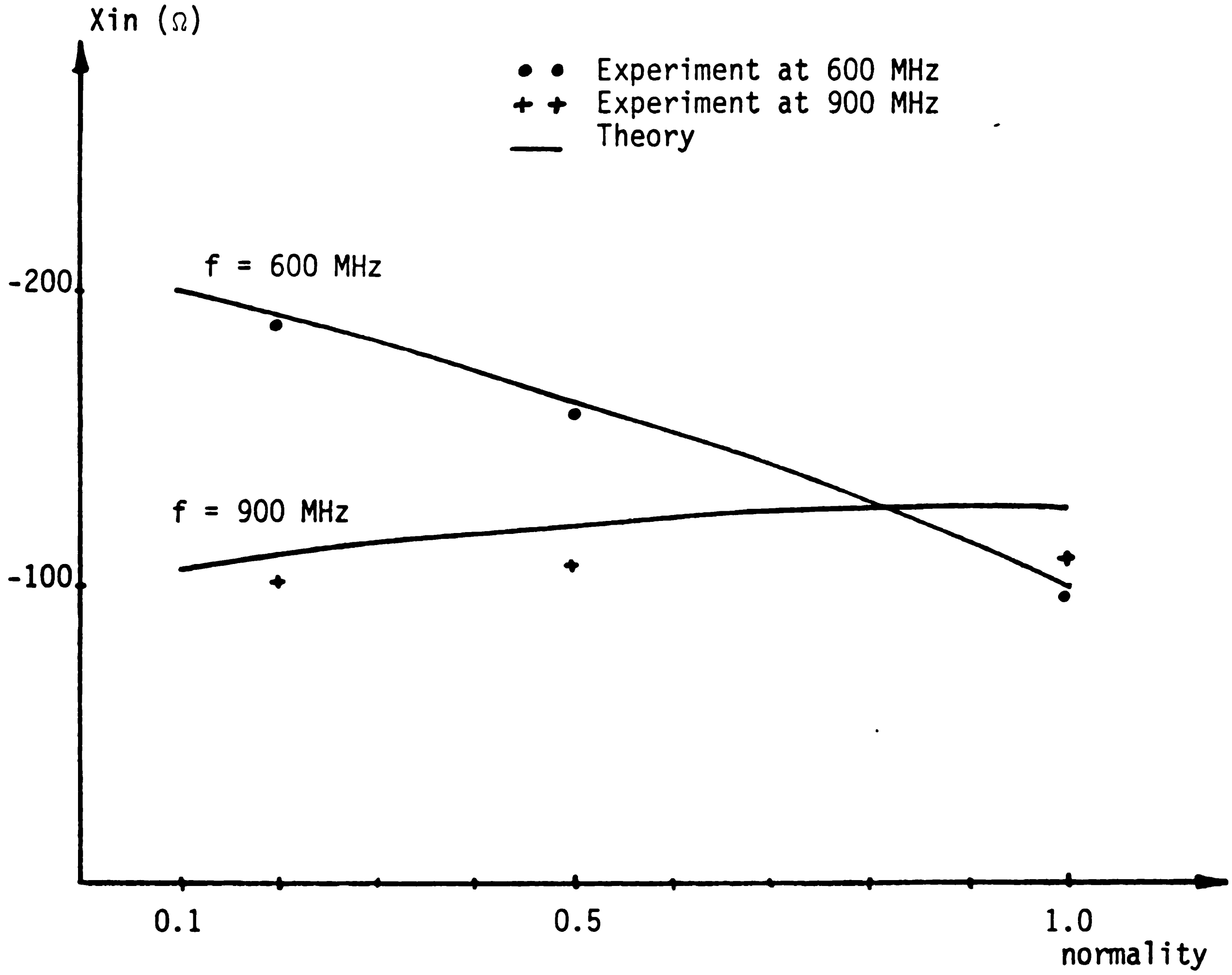

Figure 5.15. Comparison of theoretical and experimental results on the input reactance of an insulated probe with terminal impedances $Z_{e1} = \infty$, $Z_{e2} = 0.0$ in various conducting media.

assumed to be $Z_{e1} = 0$ and $Z_{e2} = 0$, but in Figures 5.14 and 5.15 the terminal impedances are $Z_{e1} = \infty$ and $Z_{e2} = 0$. From these results it is observed that the agreement between theory and experiment is very good for the case of $Z_{e1} = \infty$ and $Z_{e2} = 0$, and for the case of $Z_{e1} = 0$, $Z_{e2} = 0$ the agreement is still considered to be satisfactory. These results confirm the validity of the theory developed for the insulated probe in this chapter.

5.4.1. Current Distributions Along the Insulated Probe

The current along each section of the probe can be found by substituting for V_1 and V_2 in (5.1.15) and (5.1.17) using (5.1.6). The current can be expressed as

$$I_1(Z) =$$

$$V \frac{\sinh(\gamma_2 h_2 + \theta_2)\sinh[(\gamma_1 h_1 + \theta_1) - \gamma_1 Z]}{Z_{C1}\cosh(\gamma_1 h_1 + \theta_1)\sinh(\gamma_2 h_2 + \theta_2) + Z_{C2}\sinh(\gamma_1 h_1 + \theta_1)\cosh(\gamma_2 h_2 + \theta_2)}$$

$$0 \le Z \le h_1 \qquad (5.4.1)$$

and

$$I_2(Z) =$$

$$V \frac{\sinh(\gamma_1 h_1 + \theta_1)\sinh[(\gamma_2 h_2 + \theta_2) + \gamma_2 Z]}{Z_{C1}\cosh(\gamma_1 h_1 + \theta_1)\sinh(\gamma_2 h_2 + \theta_2) + Z_{C2}\sinh(\gamma_1 h_1 + \theta_1)\cosh(\gamma_2 h_2 + \theta_2)}$$

$$-h_2 \le Z \le 0 \qquad (5.4.2)$$

If we assume both sections of the probe to have the same radius ($a_1 = a_2$) and the same dielectric material, then $Z_{c1} = Z_{c2} = Z_c$ and $\gamma_1 = \gamma_2 = \gamma$. Equations (5.4.1) and (5.4.2) can be simplified to

$$I_1(Z) = \frac{V}{Z_c} \frac{\sinh(\gamma h_2 + \theta_2) \sinh[(\gamma h_1 + \theta_1) - \gamma Z]}{\sinh[\gamma(h_1 + h_2)]} \qquad (5.4.3)$$

$$0 \leq Z \leq h_1$$

and

$$I_2(Z) = \frac{V}{Z_c} \frac{\sinh(\gamma h_1 + \theta_1) \sinh[(\gamma h_2 + \theta_2) + \gamma Z]}{\sinh[\gamma(h_1 + h_2)]} \qquad (5.4.4)$$

$$-h_2 \leq Z \leq 0$$

The current along the probe for different terminal impedances is found as follows.

Case (1). In this case $Z_{e1} = Z_{e2} = \infty$, $\theta_1 = \theta_2 = 0$. Substituting for θ_1 and θ_2 in (5.4.3) and (5.4.4), the current along each section of the probe becomes

$$I_1(Z) = \frac{V}{Z_c} \frac{\sinh[\gamma h_2] \sinh[\gamma h_1 - \gamma Z]}{\sinh[\gamma(h_1 + h_2)]} \qquad (5.4.5)$$

$$0 \leq Z \leq h_1$$

and

$$I_2(Z) = \frac{V}{Z_c} \frac{\sinh[\gamma h_1] \sinh[\gamma h_2 + \gamma Z]}{\sinh[\gamma(h_1 + h_2)]} \qquad (5.4.6)$$

$$-h_2 \leq Z \leq 0$$

For a symmetric insulated probe $h_1 = h_2 = h$, the current along the probe can be further simplified to

$$I(Z) = \frac{V}{2Z_c} \frac{\sinh [\gamma(h - |Z|)]}{\cosh (\gamma h)} \qquad -h \leq Z \leq h \qquad (5.4.7)$$

In Figure 5.16, the current distributions along the insulated probe with the terminal impedances $Z_{e1} = Z_{e2} = \infty$ are shown. In this figure it is assumed that $a_1 = a_2 = 0.43$ mm, $a_3 = 0.96$ mm, $h_1 = 15$ mm, and h_2 is variable. The electrical properties of the insulator and the conducting medium are $\sigma_d = 0$, $\varepsilon_{rd} = 2.25$, $\sigma_2 = 1.1$, $\varepsilon_{r2} = 76.7$.

The current at the tips of the probes are zero due to infinite terminal impedances. It is observed that the current does not decay along the probe, and for the short probe $h_1 = h_2 = 15$ mm, the current has a triangular distribution which is similar to the current distributions along a short bare probe.

Case (2). Both terminal impedances are zero, $Z_{e1} = Z_{e2} = 0$, implying $\theta_1 = \theta_2 = \frac{j\pi}{2}$. Substituting for θ_1 and θ_2 in (5.4.3) and (5.4.4), the current distribution along each section of the probe is

$$I_1(Z) = \frac{V}{Z_c} \frac{\cosh (\gamma h_2) \cosh [\gamma(h_1 - Z)]}{\sinh [\gamma(h_1 + h_2)]} \qquad (5.4.8)$$

$$0 \leq Z \leq h_1$$

and

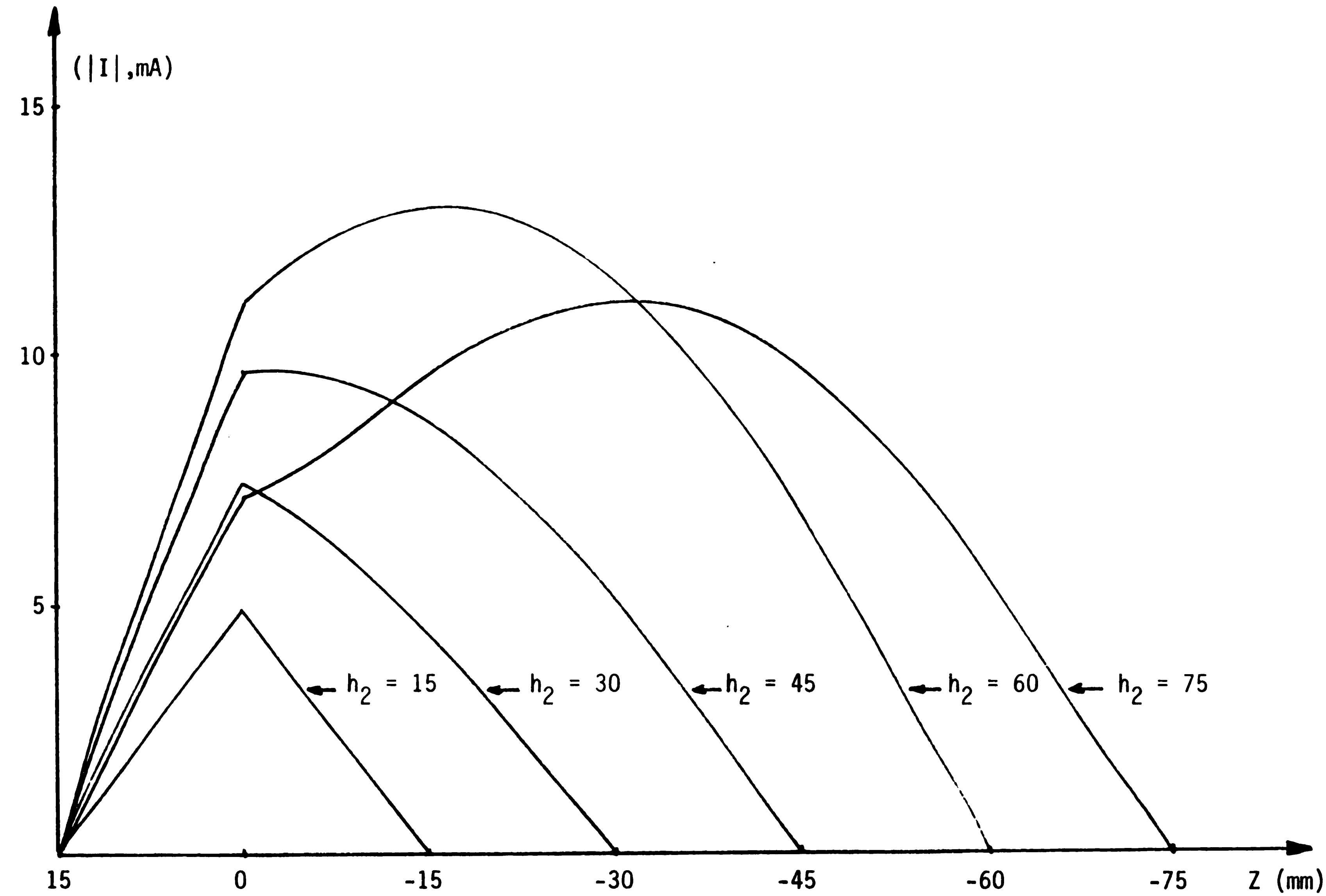

Figure 5.16. Current distributions along insulated probes with terminal impedances $Z_{e1} = Z_{e2} = \infty$, h_1 = 15 mm and h_2 is variable. The frequency is 600 MHz.

$$I_2(Z) = \frac{V}{Z_c} \frac{\cosh(\gamma h_1) \cosh[\gamma(h_2 + Z)]}{\sinh[\gamma(h_1 + h_2)]} \tag{5.4.9}$$

$$-h_2 \le Z \le 0$$

For a symmetric probe, $h_1 = h_2 = h$, the current along the probe is simplified to

$$I(Z) = \frac{V}{2Z_c} \frac{\cosh[\gamma(h - |Z|)]}{\sinh(\gamma h)} \qquad -h_2 \le Z \le h_1 \tag{5.4.10}$$

The current distributions along the probes with terminal impedances of $Z_{e1} = Z_{e2} = 0$ are shown in Figure 5.17. The physical dimensions of the probes and the electrical properties of the insulator and the conducting medium are the same as that for Figure 5.16. On the tips of the probe the current is very large because the terminal impedances are assumed to be zero.

Case (3). In this case one of the terminal impedances is zero and the other is infinity.

(a). The terminal impedances are $Z_{e1} = \infty$ and $Z_{e2} = 0$ corresponding to $\theta_1 = 0$ and $\theta_2 = \frac{j\pi}{2}$. Substituting for θ_1 and θ_2 in (5.4.3) and (5.4.4), the current along each section of the probe is

$$I_1(Z) = \frac{V}{Z_c} \frac{\cosh(\gamma h_2) \sinh[\gamma(h_1 - Z)]}{\cosh[\gamma(h_1 + h_2)]} \tag{5.4.11}$$

$$0 \le Z \le h_1$$

and

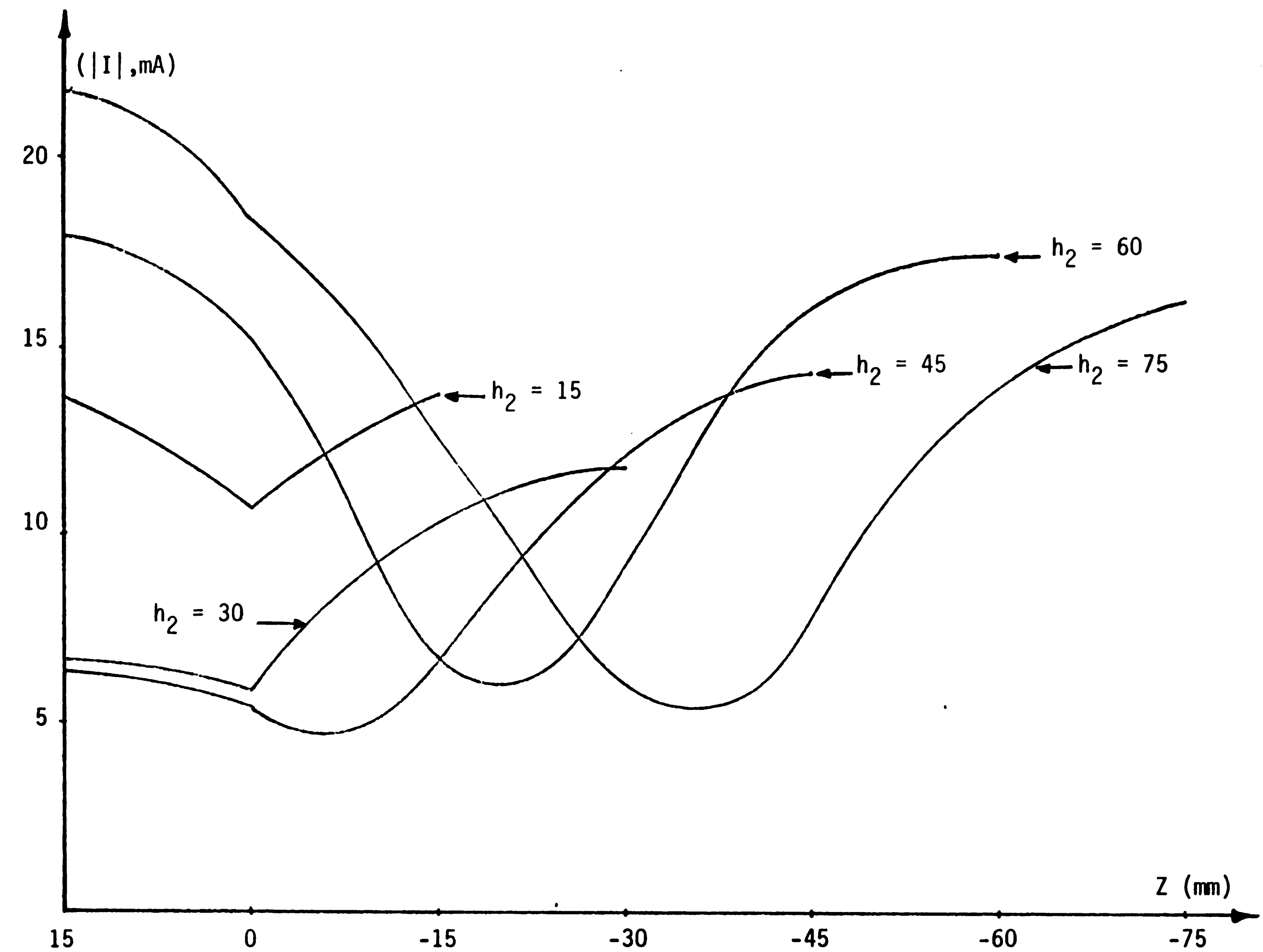

Figure 5.17. Current distributions along insulated probes with terminal impedances $Z_{e1} = Z_{e2} = 0.0$, h_1 = 15 mm and h_2 is variable. The frequency is 600 MHz.

$$I_2(Z) = \frac{V}{Z_c} \frac{\sinh(\gamma h_1) \cosh[\gamma(h_2 + Z)]}{\cosh[\gamma(h_1 + h_2)]} \tag{5.4.12}$$

$$-h_2 \leq Z \leq 0$$

For a symmetric insulated probe, $h_1 = h_2 = h$, the current in each section of the probe becomes

$$I_1(Z) = \frac{V}{Z_c} \frac{\cosh(\gamma h) \sinh[\gamma(h - |Z|)]}{\cosh(2\gamma h)} \tag{5.4.13}$$

$$0 \leq Z \leq h$$

and

$$I_2(Z) = \frac{V}{Z_c} \frac{\sinh(\gamma h) \cosh[\gamma(h - |Z|)]}{\cosh(2\gamma h)} \tag{5.4.14}$$

$$-h_2 \leq Z \leq 0$$

In Figure 5.18, the current distributions along the insulated probes are shown. The current at the tip with infinite terminal impedance is zero and at the tip with zero terminal impedance the current is very large.

(b). The terminal impedances are $Z_{e1} = 0.0$ and $Z_{e2} = \infty$ corresponding to $\theta_1 = \frac{j\pi}{2}$ and $\theta_2 = 0.0$. Substituting for θ_1 and θ_2 in (5.4.3) and (5.4.4), the current along each section of the probe is

$$I_1(Z) = \frac{V}{Z_c} \frac{\sinh(\gamma h_2) \cosh[\gamma(h_1 - Z)]}{\cosh[\gamma(h_1 + h_2)]} \tag{5.4.15}$$

$$0 \leq Z \leq h_1$$

and

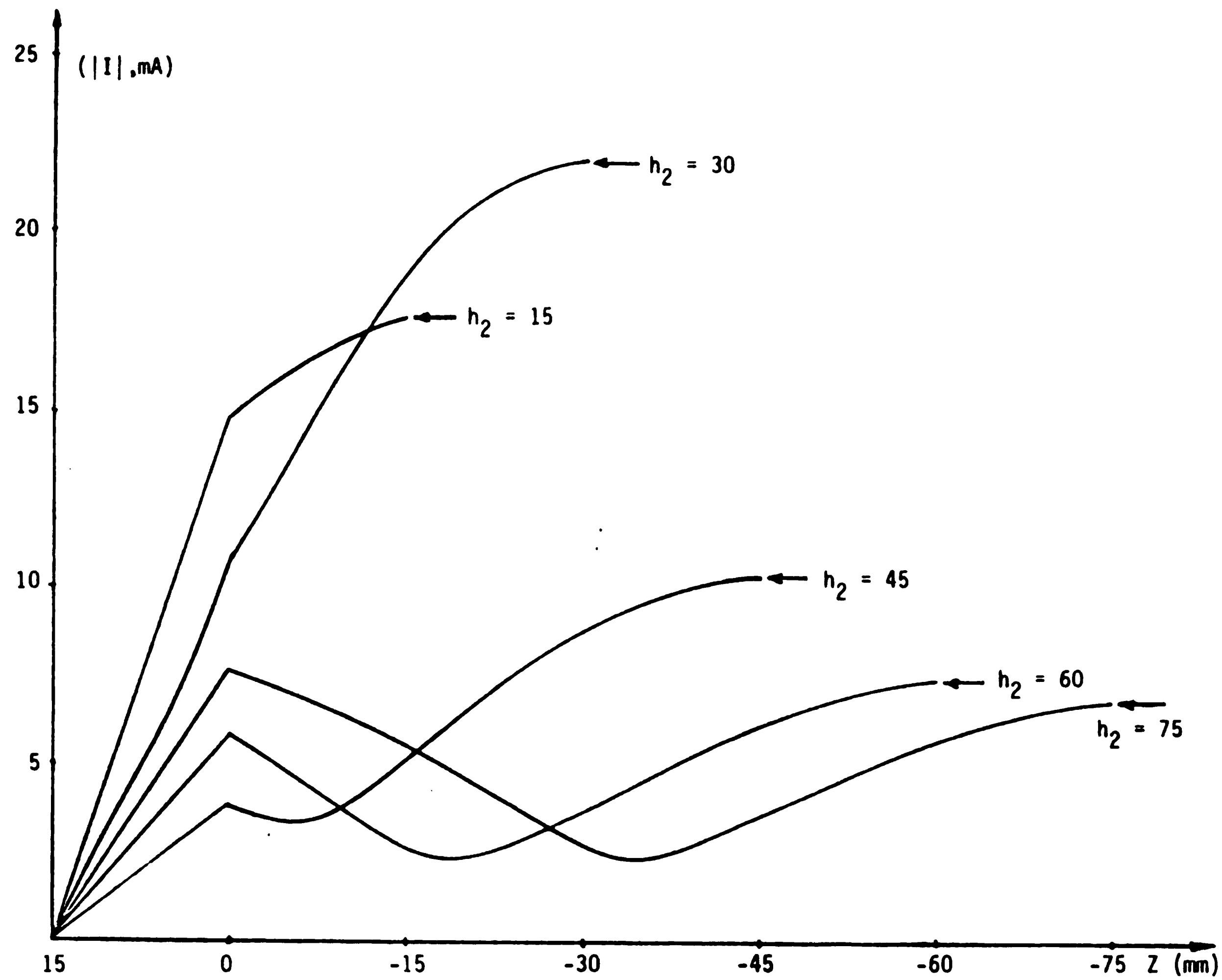

Figure 5.18. Current distributions along insulated probes with terminal impedances $Z_{e1} = \infty$, $Z_{e2} = 0.0$, $h_1 = 15$ mm, h_2 is variable. The frequency of operation is 600 MHz.

$$I_2(Z) = \frac{V}{Z_c} \frac{\cosh(\gamma h_1) \sinh[\gamma(h_2 + Z)]}{\cosh[\gamma(h_1 + h_2)]} \qquad (5.4.16)$$

$$-h_2 \leq Z \leq 0$$

For a symmetric probe, $h_1 = h_2 = h$, the current on each section of the probe becomes

$$I_1(Z) = \frac{V}{Z_c} \frac{\sinh(\gamma h) \cosh[\gamma(h - |Z|)]}{\cosh(2\gamma h)} \qquad (5.4.17)$$

$$0 \leq Z \leq h$$

and

$$I_2(Z) = \frac{V}{Z_c} \frac{\cosh(\gamma h) \sinh[\gamma(h - |Z|)]}{\cosh(2\gamma h)} \qquad (5.4.18)$$

$$-h \leq Z \leq 0$$

In Figure 5.19, the current distributions along the insulated probes with $Z_{e1} = 0.0$ and $Z_{e2} = \infty$ are shown. The dimensions of the probe and electrical properties of the insulator and the conducting medium are the same as that of case (1).

The current distributions on the probes with various terminal impedances are shown in Figure 5.20. The current along the probe changes with the change on the terminal impedances. Therefore, the heat pattern produced by the EM energy delivered by the probe changes with the change on the terminal impedances of the probe.

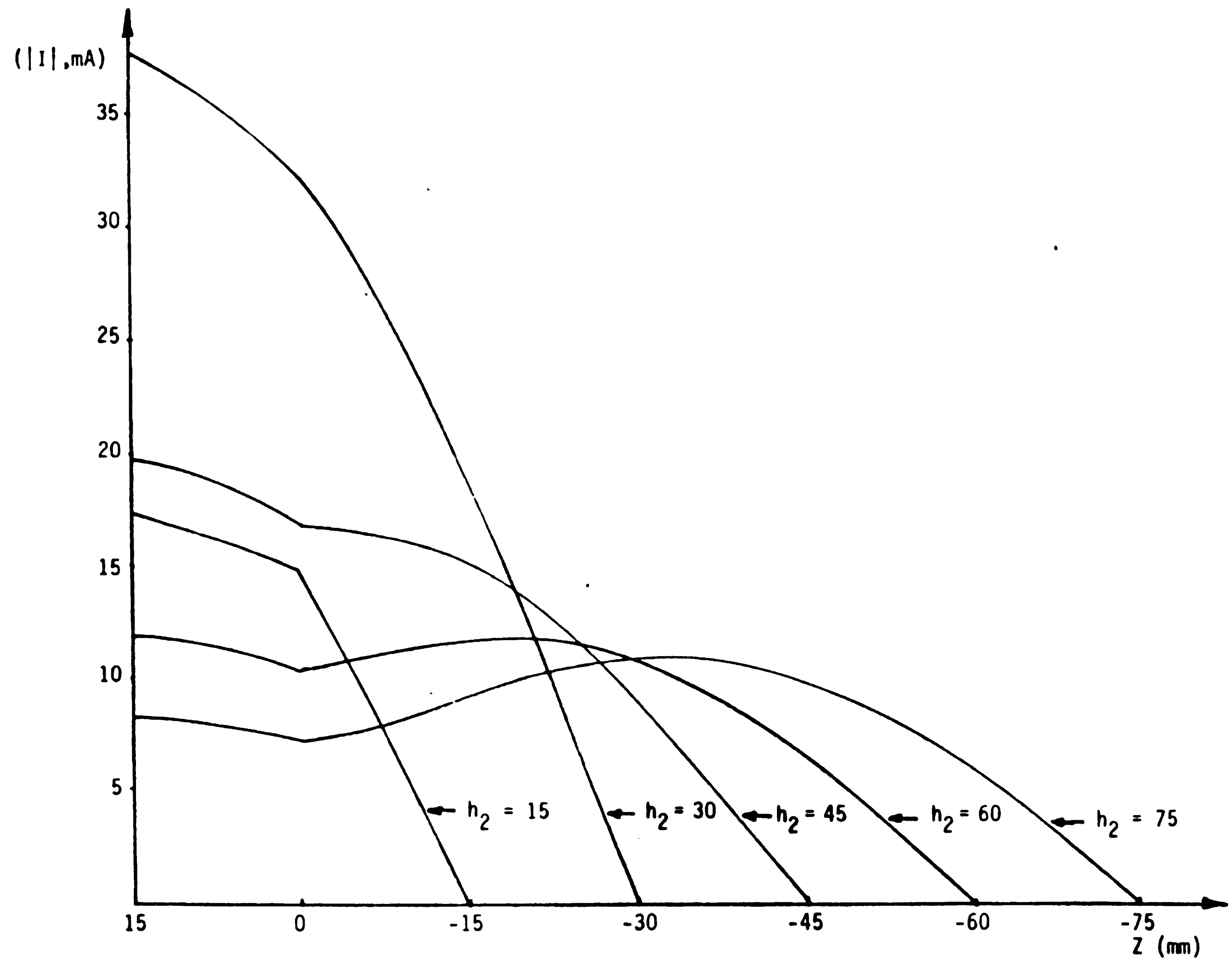

Figure 5.19. Current distributions along insulated probes with terminal impedances $Z_{e1} = 0.0$ and $Z_{e2} = \infty$, $h_1 = 15$ mm and h_2 is variable. The frequency of operation is 600 MHz.

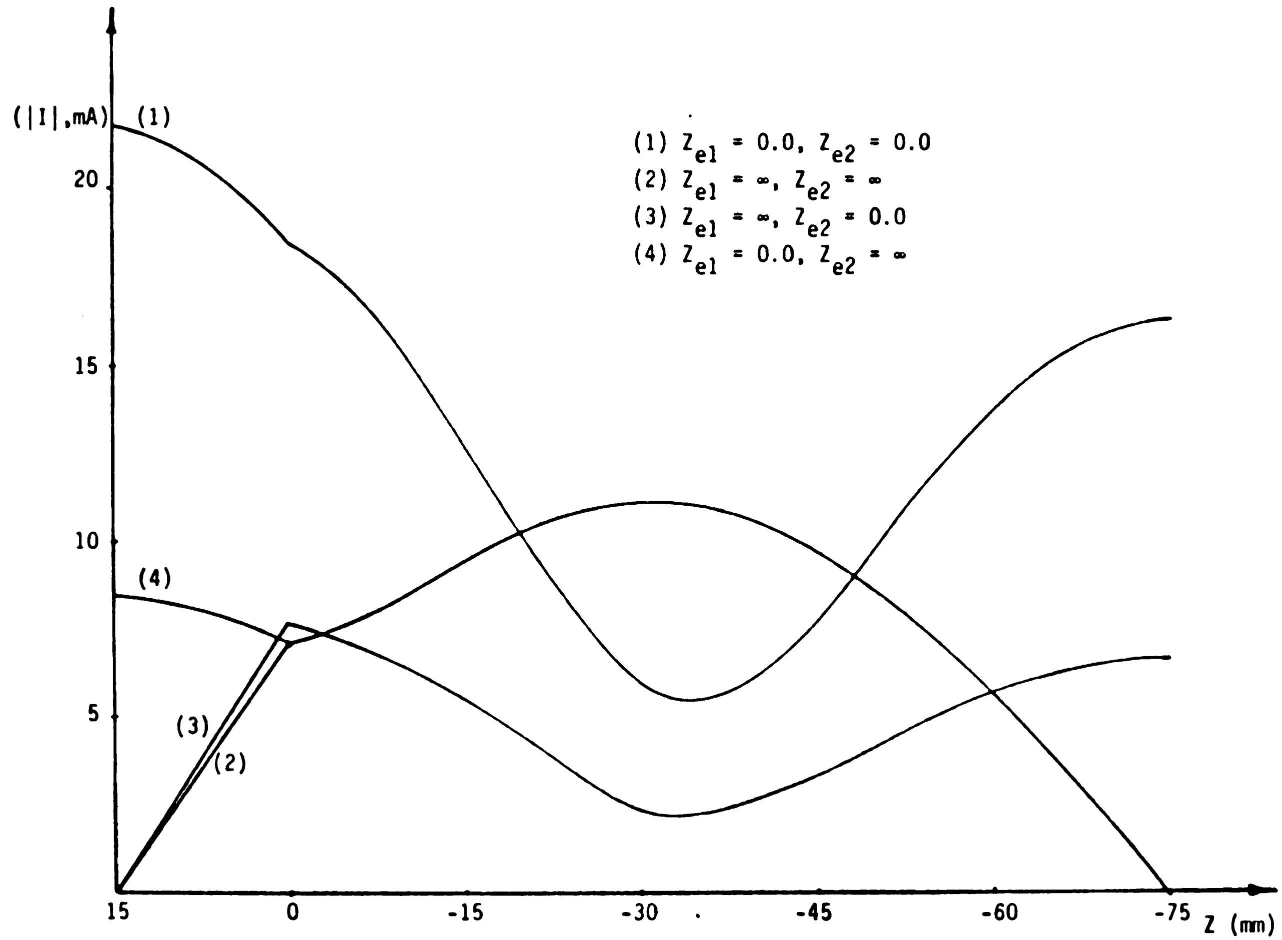

Figure 5.20. Current distributions along insulated probes with different terminal impedances.

CHAPTER VI

APPLICATION OF THE INSULATED PROBE

As mentioned earlier the input resistance of a bare probe in a conducting medium is smaller than that of a corresponding insulated probe. This implies that an insulated probe can deliver more EM energy in the surrounding medium. For this reason the insulated probe is extensively used for local heating in biological bodies.

The heat produced by the probe in the medium is given by $\frac{1}{2}\sigma|E|^2$, where σ is the conductivity of the medium and $\vec{E}$ is the electric field maintained by the probe in the medium. In the previous chapter the current distribution along the probe was determined, thus, the electric field produced by the probe current at any point in the medium can be found. It is assumed that the current is only in the z direction and there is rotational symmetry in this problem. The electric field in the medium is given by [18]

$$\vec{E}(r,z) = -\frac{j\omega}{k_2^2}\left\{\hat{r}\,\frac{\partial^2 A_z(r,z)}{\partial r \partial z} + \hat{z}\left[\frac{\partial^2 A_z(r,z)}{\partial z^2} + k_2^2 A_z(r,z)\right]\right\} \tag{6.1.1}$$

The vector potential is expressed as

$$A_z(r,z) = \frac{\mu}{4\pi}\int_{-h_2}^{h_1}\int_{-\pi}^{\pi} \frac{e^{-jk_2R}}{R} I_z(z') \frac{d\phi'}{2\pi} dz' \qquad (6.1.2)$$

where

$$R = \left\{(z - z')^2 + a_3^2 + r^2 - 2a_3r \cos \phi'\right\}^{1/2}$$

Substituting the vector potential given by (6.1.2) in (6.1.1), the r and z components of the electric field can be obtained as

$$E_r(r,z) = -\frac{j\omega\mu}{4\pi k_2^2}\int_{-h_2}^{h_1}\int_{-\pi}^{\pi} I_z(z') \frac{\partial^2}{\partial r \partial z} K(z,z') \frac{d\phi}{2\pi} dz' \qquad (6.1.3)$$

and

$$E_z(r,z) = -\frac{j\omega\mu}{4\pi k_2^2}\int_{-h_2}^{h_1}\int_{-\pi}^{\pi} I_z(z') \left(\frac{\partial^2}{\partial z^2} + k^2\right)K(z,z') \frac{d\phi'}{2\pi} dz' \qquad (6.1.4)$$

where

$$K(z,z') = \frac{e^{-jk_2R}}{R} .$$

Since the derivatives of the Kernel are

$$\frac{\partial}{\partial z} K(z,z') = -\frac{(z - z')(1 + jk_2R)}{R^2} K(z,z') ,$$

$$\frac{\partial^2}{\partial r \partial z} K(z,z') = \frac{(r - a_3 \cos \phi')(z - z')(3 + 3jk_2 R - k_2^2R^2)}{R^4} K(z,z'),$$

$$\frac{\partial^2}{\partial z^2} K(z,z') = \frac{(z-z')^2(3+3jk_2R-k_2^2R^2)-R^2-jk_2R^3}{R^4} K(z,z') \text{ ,}$$

The electric field components given by equations (6.1.3) and (6.1.4) become

$$E_r(r,z) = -\frac{j\omega\mu}{4\pi k_2^2}\left\{\int_{-h_2}^{h_1} I_z(z')(z-z')\int_{-\pi}^{\pi} \frac{(r-a_3\cos\phi')(3+3jk_2R-K_2^2R^2)}{R^4}\right.$$

$$\left. K(z,z')\,\frac{d\phi'}{2\pi}\,dz'\right\} \qquad (6.1.5)$$

and

$$E_z(r,z) = -\frac{j\omega\mu}{4\pi k_2^2}\int_{-h_2}^{h_1} I_z(z')\int_{-\pi}^{\pi} \frac{(z-z')^2(3+3jk_2R-k_2^2R^2)}{R^4}$$

$$-\frac{R^2+jk_2R^3-k_2^2R^4}{R^4}\;K(z,z')\,\frac{d\phi}{2\pi}\,d'z \qquad (6.1.8)$$

For a very thin probe we can assume that all the current on the probe is concentrated on the z axis, therefore, $R = [r^2+(z-z')^2]^{\frac{1}{2}}$, and the components of the electric field can be expressed as

$$E_r(r,z) = -\frac{j\omega\mu}{4\pi k_2^2}\int_{-h_2}^{h_1} I_z(z')\,\frac{r(z-z')\;(3+3jk_2R-k_2^2R^2)}{R^4}\,K(z,z')dz' \qquad (6.1.7)$$

and

$$E_z(r,z) = -\frac{j\omega\mu}{4\pi k_2^2}\int_{-h_2}^{h_1} I_z(z')\left[\frac{(z-z')^2(3+3jk_2R-k_2^2R^2)}{R^4}\right.$$

$$\left.-\frac{R^2+jk_2R^3-k_2^2R^4}{R^4}\right]K(z,z')dz' \qquad (6.1.8)$$

The components of the electric field are found numerically and the heat produced by the EM energy in the medium is obtained from $\frac{1}{2}\,\sigma_2|E|^2$, where $|E|^2 = |E_z|^2 + |E_r|^2$.

In Figures 6.1-6.4 the equi-power contours for insulated probes with various terminal impedances are given. The electrical properties of the insulated material are σ_d = 0.0 (s/m), ε_{rd} = 2.25, and the physical dimensions of the probe are given in these figures. In Figure 6.1 the terminal impedances are $Z_{e1} = Z_{e2} = \infty$; in this case most of the heat is concentrated along the z axis and around the driving point. In Figures 6.2 and 6.3 it is assumed that one of the terminal impedances is zero and the other is infinity; in these cases the heat is concentrated mostly near the driving point of the probe and the tip with zero terminal impedance. In Figure 6.4 both terminal impedances are zero, and the heat is almost uniformly distributed around the probe.

In general the heat produced by an insulated probe in a conducting medium is distributed in a larger volume in comparison with

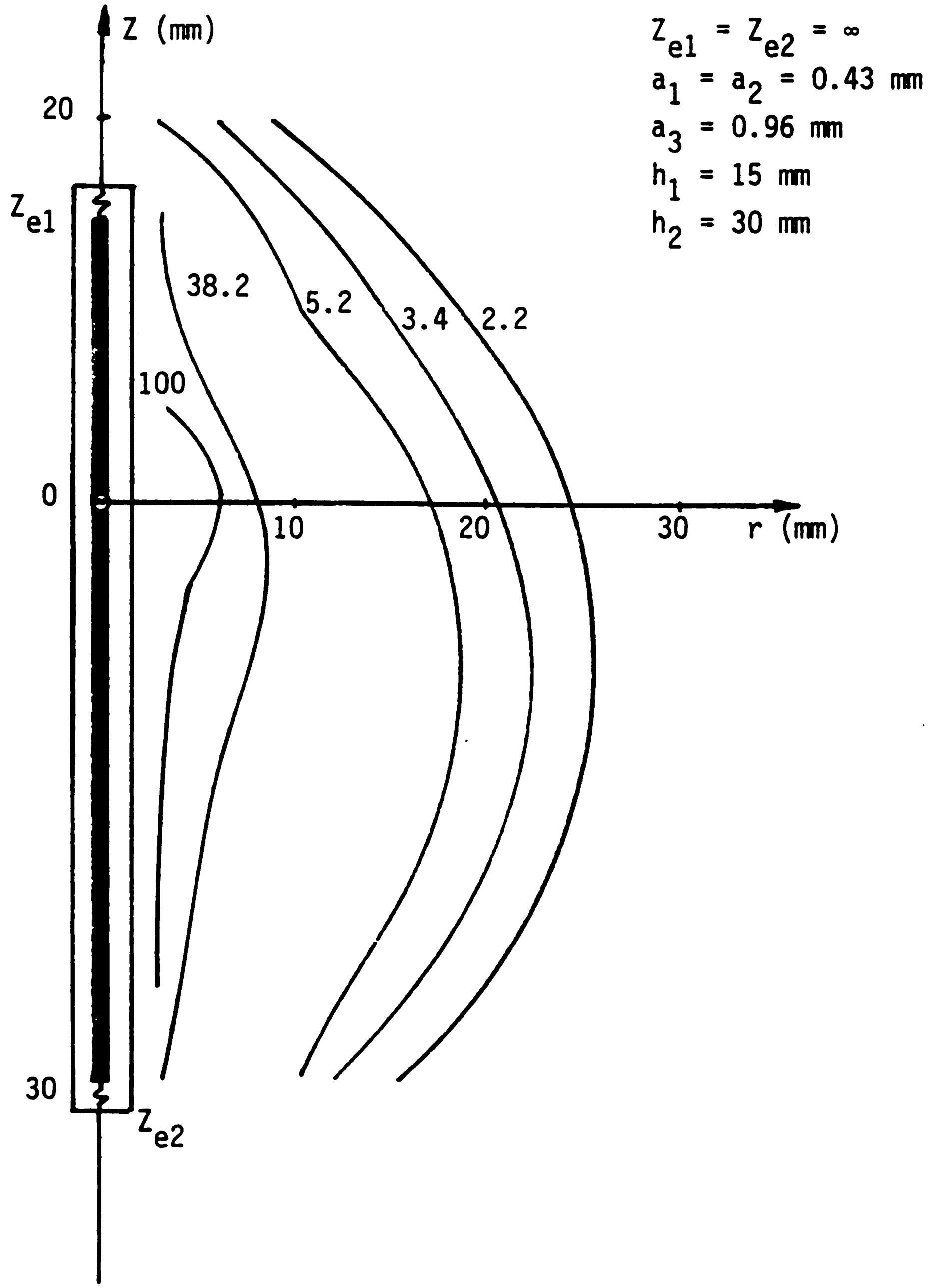

Figure 6.1. Equi-power contours for an insulated probe in the r-z plane. Characteristic impedance of the probe $Z_C = 64.5 - j13.4$, $\sigma_2 = 1.11$ (s/m), $\epsilon_{r2} = 76.7$, and the frequency is 600 MHz.

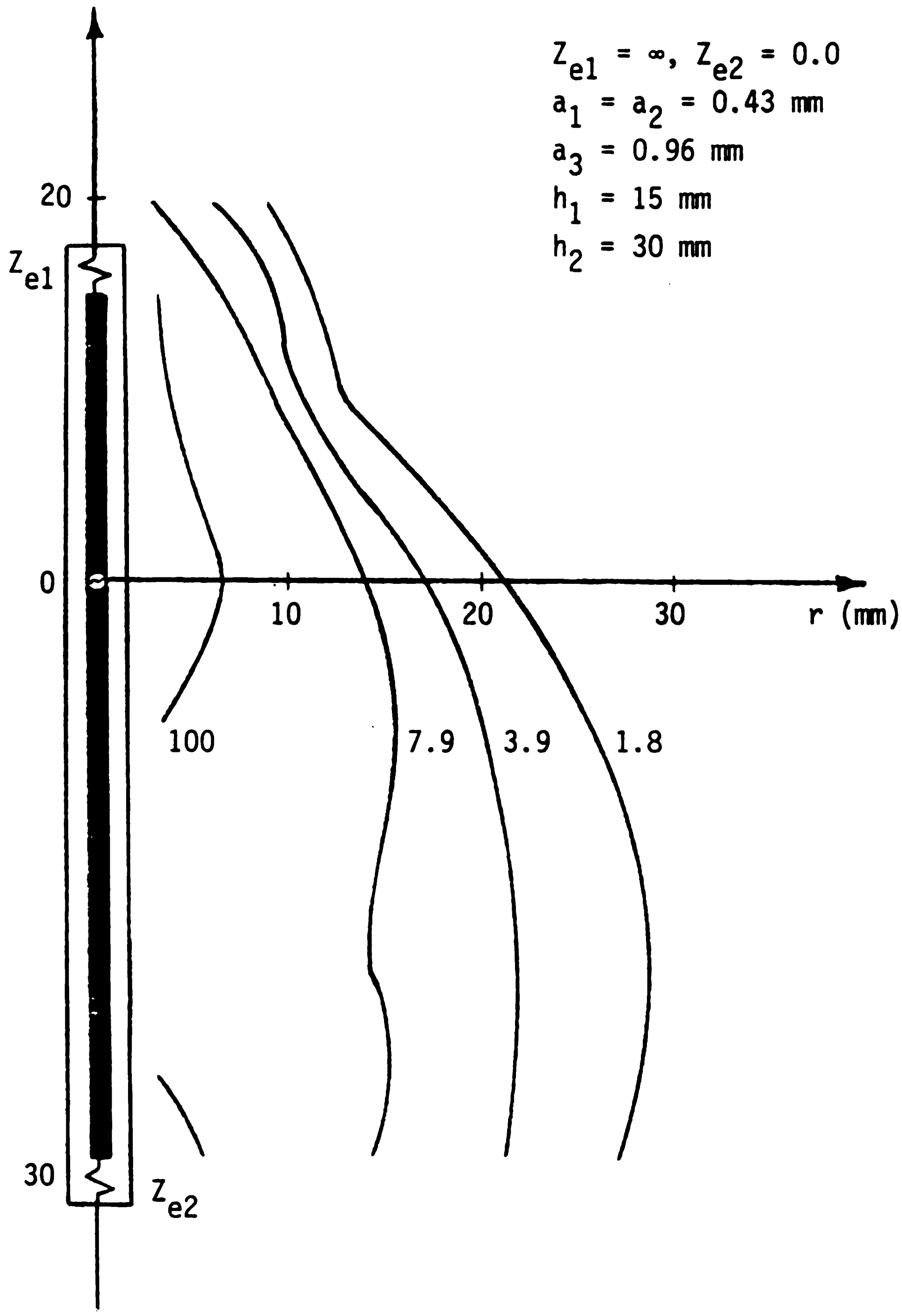

Figure 6.2. Equi-power contours for an insulated probe in the r-z plane. Characteristic impedance of the probe $Z_C = 64.5 - j13.4$, $\sigma_2 = 1.11$ (s/m), $\varepsilon_{r2} = 76.7$, and the frequency is 600 MHz.

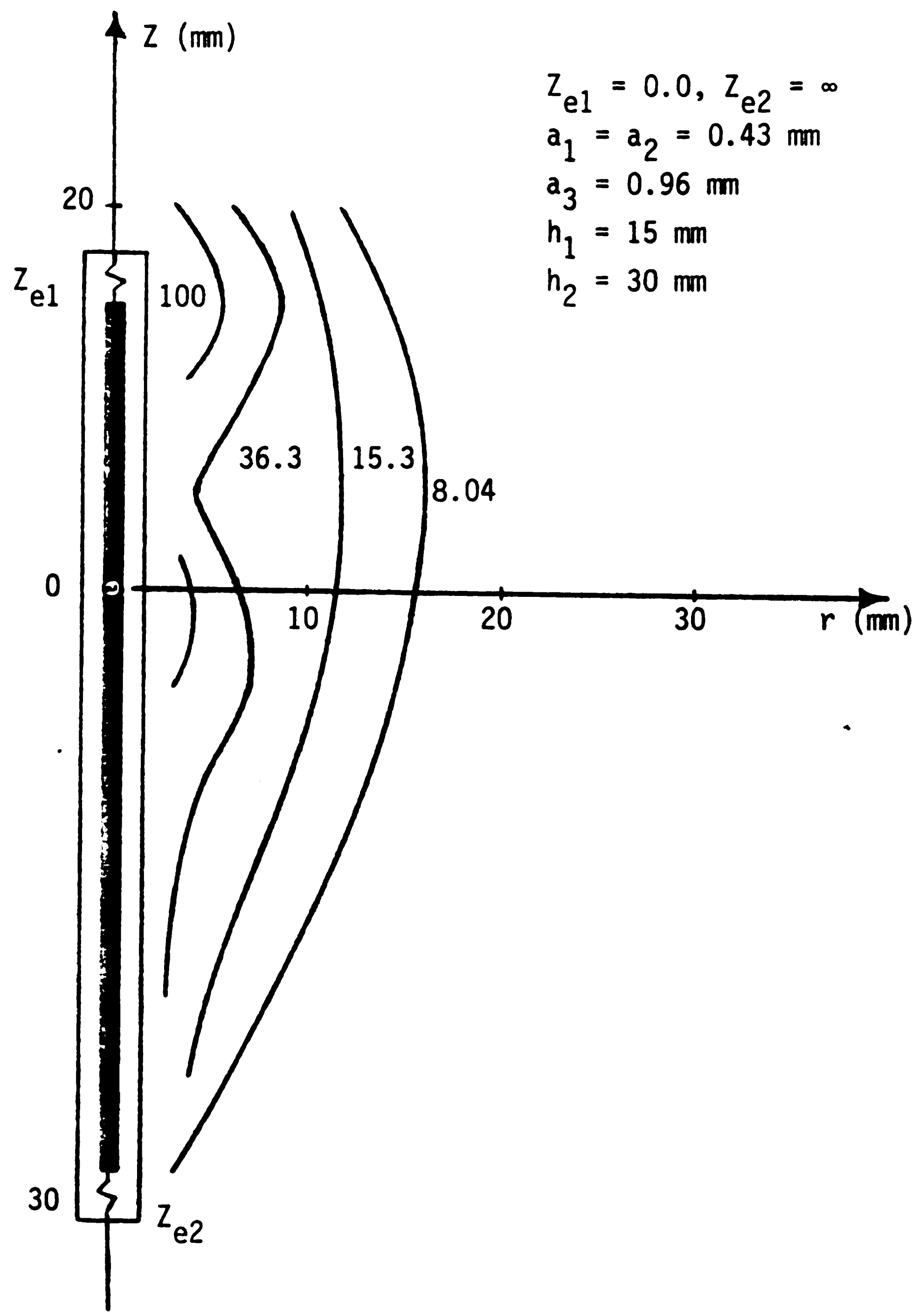

Figure 6.3. Equi-power contours for an insulated probe in the r-z plane. Characteristic impedance of the probe Z_C = 64.5 - j13.4, σ_2 = 1.11 (s/m), ε_{r2} = 76.7, and the frequency is 600 MHz.

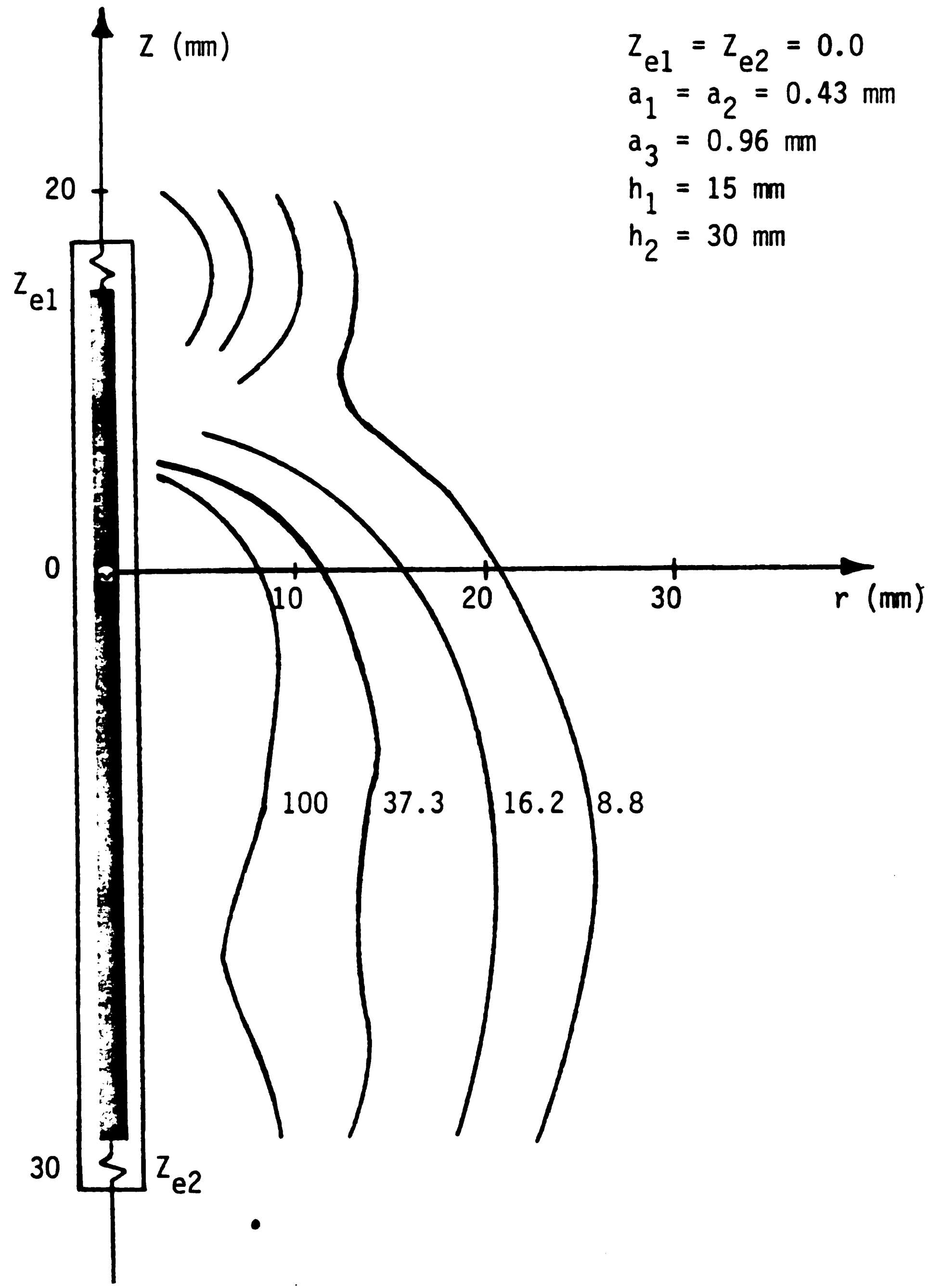

Figure 6.4. Equi-power contours for an insulated probe in the r-z plane. Characteristic impedance of the probe $Z_C = 64.5 - j13.4$, $\sigma_2 = 1.11$ (s/m), $\varepsilon_{r2} = 76.7$, and the frequency is 600 MHz.

the heat produced by the similar bare probe, and for an insulated probe the heat pattern can be changed by the changing in the terminal impedances.

CHAPTER VII

A USER'S GUIDE TO COMPUTER PROGRAMS USED TO CALCULATE THE CURRENT DISTRIBUTION AND ELECTRIC FIELD IN A BIOLOGICAL BODY INDUCED BY A BARE AND INSULATED MICROPROBE

This chapter is divided into two sections. The first section briefly explains the computer programs used to determine the current distribution and input impedance of the bare probe immersed in a conducting medium by solving Hallen's Integral Equation Method (HIEM) or Electric Field Integral Equation (EFIE). The second part gives explanation about the program used to find the parameters and the characteristic impedance of the insulated probe imbedded in the conducting medium.

7.1. Programs for the Bare Probe

Moment method is used to solve integral equations for both cases HIEM and EFIE. The probe is divided into N segments, and the current is assumed to be constant along each segment. The geometry of the bare probe is given in Figure 7.1.

7.2. Program HALIEQ

This program solves Hallen's integral equation for the bare probe. Given the necessary data the program solves equation (2.1.4)

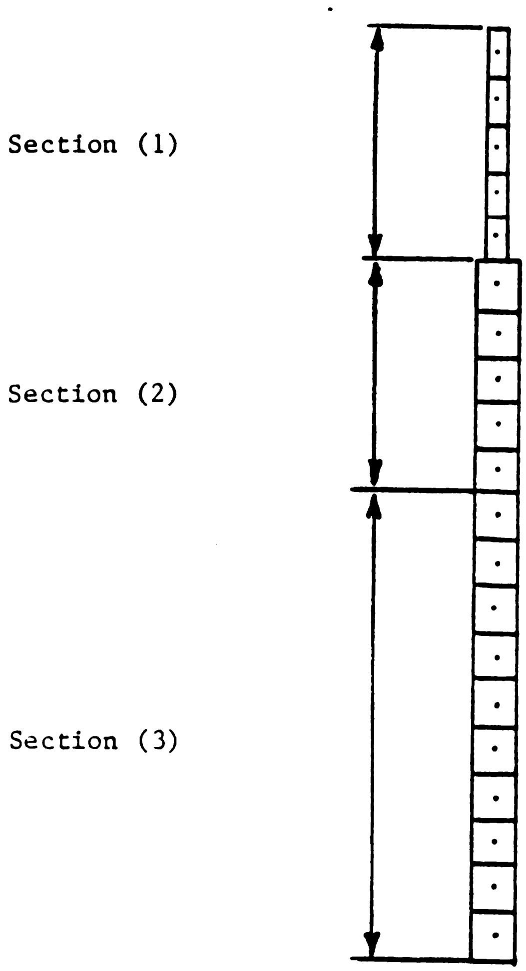

Figure 7.1. Geometry of the bare probe used in HALIEQ.

for the current distribution, and the input impedance of both symmetric and asymmetric bare probes. The main program contains a subroutine and a function as explained below.

CMATPAC is a subroutine that solves the system of linear equations by Gauss's elimination process to determine the unknown currents on the probe.

GRE is a function that computes Green's function.

7.2.1. Description of Input Variables and Input Data Files

The data deck is composed of two files with each file having only one card. The names of the variables used in this program and the format specifications are given in Table 7.1. The variables in data files are defined below.

First data file--accommodates the following variables:

N is the total number of segments on the probe.

M1 is an even integer; it is the number of segments on the section (1) and section (2) of the probe.

M2 is the number of segments on the section (3) of the probe.

Second data file--contains the following variables:

FREQ is the frequency of operation in Hz.

RR1 specifies the radius of the section (1) of the probe.

RR2 is the radius of the section (2) of the probe.

ZI specifies the surface impedance of the probe in section (2) and section (3); it is assumed that the surface impedance of section (1) is zero.

ZIG specifies the conductivity of the conducting medium.

EPR is the relative permittivity of the conducting medium.

Table 7.1. The symbolic names of the input variables and the format specifications used in program HALIEQ.

File Number	Card Number	Columns	Variable Name	Format
1	1	1-3	N	I3
		4-6	M1	I3
		7-9	M2	I3
2	1	1-12	FREQ	F12.1
		13-21	RR1	F9.5
		22-30	RR2	F9.5
		31-39	ZI	F9.1
		40-45	ZIG	F6.2
		46-50	EPR	F5.1
		51-56	HH1	F6.1
		57-62	HH2	F6.2

HH1 is the length of the section (1) of the probe.

HH2 specifies the length of the section (2) plus section (3) of the probe.

7.2.2. Example

Let us assume that the probe has the dimensions of $h_1 = 7.5$ mm, $h_2 = 15$ mm, and the diameters of the two sections are equal ($a_1 = a_2 = 0.43$ mm). The frequency is 600 MHz, and the electrical properties of the conducting medium are $\sigma = 1.11$, $\varepsilon_r = 76.7$. The surface impedance $Z^i = 100$. Following is the list of numbers and corresponding variable names should provide in file no. 1 and file no. 2.

Numbers	Variable Name	Columns
File No. 1		
024	N	1-3
016	M1	4-6
008	M2	7-9
File No. 2		
600,000,000.0	FREQ	2-12
0.00043	RR1	15-21
0.00043	RR2	24-30
100.0	ZI	35-39
1.11	ZIG	42-45
76.7	EPR	47-50
7.5	HH1	53-55
15.0	HH2	58-61

The numerical results are presented after the listing of the program HALIEQ.

7.3. Program EFZI

This program solves EFIE for the bare probe given in equation (2.2.7). Given the necessary data this program finds the current distribution and input impedance of both symmetric and asymmetric bare probes. The subroutines and functions used in the main program are as explained below.

CAMTPAC is explained in HALIEQ.

MAGRIN is a subroutine that finds the electric field on the surface of the probe, based on magnetic current ring as the driving source.

SIMCON is a subroutine that calculates the first integral in a double integral.

FCT is a function that provides the integrand of SIMCON.

SIMCOP is a subroutine that calculates second integral in a double integral.

FCTP is a function that provides the integrand of SIMCOP.

GRE is a function that computes the Green's function.

7.3.1. Description of Input Variables and Input Data Files

The data deck is composed of two files, with each file having only one card. The names of the variables used in the first data file and the format specifications are given in Table 7.2. The second data file has the same variables and formats as the variables in the second data file in HALIEQ. The information about variables in the first data file is explained below.

First data file--accommodates the following variables:

N is the total number of segments on the probe.

M1 is the number of segments on section (1) of the probe.

M2 is the number of segments on section (2) and section (3) of the probe.

NG specifies the number of subdivisions the driving point segment will undergo in the partitioning process of the probe.

ITEST is either one or two; when it is one the driving source is assumed to be a delta gap, and when it is two the driving source is modeled as a magnetic current ring.

7.3.2. Example

Let us assume that all the conditions are the same as mentioned in example 7.2.2, but the surface impedance is zero everywhere in this case. The second data file is the same as explained in example

Table 7.2. The symbolic names of the input variables and the format specifications used in the first data file in program EFZI.

File Number	Card Number	Columns	Variable Name	Format
1	1	1-3	N	I3
		4-6	M1	I3
		7-9	M2	I3
		10-12	NG	I3
		13-15	ITEST	I3

7.2.2, except we have zero for surface impedance. The list of numbers and corresponding variable names in file no. 1 are given below.

Numbers	Variable Name	Columns
File No. 1		
024	N	1-3
008	M1	4-6
016	M2	7-9
001	NG	10-12
002	ITEST	13-15

The numerical results are presented after the listing of the program EFZI.

7.4. Program Used for Insulated Probe

This section briefly explains the computer program used to determine the parameters and the input impedance of the insulated probe, with various terminal impedances. The probe is treated as a lossy transmission line. The symbolic name of the program is INPIMP. The main program contains a subroutine COMBES, which finds the Bessel's functions of first and second kind for complex argument and complex order. The subroutine COMBES is explained in more detail in [16].

7.4.1. Description of Input Variables and Input Data Files

The data deck is composed of five files, with each file having only one card. The names of the variables used in this program and the format specifications are given in Table 7.3. The variables in data files are defined as below.

First data file--accommodates the following variables:

H1 is the length of the section (1) of the probe.

H2 is the length of the section (2) of the probe.

Second data file--contains the following variables:

ZIGD is conductivity of the insulating material.

EPRD is relative permittivity of the insulating material.

Third data file--contains the following variables:

ZIG2 is conductivity of the conducting medium.

EPR2 is relative permittivity of the conducting medium.

Fourth data file--contains the following variables:

A_1 is the radius of the conductor in section (1).

A_2 is the radius of the conductor in section (2).

A_3 is the outer radius of the insulator.

Fifth data file--contains the following variable:

FREQ is the frequency of operation.

Table 7.3. The symbolic names of the input variables and the format specifications used in program INPIMP.

File Number	Card Number	Columns	Variable Name	Format
1	1	1-8	H1	F8.5
		9-16	H2	F8.5
2	1	1-6	ZIGD	F6.2
		7-12	EPRD	F6.2
3	1	1-8	ZIG2	F8.4
		9-13	EPR2	F5.2
4	1	1-8	A1	F8.5
		9-16	A2	F8.5
		17-24	A3	F8.5
5	1	1-12	FREQ	F12.1

7.4.2. Example

The input impedance of insulated probe with $a_1 = a_2 = 0.43$ mm, $a_3 = 0.96$ mm, $h_1 = 15$ mm, and $h_2 = 45$ mm is found by INPIMP. The electrical properties of the insulator and the conducting medium are $\sigma_d = 0.0$, $\varepsilon_{rd} = 2.25$, $\sigma_2 = 1.11$, and $\varepsilon_{r2} = 76.7$. Following is the list of numbers and corresponding variable names

Numbers	Variable Name	Columns
File No. 1		
0.015	H1	2-6
0.045	H2	10-14
File No. 2		
0.0	ZIGD	3-5
2.25	EPRD	9-12
File No. 3		
1.11	ZIG2	3-6
76.7	EPR2	9-12
File No. 4		
0.00043	A1	2-8
0.00043	A2	10-16
0.00096	A3	18-24
File No. 5		
600,000,000.0	FREQ	2-12

The numerical results are presented after the listing of the program INPIMP.

```
C*********************************************************************
C  THIS PROGRAM DETERMINS  THE CURRENT DISTRIBUTION ON THE PROBE AND
C  INPUT IMPEDANCE OF THE PROBE BY SOLVING HALLEN.S INTEGRAL EQUATION.
C*********************************************************************
      PROGRAM HALIEQ (INPUT,OUTPUT)
      COMMON/HALGRE/JK
      DIMENSION G(100,100),Z(100),S(100),D3(3)
      COMPLEX G,K,F,F1,D2,D3,B2,B4,DET,A,E,E1,E2,E3,E4,ZIN,B1,JK,GRE
      REAL MU,IREA,IIMA,LA
      READ 100,N,M1,M2
      READ 101,FREQ,RR1,RR2,ZI,ZIG,EPR,HH1,HH2
      FREQ=FREQ/1.0E+6
      PRINT 102,FREQ,RR1,RR2,ZI
      R1=RR1    $ R2=RR2
      PI=4.0*ATAN(1.0)    $ V0=1.0
      MU=4.0*PI*1.0E-7
      OME=2.0*PI*FREQ*1.0E+6
      M3=M1+1    $ M4=M1/2     $ M6=M4+1
      H1=HH1/1000.0  $ H2=HH2/1000.0    $ H3=H1
      DEL1=(H1+H3)/M1
      DEL2=(H2-H3)/M2
      DEL3=(DEL1+DEL2)/2.0
C*********************************************************************
C  PARTITION THE PROBE IN N SEGMENTS.
C*********************************************************************
      DO 10 JJ=1,N
      IF(JJ-M3) 11,12,13
   11 IF(JJ.EQ.1) GO TO 14
      DEL=DEL1    $ JJ1=JJ-1
      Z(JJ)=Z(JJ1)-DEL  $ GO TO 10
   14 DEL=DEL1
      Z(JJ)=H1-0.5*DEL    $ GO TO 10
   12 DEL=DEL3
      JJ2=JJ-1
      Z(JJ)=Z(JJ2)-DEL    $ GO TO 10
   13 DEL=DEL2
      JJ3=JJ-1
      Z(JJ)=Z(JJ3)-DEL
   10 CONTINUE
      EP=1.0E-9*EPR/(36.0*PI)
      PRINT 93,H1,H2,ZIG,EPR
      PRINT 39,N,M1,M2
      K=OME*CSQRT(MU*EP-CMPLX(0.0,1.0)*MU*ZIG/OME)
      ALPHA=-AIMAG(K)     $ BETA=REAL(K)
      PRINT 81,ALPHA,BETA
      JK=CMPLX(0.0,1.0)*K
C*********************************************************************
C  FIND THE DIAGONAL TERMS OF THE IMPEDANSE MATRIX.
C*********************************************************************
      DO 2 II=1,3
      IF(II-2) 3,4,5
    3 DEL=DEL1
      R=R1     $ GO TO 6
    4 DEL=DEL1
      R=R2      $ GO TO 6
    5 DEL=DEL2
      R=R2
    6 HDEL=DEL/2.0
      D=HDEL/R
      D1=2.0*ALOG(D+SQRT(1.0+D**2.0))
      D2=D1-JK*DEL
      D3(II)=D2
    2 CONTINUE
```

```
      B=(4.0*PI)/(OME*MU)
      B1=CMPLX(ALPHA,BETA)
      B2=B*B1    $ B3=B*ZI
      B4=CMPLX(0.0,-B3)
      M=N+1
C*********************************************************************
C  THIS SECTION FINDS THE ELEMENTS OF THE IMPEDANCE MATRIX.
C*********************************************************************
      DO 15 L=1,N
      G(L,1)=B2*CCOS(K*Z(L))
      G(L,N)=B2*CSIN(K*Z(L))
      G(L,M)=-B2*(V0/2.0)*CSIN(K*ABS(Z(L)))
   15 CONTINUE
      E1=(1-CCOS(K*DEL1/2.0))*B4
      E2=(1-CCOS(K*DEL2/2.0))*B4
      M5=N-M4
      DO 30 J=1,M5
      DEL=DEL2
      IF(J.LE.M4) DEL=DEL1
      L=J+M4
      S(J)=Z(L)-DEL/2.0
   30 CONTINUE
      N1=N-1
      DO 40 I=1,N
      DO 40 J=2,N1
      IF(I.EQ.J) GO TO 41
      DEL=DEL2
      IF(J.LE.M1) DEL=DEL1
      R=R2
      IF(I.LE.M4) R=R1
      R3=SQRT((Z(I)-Z(J)) **2.0+R**2.0)
      IF(I.GT.M4.AND.J.GT.M4) GO TO 42
   43 G(I,J)=GRE(R3)*DEL     $ GO TO 40
   42 IF(J.GT.I) GO TO 43
      L=I-M4    $ LL=J-M4      $ LP=LL+1
      F=B4*(CCOS(K*(Z(I)-S(LP)))-CCOS(K*(Z(I)-S(LL))))
      G(I,J)=GRE(R3)*DEL+F
      GO TO 40
   41 IF(I.GT.M1) GO TO 44
      IF(I.GT.M4) GO TO 45
      JJ=1
      G(I,J)=D3(JJ)        $ GO TO 40
   44 JJ=3
      G(I,J)=D3(JJ)+E2
      GO TO 40
   45 JJ=2
      G(I,J)=D3(JJ)+E1
   40 CONTINUE
      CALL CMATPAC(-1,G,N,1,DET,1.0E-200)
      AYIN=CABS(G(M4,M))
      PRINT 111,AYIN,G(M4,M)
      ZIN=1/(G(M4,M))
      AZIN=CABS(ZIN)
      PHI=ATAN(AIMAG(ZIN)/REAL(ZIN))*180.0/(2.0*PI)
      PRINT 107,AZIN,ZIN,PHI
      PRINT 103
      DO 95 I1=1,N
      IF(I1.EQ.1) GO TO 19
      IF(I1.EQ.N) GO TO 19
      AMPI=CABS(G(I1 ,M))
      GO TO 21
```

```
   19 G(I1,M)=0.0
      AMPI=0.0
   21 PRINT 25,I1,Z(I1),AMPI,G(I1,M)
   95 CONTINUE
C*********************************************************************
C  READ AND WRITE FORMATS.
C*********************************************************************
   25 FORMAT(1H0,10X,I3,4X,*Z=*,F6.4,4X,*AMP(I)=*,F8.4,4X,*I=*,
     C2(F8.4,2X))
   39 FORMAT(1H0,20X,2HN=,I3,4X,3HM1=,I3,4X,3HM2=,I3,/)
   81 FORMAT(1H0,20X,*ALPHA=*,F8.2,4X,*BETA=*,F8.2,/)
   93 FORMAT(1H0,10X,*H1=*,F8.4,4X,*H2=*,F8.4,4X,*SIG=*,F8.4,4X,
     C*EPR=*,F8.4,/)
  100 FORMAT(3I3)
  101 FORMAT(F12.1,2(F9.5),F9.1,F6.2,F5.1,2(F6.1))
  102 FORMAT(1H0,10X,*FREQ=*,F7.2,*MHZ*,4X,*A=*,F8.5,4X,*B=*,F8.5,4X,
     **ZI=*,F8.1,/)
  103 FORMAT(1H0,135(*+*),/)
  105 FORMAT(2(F14.8))
  107 FORMAT(1H0,20X,*ABS(ZIN)=*,F8.2,4X,*ZIN=*,2(F8.2,2X),*PHI=*,
     CF8.2,/)
  111 FORMAT(1H0,20X,*ABS(YIN)=*,F8.4,4X,*YIN=*,2(F8.4,2X),/)
      END
C*********************************************************************
      COMPLEX FUNCTION GRE(R1)
C*********************************************************************
      COMMON/HALGRE/JK
      COMPLEX JK
      GRE=CEXP(-JK*R1)/R1
      RETURN
      END
C*********************************************************************
C  SUBROUTINE CMATPAC SOLVES THE SYSTEM OF EQUATIONS BY
C  GAUSS-ELIMINATION PROCESS.
C*********************************************************************
      SUBROUTINE CMATPAC(IJOB,A,N,M,DET,EP)                             CMA00001
      DIMENSION A(100,100)
      TYPE COMPLEX A,B,DET,CONST,S                                      CMA00002
   30 FORMAT(1X,42HTHE DETERMINANT OF THE SYSTEM EQUALS ZERO./          CMA00004
     11X,36HTHE PROGRAM CANNOT HANDLE THIS CASE.//)                     CMA00005
      DET=1.                                                            CMA00006
      NP1=N+1                                                           CMA00007
      NPM=N+M                                                           CMA00008
      NM1=N-1                                                           CMA00009
      IF(IJOB) 2,1,2                                                    CMA00010
    1 DO 3 I=1,N                                                        CMA00011
      NPI=N+I                                                           CMA00012
      A(I,NPI)=1.                                                       CMA00013
      IP1=I+1                                                           CMA00014
      DO 3 J=IP1,N                                                      CMA00015
      NPJ=N+J
      A(I,NPJ)=0.                                                       CMA00017
    3 A(J,NPI)=0.                                                       CMA00018
    2 DO 4 J=1,NM1                                                      CMA00019
      C=CABS(A(J,J))
      JP1=J+1                                                           CMA00021
      DO 5 I=JP1,N                                                      CMA00022
      D=CABS(A(I,J))
      IF(C-D) 6,5,5                                                     CMA00024
    6 DET=-DET
      DO 7 K=J,NPM
```

```
    6 DET=-DET
      DO 7 K=J,NPM
      B=A(I,K)                                                        CMA00027
      A(I,K)=A(J,K)                                                   CMA00028
    7 A(J,K)=B                                                        CMA00029
      C=D                                                             CMA00030
    5 CONTINUE                                                        CMA00031
      IF(CABS(A(J,J))-EP) 14,15,15
   15 DO 4 I=JP1,N                                                    CMA00033
      CONST=A(I,J)/A(J,J)                                             CMA00034
      DO 4 K=JP1,NPM                                                  CMA00035
    4 A(I,K)=A(I,K)-CONST*A(J,K)                                      CMA00036
      IF(CABS(A(N,N)-EP))14,18,18
   14 DET=0.                                                          CMA00038
      IF(IJOB) 16,16,17                                               CMA00039
   16 PRINT 30                                                        CMA00040
   17 RETURN                                                          CMA00041
   18 DO 11 I=1,N                                                     CMA00042
   11 DET=DET*A(I,I)                                                  CMA00043
      IF(IJOB) 10,10,17
   10 DO 12 I=1,N                                                     CMA00045
      K=N-I+1                                                         CMA00046
      KP1=K+1                                                         CMA00047
      DO 12 L=NP1,NPM
      S=0.                                                            CMA00049
      IF(N-KP1) 12,19,19                                              CMA00050
   19 DO 13 J=KP1,N                                                   CMA00051
   13 S=S+A(K,J)*A(J,L)                                               CMA00052
   12 A(K,L)=(A(K,L)-S)/A(K,K)                                        CMA00053
      RETURN                                                          CMA00054
      END
24 16  8
600000000.0  0.00043  0.00043    100.0  1.11 76.7   7.5  15.0
```

FREQ= 600.00MHZ A= .00043 B= .00043 ZI= 100.0

H1= .0075 H2= .0150 SIG= 1.1100 EPR= 76.7000

N= 24 M1= 16 M2= 8

ALPHA+ 23.37 BETA+ 112.51

ABS(YIN)= .0505 YIN= .0434 .0258

ABS(ZIN)= 19.80 ZIN= 17.03 -10.11 PHI= -15.34

+ +

1	Z=	.0070	AMP(I)=	0.0000	I=	0.0000	0.0000
2	Z=	.0061	AMP(I)=	.0117	I=	.0110	.0038
3	Z=	.0052	AMP(I)=	.0181	I=	.0170	.0062
4	Z=	.0042	AMP(I)=	.0244	I=	.0227	.0088
5	Z=	.0033	AMP(I)=	.0303	I=	.0280	.0115
6	Z=	.0023	AMP(I)=	.0360	I=	.0329	.0146
7	Z=	.0014	AMP(I)=	.0415	I=	.0374	.0179
8	Z=	.0005	AMP(I)=	.0505	I=	.0434	.0258
9	Z=	-.0005	AMP(I)=	.0522	I=	.0454	.0258
10	Z=	-.0014	AMP(I)=	.0469	I=	.0434	.0178
11	Z=	-.0023	AMP(I)=	.0453	I=	.0429	.0145
12	Z=	-.0033	AMP(I)=	.0435	I=	.0419	.0116
13	Z=	-.0042	AMP(I)=	.0417	I=	.0406	.0092
14	Z=	-.0052	AMP(I)=	.0396	I=	.0390	.0071
15	Z=	-.0061	AMP(I)=	.0373	I=	.0369	.0053
16	Z=	-.0070	AMP(I)=	.0348	I=	.0345	.0038
17	Z=	-.0080	AMP(I)=	.0319	I=	.0318	.0025
18	Z=	-.0089	AMP(I)=	.0288	I=	.0287	.0015
19	Z=	-.0098	AMP(I)=	.0253	I=	.0253	.0008
20	Z=	-.0108	AMP(I)=	.0216	I=	.0216	.0002
21	Z=	-.0117	AMP(I)=	.0176	I=	.0176	-.0001
22	Z=	-.0127	AMP(I)=	.0131	I=	.0131	-.0003
23	Z=	-.0136	AMP(I)=	.0085	I=	.0085	-.0003
24	Z=	-.0145	AMP(I)=	0.0000	I=	0.0000	0.0000

```
C*********************************************************************
C  THIS PROGRAM SOLVES ELECTRIC FIELD INTEGRAL EQUATION TO FIND CURRENT
C  DISTRIBUTION AND INPUT IMPEDANCE OF THE PROBE.
C*********************************************************************
      PROGRAM EFZI(INPUT,OUTPUT,TAPE1)
      DIMENSION D6(4),B(60),Z(60),G(60,61),EZ(60)
      COMPLEX K,JK,D2,D3,D6,D7,B,B2,E3,E4,E7,G,ZIN,A,EZ,GRE,BA,ALR
     *,JJK
      COMMON/EZIMAG/A1,A2,JK,DELG
      COMMON/EFGRE/JJK
      REAL LA,MU
      READ 100,N,M1,M2,NG,ITEST
      READ 103,FREQ,RR1,RR2,ZI,ZIG,EPR,HH1,HH2
      FREQ=FREQ/1.0E+6
      H1=HH1/1000.0
      H2=HH2/1000.0
      PRINT 101,FREQ,RR1,RR2,ZI,ZIG,EPR,H1,H2
      PRINT 39,N,M1,M2,NG,ITEST
      PI=4.0*ATAN(1.0)      $ V=1.0
      MU=4.0*PI*1.0E-7
      OME=2.0*PI*FREQ*1.0E+6
      M3=M1+1  $ M4=M1+NG   $ M5=M4+1   $ NC=M1+1   $ NP=N+NG
      A1=RR1       $ A2=RR2
      DEL1=H1/M1
      DEL2=H2/M2
      DO 56 INM=1,1
      DELG=0.001
      DEL3=(DEL1+DELG)/2.0
      DEL4=(DEL2+DELG)/2.0
      H1=HH1/1000.0+0.5*DELG
      H2=HH2/1000.0+0.5*DELG
      DO 10 J=1,NP
      IF(J.LE.M1) GO TO 11
      IF(J.GT.M4) GO TO 13
      DEL=DEL3
      J3=J-1
      Z(J)=Z(J3)-DEL    $ GO TO 10
   13 DEL=DEL2
      IF(J.EQ.M5) DEL=DEL4
      J2=J-1
      Z(J)=Z(J2)-DEL    $ GO TO 10
   11 IF(J.EQ.1) GO TO 12
      J1=J-1
      Z(J)=Z(J1)-DEL1    $ GO TO 10
   12 Z(J)=H1-DEL1*0.5
   10 CONTINUE
      EP=EPR*1.0E-9/(36.0*PI)
      K=OME*CSQRT(MU*EP-CMPLX(0.0,1.0)*MU*ZIG/OME)
      JK=K*CMPLX(0.0,1.0)
      JJK=JK
      ALPHA=-AIMAG(K)   $ BETA=REAL(K)
      PRINT 81,ALPHA,BETA
      LA=2.0*PI/BETA
      PRINT 57,EPR,ZIG
      PRINT 67,DELG
C*********************************************************************
C  FIND THE DIAGONAL TERMS OF THE IMPEDANCE MATRIX.
C*********************************************************************
      DO 2 II=1,4
      IF(II.GT.2) GO TO 4
      A3=A1      $ DEL=DEL1
      IF(II.EQ.2)DEL=DELG
      GO TO 7
```

```
 4  A3=A2
    DEL=DEL2
    IF(II.EQ.3) DEL=DELG
 7  HDEL=DEL/2.0
    D=HDEL/A3
    D1=2.0*ALOG(D+SQRT(1.0+D**2.0))
    D2=D1-JK*DEL
    R=SQRT(HDEL**2.0+A3**2.0)
    RRE=1.0/R  $ RSQ=RRE**2.0
    D3=-DEL*(RSQ+JK*RRE)*GRE(R)/(K**2)
    IF(II.LT.2) D7=0.0
    IF(II.GE.2) D7=CMPLX(0.0,-4.0*PI/(OME*MU))*ZI
    D6(II)=D2+D3+D7
 2  CONTINUE
    B1=(4.0*PI)/(OME*MU)
    B2=CMPLX(0.0,-B1)
    IF(ITEST-2) 44,47,47
 47 CALL MAGRIN(NP,Z,EZ)
    DO 45 IR=1,NP
 45 B(IR)=B2*EZ(IR)
    GO TO 3
 44 DO 48 NN=1,NP
    B(NN)=0.0
    IF(NN.EQ.NC) B(NN)=B2*(1.0/DELG)
 48 CONTINUE
C**********************************************************************
C  THIS SECTION FINDS ELEMENTS OF THE IMPEDANCE MATRIX.
C**********************************************************************
 3  DO 15 I=1,NP
    DO 15 JJ=1,NP
    IF(I.EQ.JJ) GO TO 17
    A3=A2
    IF(I.LE.NC) A3=A1
    R=SQRT((Z(I)-Z(JJ)) **2.0+A3**2.0)
    DEL=DEL1
    IF(JJ.GE.M3) DEL=DELG
    IF(JJ.GT.M4) DEL=DEL2
    HDEL=DEL/2.0
    E1=Z(I)-Z(JJ)+HDEL     $ E2=Z(I)-Z(JJ)-HDEL
    R1=SQRT(E1**2.0+A3**2.0)
    R2=SQRT(E2**2.0+A3**2.0)
    F1=1.0/R1  $ F2=F1**2.0
    E3=-E1*(F2+JK*F1)*GRE(R1)
    F3=1.0/R2   $ F4=F3**2.0
    E4=-E2*(F4+JK*F3)*GRE(R2)
    G(I,JJ)=(E3-E4)/(K**2)+DEL*GRE(R)
    GO TO 15
 17 IF(I-NC) 31,32,33
 31 J=1        $ GO TO 34
 32 J=2      $ GO TO 34
 33 J=4
 34 G(I,JJ)=D6(J)
 15 CONTINUE
    MP=NP+1
    DO 55 L=1,NP
    G(L,MP)=B(L)
 55 CONTINUE
    CALL CMATPAC(-1,G,NP,1,DET,1.0E-200)
    AYIN=CABS(G(NC,MP))
    PRINT 111,AYIN,G(NC,MP)
    ZIN=1.0/G(NC,MP)       $ AZIN=CABS(ZIN)
```

```
      PHI=ATAN(AIMAG(ZIN)/REAL(ZIN))*180.0/(2.0*PI)
      PRINT 107,AZIN,ZIN,PHI
      PRINT 102
      DO 95 I1=1,NP
      AMPI=CABS(G(I1,MP))
      PRINT 23,I1,Z(I1),AMPI,G(I1,MP)
   95 CONTINUE
   56 CONTINUE
C**********************************************************************
C  READ AND WRITE FORMATS.
C**********************************************************************
   23 FORMAT(10X,I3,4X,4(F8.6,4X),/)
   39 FORMAT(1H0,20X,2HN=,I3,4X,3HM1=,I3,4X,3HM2=,I3,4X,3HNG=,I3,,2X,
     **ITEST=*,I3,/)
   57 FORMAT(1H0,20X,4HEPR=,F8.3,4X,4HZIG=,F8.4,/)
   67 FORMAT(1H0,30X,5HDELG=,F8.6,/)
  81  FORMAT(1H0,10X,6HALPHA=,E12.5,4X,5HBETA=,E12.5,/)
  100 FORMAT(5(I3))
  101 FORMAT(1H0,5X,5HFREQ=,F6.2,4HMHZ ,2X,2HA=,F7.5,2X,2HB=,F7.5,2X,4H
     *ZI=,F7.1,2X,4HZIG=,F6.2,2X,4HEPR=,F5.1,2X,3HH1=,F7.4,2X,3HH2=,F7.4
     *,/)
102   FORMAT(1H0,135(*+*),/)
 103 FORMAT(F12.1,2(F9.5),F9.1,F6.2,F5.1,2(F6.1))
107   FORMAT(1H0,20X,9HABS(ZIN)=,E12.5,4X,4HZIN=,2(E12.5,2X),4HPHI=,
     *E12.5,/)
111   FORMAT(1H0,20X,9HABS(YIN)=,E12.5,4X,4HYIN=,2(E12.5,2X),/)
      END
C **********************************************************************
      SUBROUTINE MAGRIN(NP,Z,EZ)
C **********************************************************************
      COMMON/MAGFCT/PI,ZZ,RO,ROP,EROP   /MAGFCP/ZZI,RRO,RROP,EEJK
      COMMON/EZIMAG/A1,A2,JK,DELG
      DIMENSION Z(60),F(4),EZ(60)
      COMPLEX K,JK,EEJK,SUM1,EZ,F,SUM4,SUM5,SUM6,PATCH
      REAL MU,LA
      PI=4.0*ATAN(1.0)
      EEJK=JK
      DA=0.001*A1
      XX=DELG/2.0
      FACT=1.0/(8.0*PI*XX)
      XEND=XX
      ROP=A2
      RROP=ROP
      X1=-XX
      ERR=0.001
      EPS=XX/100.0
      EPOR=EPS/ROP
      PATCH=PI*EPS*0.5-JK*PI*0.25*(EPS**2.0)
      DO 20 INDEX=1,NP
      ZZ=Z(INDEX)
      ZZI=ZZ
      DO 21 J=1,2
      RO=0.9*A1-(2-J)*DA
      RRO=RO
      IF((RO.EQ.ROP).AND.(INDEX.EQ.NC)) GO TO 23
      CALL SIMCON(INDEX,X1,XEND,ERR,25,SUM1,NOI,R)
      F(J)=SUM1*RO*ROP*2.0
      GO TO 21
   23 II=100+INDEX
      CALL SIMCON(INDEX,EPS,XEND,ERR,25,SUM4,NOI,R)
      CALL SIMCON(II,0.0,EPS,ERR,25,SUM5,NOI,R)
```

```
   41 FORMAT(1HO,50X,2(E12.5,4X,E12.5),/)
      F(J)=4.0*RO*(ROP*SUM4+ROP*SUM5+PATCH)
   21 CONTINUE
      EZ(INDEX)=FACT*(F(2)-F(1))/(RO*DA)
      PRINT 22,Z(INDEX),RO,EZ(INDEX)
   22 FORMAT(1HO,20X,2HZ=,F9.6,4X,4HRAD=,F9.6,4X,3HEF=,F9.4,2X,F9.4,/)
   20 CONTINUE
   59 CONTINUE
      END
C*********************************************************************
      SUBROUTINE SIMCON(INDEX,X1,XEND,TEST,LIM,AREA,NOI,R)
C*********************************************************************
      COMPLEX AREA,ODD,EVEN,AREA1,ENDS,FCT
      NOI=0
      ODD=0.0
      INT=1
      V=1.0
      EVEN=0.0
      AREA1=0.0
      ENDS=FCT(INDEX,X1)+FCT(INDEX,XEND)
    2 H=(XEND-X1)/V
      ODD=EVEN+ODD
      X=X1+.5*H
      EVEN=0.0
      DO 3 I=1,INT
      EVEN=EVEN+FCT(INDEX,X)
      X=X+H
    3 CONTINUE
      AREA=(ENDS+4.0*EVEN+2.0*ODD)*H/6.0
      NOI=NOI+1
      A3=CABS(AREA)
      IF((A3.LE.1.E-14).AND.(NOI.LE.2)) GO TO 4
      IF((A3.LE.1.E-14).AND.(NOI.GE.2)) GO TO 50
      R=CABS((AREA1-AREA)/AREA)
      R=CABS((AREA1-AREA)/AREA)
   31 IF(R-TEST) 32,32,4
   32 RETURN
    4 AREA1=AREA
      INT=2*INT
      V=2.0*V
      GO TO 2
   50 AREA=1.E-14
      RETURN
      END
C*********************************************************************
      COMPLEX FUNCTION FCT(INDEX,ZP)
C*********************************************************************
      COMMON/MAGFCT/PI,ZZ,RO,ROP,EPOR      /FCTFCT/ZZP
      COMPLEX SUM2
      ZZP=ZP
      IF(INDEX.GT.100) GO TO 41
      CALL SIMCOP(INDEX,0.0,PI,0.001,25,SUM2,NOI,R)
      FCT=SUM2
      RETURN
   41 CALL SIMCOP(INDEX,EPOR,PI,0.001,25,SUM2,NOI,R)
      FCT=SUM2
      RETURN
      END
C*********************************************************************
      SUBROUTINE SIMCOP(INDEX,X1,XEND,TEST,LIM,AREA,NOI,R)
C*********************************************************************
```

```
      COMPLEX AREA,ODD,EVEN,AREA1,ENDS,FCTP
      NOI=0
      ODD=0.0
      INT=1
      V=1.0
      EVEN=0.0
      AREA1=0.0
      ENDS=FCTP(INDEX,X1)+FCTP(INDEX,XEND)
    2 H=(XEND-X1)/V
      ODD=EVEN+ODD
      X=X1+.5*H
      EVEN=0.0
      DO 3 I=1,INT
      EVEN=EVEN+FCTP(INDEX,X)
      X=X+H
    3 CONTINUE
      AREA=(ENDS+4.0*EVEN+2.0*ODD)*H/6.0
      NOI=NOI+1
      A3=CABS(AREA)
      IF((A3.LE.1.E-14).AND.(NOI.LE.2)) GO TO 4
      IF((A3.LE.1.E-14).AND.(NOI.GE.2)) GO TO 50
      R=CABS((AREA1-AREA)/AREA)
      IF(NOI-LIM) 31,32,32
   31 IF(R-TEST) 32,32,4
   32 RETURN
    4 AREA1=AREA
      INT=2*INT
      V=2.0*V
      GO TO 2
   50 AREA=1.E-14
      RETURN
      END
C*********************************************************************
      COMPLEX FUNCTION FCTP(INDEX,PHI)
C*********************************************************************
      COMPLEX GRE,EEJK
      COMMON/MAGFCP/ZZI,RRO,RROP,EEJK    /FCTFCT/ZZP
      COPH=COS(PHI)
      R1=SQRT((ZZI-ZZP)**2.0+RRO**2.0+RROP**2.0-2.0*RRO*RROP*COPH)
      FCTP=GRE(R1)*COPH
      RETURN
      END
C*********************************************************************
      COMPLEX FUNCTION GRE(RR)
C*********************************************************************
      COMMON/EFGRE/JJK
      COMPLEX JJK
      GRE=CEXP(-JJK*RR)/RR
      RETURN
      END
```

```
FREQ=600.MHZ A=.00043 B=.00043 ZI=).0 ZIG=1.11 EPR=76.7 H1=.0075 H2=.0150
        N= 24    M1=  8    M2= 16    NG=  1    ITEST=  2

    ALPHA=  .23370E+02   BETA=  .11251E+03

            EPR=  76.700   ZIG=  1.1100

                      DELG=  .001000

            Z=   .007531     RAD=  .000387   EF=     .2553    -.0580
            Z=   .006594     RAD=  .000387   EF=     .3715    -.0641
            Z=   .005656     RAD=  .000387   EF=     .5723    -.0718
            Z=   .004719     RAD=  .000387   EF=     .9556    -.0817
            Z=   .003781     RAD=  .000387   EF=    1.7953    -.0957
            Z=   .002844     RAD=  .000387   EF=    4.0563    -.1174
            Z=   .001906     RAD=  .000387   EF=   12.6046    -.1570
            Z=   .000969     RAD=  .000387   EF=   72.4910    -.2482
            Z=  -.000000     RAD=  .000387   EF=  830.8496    -.3941
            Z=  -.000969     RAD=  .000387   EF=   72.4910    -.2482
            Z=  -.001906     RAD=  .000387   EF=   12.6046    -.1570
            Z=  -.002844     RAD=  .000387   EF=    4.0563    -.1174
            Z=  -.003781     RAD=  .000387   EF=    1.7953    -.0957
            Z=  -.004719     RAD=  .000387   EF=     .9556    -.0817
            Z=  -.005656     RAD=  .000387   EF=     .5723    -.0718
            Z=  -.006594     RAD=  .000387   EF=     .3715    -.0641
            Z=  -.007531     RAD=  .000387   EF=     .2553    -.0580
            Z=  -.008469     RAD=  .000387   EF=     .1829    -.0528
            Z=  -.009406     RAD=  .000387   EF=     .1351    -.0484
            Z=  -.010344     RAD=  .000387   EF=     .1020    -.0445
            Z=  -.011281     RAD=  .000387   EF=     .0783    -.0410
            Z=  -.012219     RAD=  .000387   EF=     .0607    -.0378
            Z=  -.013156     RAD=  .000387   EF=     .0474    -.0348
            Z=  -.014094     RAD=  .000387   EF=     .0371    -.0321
            Z=  -.015031     RAD=  .000387   EF=     .0290    -.0295
            ABS(YIN)=  .52670E-01.   YIN=  .48716E-01    .20023E-01
            ABS(ZIN)=  .18986E+02    ZIN=  .17561E+02   -.72176E+01
                                               PHI= -.11172E+02

+ + + + + + + + + + + + + + + + + + + + + + + + + + + + + + + + + +
```

1	.007531	.009232	.009135	.001334
2	.006594	.015583	.015386	.002467
3	.005656	.021343	.021017	.003716
4	.004719	.026729	.026229	.005146
5	.003781	.031829	.031091	.006812
6	.002844	.036706	.035637	.008791
7	.001906	.041455	.039909	.011216
8	.000969	.046337	.044033	.014428
9	-.000000	.052670	.048716	.020023
10	-.000969	.049592	.047652	.013736
11	-.001906	.048082	.047058	.009870
12	-.002844	.046793	.046290	.006840
13	-.003781	.045427	.045221	.004325
14	-.004719	.043869	.043813	.002216
15	-.005656	.042062	.042059	.000462
16	-.006594	.039975	.039964	-.000965
17	-.007531	.037594	.037537	-.002084
18	-.008469	.034913	.034792	-.002910
19	-.009406	.031932	.031744	-.003457
20	-.010344	.028654	.028409	-.003738
21	-.011281	.025082	.024797	-.003767
22	-.012219	.021215	.020914	-.003557
23	-.013156	.017038	.016750	-.003120
24	-.014094	.012499	.012255	-.002459
25	-.015031	.007436	.007272	-.001553

```
C*******************************************************************
C   THIS PROGRAM FINDS INPUT IMPEDANCE OF INSULATED PROBE.
C*******************************************************************
      PROGRAM INPIMP(INPUT,OUTPUT)
      DIMENSION S(10),RR(10),BJRE(40),BJIM(40),YRE(12),YIM(12),
     $ZIN(4)
      COMPLEX JO(2),J1(2),GAMA(2),ZC(2)
      COMPLEX YC,HO2,H12,Z1I,Z2I,ZEL,K1,K2,X,SHGH1,ER,ERR,D,KL,KD,ZI,
     *GH1,GH2,GH3,GH4,Z,ARG,CHGH1,CHGH2,SHGH2,TETA1,TETA2,ZIN
      REAL MU,L
      N=3
      READ 71,H1,H2
      PI=ATAN(1.)*4.0
      ZIG1=5.777E+7
      EPR1=1.0
      AL=0.0
      BE=0.0
      READ 103,ZIGD,EPRD
      PRINT 104,ZIGD,EPRD
      READ 52,ZIG2,EPR2
      READ 100,A1,A2,A3
      PRINT 101,A1,A2,A3
      READ 106,FREQ
      PRINT 108,FREQ
      OME=2.0*PI*FREQ
      EP1=EPR1*1.0E-9/(36.0*PI)
      EPD=EPRD*1.0E-9/(36.0*PI)
      MU=4.0*PI*1.0E-7
      K1=CSQRT(CMPLX(OME**2.0*MU*EP1,-OME*MU*ZIG1))
      DO 7 J=1,1
      IF(J.EQ.1) A=A1
      IF(J.EQ.2) A=A2
      X=K1*A
      JO(J)=CSQRT(2.0/PI*X)*CCOS(X-PI/4.0)
    7 J1(J)=CSQRT(2.0/PI*X)*CCOS(X-3.0*PI/4.0)
      EP2=EPR2*1.0E-9/(36.0*PI)
      K2=CSQRT(CMPLX(OME**2.0*MU*EP2,-OME*MU*ZIG2))
      PRINT 33,K1,K2
      DO 10 I=1,1
      IF(I.EQ.1) GO TO 1
      A=A2
      GO TO 3
    1 A=A1
    3 G=2.0*PI*ZIGD/ALOG(A3/A)
      C=2.0*PI*EPD/ALOG(A3/A)
      YC=CMPLX(G,OME*C)
      ARG=K2*A3
      U=REAL(ARG)
      V=AIMAG(ARG)
      CALL COMBES(U,V,AL,BE,N,BJRE,BJIM,YRE,YIM)
      HO2=CMPLX(BJRE(1),BJIM(1))-CMPLX(0.0,1.0)*CMPLX(YRE(1),YIM(1))
      H12=CMPLX(BJRE(2),BJIM(2))-CMPLX(0.0,1.0)*CMPLX(YRE(2),YIM(2))
      PRINT 31,JO(I),J1(I)
      PRINT30,HO2,H12
      Z1I=CMPLX(0.0,1.0)*K1/(2.0*PI*A*ZIG1)
      Z2I=(-K2*HO2)/(2.0*PI*A3*CMPLX(ZIG2,OME*EP2)*H12)
      ZE=(OME*MU/(2.0*PI))*ALOG(A3/A)
      ZEL=CMPLX(0.0,ZE)
      ZI=Z1I+Z2I
      RI=REAL(ZI)
      XI=AIMAG(ZI)
      PL=RI/(XI+ZE)
      P=SQRT(1.0+PL**2.0)
```

```
      FP=SQRT(0.5*(P+1.0))
      GP=SQRT(0.5*(P-1.0))
      KD=CSQRT(-YC*ZEL)
      KL=KD*SQRT(1.0+XI/ZE)*(FP-CMPLX(0.0,1.0)*GP)
      ALPHA=-AIMAG(KL)
      BETA=REAL(KL)
      Z=Z1I+Z2I+ZEL
      R=REAL(Z)
      L=AIMAG(Z)/OME
      HC=(OME*(R*C-L*G))/(OME**2.0*L*C+R*G)
      FHC=SQRT(0.5*(SQRT(1.0+HC**2.0)+1.0))
      PHC=SQRT(0.5*(SQRT(1.0+HC**2.0)-1.0))
      ZC(I)=SQRT((OME**2.0*L*C+R*G)/((OME*C)**2.0+G**2.0))*(FHC-
     *CMPLX(0.0,1.0)*PHC)
      PRINT 40,ZC(I)
      PRINT 21,I,ALPHA,BETA
      GAMA(I)=CMPLX(ALPHA,BETA)
   10 CONTINUE
      IF(A1.NE.A2) GO TO 8
      GAMA(2)=GAMA(1)
      ZC(2)=ZC(1)
 8    DO 51 II=1,3
      IF(II-2) 73,74,75
   73 TETA1=CMPLX(0.0,PI/2.0)
      TETA2=TETA1
      GO TO 76
   74 TETA1=0.0
      TETA2=CMPLX(0.0,PI/2.0)
      GO TO 76
   75 TETA2=0.0
      TETA1=0.0
   76 GH2=CEXP(GAMA(2)*H2+TETA2)
      GH1=CEXP(GAMA(1)*H1+TETA1)
      GH3=1.0/GH1
      GH4=1.0/GH2
      SHGH1=(GH1-GH3)/2.0
      SHGH2=(GH2-GH4)/2.0
      CHGH1=(GH1+GH3)/2.0
      CHGH2=(GH2+GH4)/2.0
      ZIN(II)=(ZC(1)*CHGH1*SHGH2+ZC(2)*SHGH1*CHGH2)/(SHGH1*SHGH2)
      PRINT 25,TETA1,TETA2,ZIN(II)
 51   CONTINUE
C*****************************************************************
C   INPUT,OUTPUT FORMATS.
C*****************************************************************
 21   FORMAT(1H0,20X,2HI=,I2,4X,6HALPHA=,F12.5,4X,5HBETA=,F12.5,//)
   25 FORMAT(1H0,20X,*TETA1=*,2(F5.2,2X),2X,*TETA2=*,2(F5.2,2X),2X,
     **ZIN=*,2(F12.3,2X),/)
 30   FORMAT(1H0,20X,4HH02=,2(E12.5,2X),4HH12=,2(E12.5,2X),/)
 31   FORMAT(1H0,20X,3HJ0=,2(E12.5,2X),3HJ1=,2(E12.5,2X),/)
 33   FORMAT(1H0,20X,3HK1=,2(E12.5,2X),3HK2=,2(E12.5,2X),/)
 40   FORMAT(1H0,20X,25HCHARACTERISTIC IMPEDANCE=,2(F12.5,4X),/)
 52   FORMAT(F8.4,F5.2)
   58 FORMAT(1H0,20X,5HZIG2=,F8.4,2X,5HEPR2=,F5.2,/)
 71   FORMAT(2(F8.5))
  100 FORMAT(5(F8.5))
 101  FORMAT(1H0,20X,3HA1=,F8.5,2X,3HA2=,F8.5,2X,3HA3=,F8.5,/)
  103 FORMAT(2(F6.2))
 104  FORMAT(1H0,20X,5HZIGD=,F6.2,2X,5HEPRD=,F6.2,/)
  106 FORMAT(F12.1)
  108 FORMAT(1H0,20X,*FREQUENCY=*,F12.1,/)
```

```
      END
      SUBROUTINE COMBES(X,Y,ALPHA,BETA,N,BJRE,BJIM,YRE,YIM)
      DIMENSION BJRE(40),BJIM(40),YRE(12),YIM(12)
      CALL BEGIN(X,Y,N,K,R)
      CALL JRECUR(X,Y,ALPHA,BETA,K,R,BJRE,BJIM)
      CALL JSUM(ALPHA,BETA,K,BJRE,BJIM,SUMRA,SUMIA)
      CALL FACTOR(X,Y,ALPHA,BETA,Q,R)
      CALL JNORM(K,Q,R,SUMRA,SUMIA,BJRE,BJIM)
7     CALL YSUM (X,Y,ALPHA,BETA,K,BJRE,BJIM,ASUMR,ASUMI)
8     CALL YGNU (X,Y,ALPHA,BETA,Q,R,ASUMR,ASUMI,BJRE,BJIM,YRE,YIM)
9     CALL WRONSK (X,Y,BJRE,BJIM,YRE,YIM)
       BJSQ=BJRE(1)**2+BJIM(1)**2
       IF(BJSQ-.00000005) 14,14,15
 14   CALL YSUMP(X,Y,ALPHA,BETA,K,BJRE,BJIM,ASUMR,ASUMI)
      CALL YGNUP(X,Y,ALPHA,BETA,Q,R,ASUMR,ASUMI,BJRE,BJIM,YRE,YIM)
15    IF (N-1)10,12,11
10    IF (N)13,12,12
13    CALL NEGN (X,Y,ALPHA,BETA,N,BJRE,BJIM,YRE,YIM)
      GO TO 12
  11  CALL YRECUR(X,Y,N,BJRE,BJIM,YRE,YIM)
12    RETURN
       END
CBES402  BEGIN SUBROUTINE                          PART 2 OF 16
      SUBROUTINE BEGIN(X,Y,N,K,R)
      SSQ=X**2+Y**2
      KTEN=SQRT(SSQ)+20.0
      NTEN=IABS(N)+10
      M=MAX0(KTEN,NTEN) /2
      K=2*M+1
          R = K + 1
      RETURN
      END
CBES403  JRECUR SUBROUTINE                         PART 3 OF 16
      SUBROUTINE JRECUR(X,Y,ALPHA,BETA,K,R,BJRE,BJIM)
      DIMENSION BJRE(100),BJIM(100)
      RALPHA=R+ALPHA
      SSQ=X**2+Y**2
      BJRE(K+2)=0
      BJIM(K+2)=0
      BJRE(K+1)=1.0E-37
      BJIM(K+1)=0.0
      DO4I=1,K
      L1=K+1-I
      RALPHA=RALPHA-1.0
      A=((2.0*X*RALPHA)+(2.0*BETA*Y))/SSQ
      B=((-2.0*Y*RALPHA)+(2.0*BETA*X))/SSQ
      BJRE(L1)=(A*BJRE(L1+1))-(B*BJIM(L1+1))-BJRE(L1+2)
4     BJIM(L1)=(B*BJRE(L1+1))+(A*BJIM(L1+1))-BJIM(L1+2)
      RETURN
      END
CBES404  JSUM SUBROUTINE                           PART 4 OF 16
      SUBROUTINE JSUM(ALPHA,BETA,K,BJRE,BJIM,SUMRA,SUMIA)
      DIMENSION BJRE(100),BJIM(100)
801   SUMRA=(BJRE(3)*(ALPHA+2.0))-(BJIM(3)*BETA)
      SUMIA=(BETA*BJRE(3))+((ALPHA+2.0)*BJIM(3))
      GRE=1.0
      GIM=0
      S=1.0
      DO6I=5,K,2
      S=S+1.0
      GREN=((GRE*(ALPHA+S-1.0))-(BETA*GIM))/S
```

```
      GIM=((GIM*(ALPHA+S-1.0))+(BETA*GRE))/S
      GRE=GREN
      ALPTS=ALPHA+2.0*S
      GJR=GRE*BJRE(I)
      GJI=GIM*BJIM(I)
      GJRI=GRE*BJIM(I)
      GJIR=GIM*BJRE(I)
      SUMRB=ALPTS*(GJR-GJI)-BETA*(GJIR+GJRI)+SUMRA
      SUMIB=ALPTS*(GJIR+GJRI)-BETA*(GJI-GJR)+SUMIA
      IF(SUMRA)15,21,15
   15 IF(ABS((SUMRB/SUMRA)-1.0)-.00000005)21,21,10
21    IF(SUMIA)20,11,20
20    IF(ABS((SUMIB/SUMIA)-1.0)-.00000005)11,11,10
10    SUMRA=SUMRB
6     SUMIA=SUMIB
   11 RETURN
       END
CBES405  FACTOR SUBROUTINE                          PART 5 OF 16
      SUBROUTINE FACTOR(X,Y,ALPHA,BETA,Q,R)
      CALL LOGGAM(ALPHA+1.0,BETA,U,V)
      CALL COMLOG(X,Y,A1,B1)
      A2=ALPHA*A1-BETA*B1
      B2=BETA*A1+ALPHA*B1
      A2=-A2
      B2=-B2
      CALL COMEXP(A2,B2,A3,B3)
      A4=.6931471806*ALPHA
      B4=.6931471806*BETA
      CALL COMEXP(A4,B4,A5,B5)
      A6=A3*A5-B3*B5
      B6=B3*A5+A3*B5
      CALL COMEXP(U,V,A7,B7)
      Q=A6*A7-B6*B7
      R=B6*A7+A6*B7
      RETURN
       END
CBES406  COMLOG SUBROUTINE                          PART 6 OF 16
C      COMPLEX LOGARITHM - BRANCH CUT ON NEGATIVE REAL AXIS
      SUBROUTINE COMLOG(X,Y,A,B)
      PI=3.141592654
      A=.5*ALOG(X*X+Y*Y)
      IF(X)5,1,4
1     B=.5*PI
      IF(Y)2,3,8
2     B=-B
      GO TO 8
3     B=0.
      GO TO 8
    4 B=ATAN(Y/X)
      GO TO 8
    5 B=ATAN(Y/X)
      IF(Y)6,7,7
6     B=B-PI
      GO TO 8
7     B=B+PI
8     RETURN
       END
CBES407  COMEXP SUBROUTINE                          PART 7 OF 16
      SUBROUTINE COMEXP(X,Y,A,B)
      C=EXP(X)
      A=C*COS(Y)
```

```
      B=C*SIN(Y)
      RETURN
       END
CBES408  JNORM SUBROUTINE                            PART 8 OF 16
      SUBROUTINE JNORM(K,Q,R,SUMRA,SUMIA,BJRE,BJIM)
      DIMENSION BJRE(100),BJIM(100)
      S=((SUMRA+BJRE(1))*Q)-((SUMIA+BJIM(1))*R)
      T=((SUMIA+BJIM(1))*Q)+((SUMRA+BJRE(1))*R)
      IF(ABS(S)-ABS(T))100,101,101
101   TS=T/S
      TSSQ=S*(1.0+(TS**2))
12    DO13I=1,K
      BJREN=(BJRE(I)+BJIM(I)*TS)/TSSQ
      BJIM(I)=(BJIM(I)-BJRE(I)*TS)/TSSQ
13    BJRE(I)=BJREN
      GO  TO  14
100   ST=S/T
      STSQ=T*((ST**2)+1.0)
102   DO103I=1,K
      BJREN=(BJRE(I)*ST+BJIM(I))/STSQ
      BJIM(I)=(BJIM(I)*ST-BJRE(I))/STSQ
103   BJRE(I)=BJREN
   14 RETURN
       END
CBES409  YSUM SUBROUTINE                             PART 9 OF 16
      SUBROUTINE YSUM (X,Y,ALPHA,BETA,K,BJRE,BJIM,ASUMR,ASUMI)
      DIMENSION BJRE(100),BJIM(100)
      A1=ALPHA-1.0
      A2=A1-1.0
      A3=A1+ALPHA
      A4=BETA**2
      A5=2.0*A4
      ABSQ=(-A1)**2+A4
      GAMRE=((2.0+ALPHA)*(-A1)-A4)/ABSQ
      GAMIM=(BETA*3.0)/ABSQ
      ASUMR=GAMRE*BJRE(3)-GAMIM*BJIM(3)
      ASUMI=GAMIM*BJRE(3)+GAMRE*BJIM(3)
      T=1.0
      DO 500 I=5,K,2
      T=T+1.0
      B1=2.0*T
      F1=B1+ALPHA
      F2=A3+T
      F3=A1+T
      F5=T-ALPHA
      F6=A2+B1
      G1=F1*F2-A5
      G2=(F2+2.0*F1)*BETA
      H1=G1*F3-G2*BETA
      H2=G2*F3+G1*BETA
      P1=F5*F6+A4
      P2=(F5-F6)*BETA
      P3=P1**2+P2**2
      CRE=((H1*P1+H2*P2)/P3)/T
      CIM=((H2*P1-H1*P2)/P3)/T
      TEMP=-(CRE*GAMRE-CIM*GAMIM)
      GAMIM=-(CIM*GAMRE+CRE*GAMIM)
      GAMRE=TEMP
      BSUMR=GAMRE*BJRE(I)-GAMIM*BJIM(I)+ASUMR
      BSUMI=GAMIM*BJRE(I)+GAMRE*BJIM(I)+ASUMI
      IF(ABS((BSUMR/ASUMR)-1.0)-.00000005)521,521,510
```

```
521   IF(ASUMI)520,511,520
520   IF(ABS((BSUMI/ASUMI)-1.0)-.00000005)511,511,510
510   ASUMR=BSUMR
500   ASUMI=BSUMI
511   RETURN
       END
CBES410  YGNU SUBROUTINE                          PART 10 OF 16
      SUBROUTINE YGNU(X,Y,ALPHA,BETA,Q,R,ASUMR,ASUMI,BJRE,BJIM,YRE,YIM)
      DIMENSION BJRE(100),BJIM(100),YRE(50),YIM(50)
      PI=3.141592654
      TPI=2.0/PI
      QRE=TPI*(Q**2-R**2)
      QIM=TPI*2.0*Q*R
      DRE=QRE*ASUMR-QIM*ASUMI
      DIM=QIM*ASUMR+QRE*ASUMI
      IF(ALPHA)1,2,1
2     IF(BETA)1,3,1
3     CALL YZERO(X,Y,ALPRE,ALPIM)
      GO TO 720
1     PALPHA=PI*ALPHA
      COX=COS(PALPHA)
      SIX=SIN(PALPHA)
      EXY=EXP(PI*BETA)
      EXY1=1.0/EXY
      COSH=.5*(EXY+EXY1)
      SINH=.5*(EXY-EXY1)
      DEN=(SIX*COSH)**2+(COX*SINH)**2
      ERE=(SIX*COX)/DEN
      EIM=(-COSH*SINH)/DEN
      ABSQ3=2.0*(ALPHA**2+BETA**2)
      ALPRE=ERE-((QRE*ALPHA+BETA*QIM)/ABSQ3)
      ALPIM=EIM-((QIM*ALPHA-BETA*QRE)/ABSQ3)
720   YRE(1)=ALPRE*BJRE(1)-ALPIM*BJIM(1)+DRE
      YIM(1)=ALPIM*BJRE(1)+ALPRE*BJIM(1)+DIM
      RETURN
       END
CBES411  YZERO SUBROUTINE                         PART 11 OF 16
      SUBROUTINE YZERO(X,Y,ALPRE,ALPIM)
      TPI=2.0/3.141592654
      CALL COMLOG(X,Y,A,B)
      ALPRE=TPI*(-.1159315157+A)
      ALPIM=TPI*B
      RETURN
       END
CBES412  WRONSK SUBROUTINE                        PART 12 OF 16
      SUBROUTINE WRONSK(X,Y,BJRE,BJIM,YRE,YIM)
      DIMENSION BJRE(100),BJIM(100),YRE(50),YIM(50)
      SSQ=X**2+Y**2
      TPI=2.0/3.141592654
      AZRE=TPI*X/SSQ
      AZIM=-TPI*Y/SSQ
      ZRE=BJRE(2)*YRE(1)-BJIM(2)*YIM(1)
      ZIM=BJIM(2)*YRE(1)+BJRE(2)*YIM(1)
      BZRE=ZRE-AZRE
      BZIM=ZIM-AZIM
      BJSQ=BJRE(1)**2+BJIM(1)**2
      CZRE=BJRE(1)/BJSQ
      CZIM=(-BJIM(1))/BJSQ
      YRE(2)=BZRE*CZRE-BZIM*CZIM
      YIM(2)=BZIM*CZRE+BZRE*CZIM
      RETURN
```

```
      END
CBES413  NEGN SUBROUTINE                          PART 13 OF 16
      SUBROUTINE NEGN(X,Y,ALPHA,BETA,N,BJRE,BJIM,YRE,YIM)
      DIMENSION BJRE(100),BJIM(100),YRE(50),YIM(50)
      L=IABS(N)+1
      SSQ=X**2+Y**2
      TX=2.0*X
      TY=2.0*Y
      RALPHA=ALPHA
      A=(TX*RALPHA+TY*BETA)/SSQ
      B=(-TY*RALPHA+TX*BETA)/SSQ
      BJRE(2)=A*BJRE(1)-B*BJIM(1)-BJRE(2)
      BJIM(2)=B*BJRE(1)+A*BJIM(1)-BJIM(2)
      YRE(2)=A*YRE(1)-B*YIM(1)-YRE(2)
      YIM(2)=B*YRE(1)+A*YIM(1)-YIM(2)
      IF(L-3)3,2,2
    2 DO 1 I=3,L
      RALPHA=RALPHA-1.0
      A=(TX*RALPHA+TY*BETA)/SSQ
      B=(-TY*RALPHA+TX*BETA)/SSQ
      BJRE(I)=A*BJRE(I-1)-B*BJIM(I-1)-BJRE(I-2)
      BJIM(I)=B*BJRE(I-1)+A*BJIM(I-1)-BJIM(I-2)
      YRE(I)=A*YRE(I-1)-B*YIM(I-1)-YRE(I-2)
1     YIM(I)=B*YRE(I-1)+A*YIM(I-1)-YIM(I-2)
    3 CONTINUE
      RETURN
      END
CBES414  YRECUR SUBROUTINE                        PART 14 OF 16
      SUBROUTINE YRECUR(X,Y,N,BJRE,BJIM,YRE,YIM)
      DIMENSION BJRE(100),BJIM(100),YRE(50),YIM(50)
      SSQ=X**2+Y**2
      TPI=2.0/3.141592654
      AZRE=TPI*X/SSQ
      AZIM=-TPI*Y/SSQ
      L=N+1
      IF(L-3)3,2,2
    2 DO 1 I=3,L
      ZRE=BJRE(I)*YRE(I-1)-BJIM(I)*YIM(I-1)
      ZIM=BJIM(I)*YRE(I-1)+BJRE(I)*YIM(I-1)
      BZRE=ZRE-AZRE
      BZIM=ZIM-AZIM
      BJSQ=BJRE(I-1)**2+BJIM(I-1)**2
      CZRE=BJRE(I-1)/BJSQ
      CZIM=(-BJIM(I-1))/BJSQ
      YRE(I)=BZRE*CZRE-BZIM*CZIM
    1 YIM(I)=BZIM*CZRE+BZRE*CZIM
    3 CONTINUE
      RETURN
      END
CBES415  YGNUP SUBROUTINE                         PART 15 OF 16
      SUBROUTINE YGNUP(X,Y,ALPHA,BETA,Q,R,ASUMR,ASUMI,BJRE,BJIM,YRE,YIM)
      DIMENSION BJRE(100),BJIM(100),YRE(50),YIM(50)
      PI=3.141592654
      TPI=2.0/PI
      QRE=TPI*(Q**2-R**2)
      QIM=TPI*2.0*Q*R
      DRE=QRE*ASUMR-QIM*ASUMI
      DIM=QIM*ASUMR+QRE*ASUMI
      IF(ALPHA)1,2,1
2     IF(BETA)1,3,1
3     CALL YZERO(X,Y,ALPRE,ALPIM)
```

```
      GO TO 720
1     PALPHA=PI*ALPHA
      COX=COS(PALPHA)
      SIX=SIN(PALPHA)
      EXY=EXP(PI*BETA)
      EXY1=1.0/EXY
      COSH=.5*(EXY+EXY1)
      SINH=.5*(EXY-EXY1)
      DEN=(SIX*COSH)**2+(COX*SINH)**2
      ERE=(SIX*COX)/DEN
      EIM=(-COSH*SINH)/DEN
      ABSQ3=2.0*(ALPHA**2+BETA**2)
      ALPRE=ERE-((QRE*ALPHA+BETA*QIM)/ABSQ3)
      ALPIM=EIM-((QIM*ALPHA- ETA*QRE)/ABSQ3)
720   TRE=ALPRE*BJRE(2)-ALPIM*BJIM(2)+DRE
      TIM=ALPIM*BJRE(2)+ALPRE*BJIM(2)+DIM
      ALPRE=-(Q*X+R*Y)/(X**2+Y**2)
      ALPIM=-(X*R-Q*Y)/(X**2+Y**2)
      YRE(2)=ALPRE*BJRE(1)-ALPIM*BJIM(1)+TRE
      YIM(2)=ALPIM*BJRE(1)+ALPRE*BJIM(1)+TIM
      RETURN
       END
CBES416  YSUMP SUBROUTINE                          PART 16 OF 16
      SUBROUTINE YSUMP(X,Y,ALPHA,BETA,K,BJRE,BJIM,ASUMR,ASUMI)
      DIMENSION BJRE(100),BJIM(100)
      A1=ALPHA-1.0
      A2=A1-1.0
      A3=A1+ALPHA
      A4=BETA**2
      A5=2.0*A4
      ABSQ=(-A1)**2+A4
      ROLDRE=((2.0+ALPHA)*(-A1)-A4)/ABSQ
      ROLDIM=(BETA*3.0)/ABSQ
      RES1=-ROLDRE/2.0
      VMS1=-ROLDIM/2.0
      STORE=3.*(ALPHA*X+BETA*Y)/(X**2+Y**2)
      STOIM=3.*(X*BETA-ALPHA*Y)/(X**2+Y**2)
      RES2=(ROLDRE*STORE-ROLDIM*STOIM)
      VMS2=(ROLDRE*STOIM+ROLDIM*STORE)
      ASUMR=RES1*BJRE(2)-VMS1*BJIM(2)
      ASUMR=ASUMR+RES2*BJRE(3)-VMS2*BJIM(3)
      ASUMI=VMS1*BJRE(2)+RES1*BJIM(2)
      ASUMI=ASUMI+VMS2*BJRE(3)+RES2*BJIM(3)
      T=1.0
      DO 500 I=3,K,2
      T=T+1.0
      B1=2.0*T
      F1=B1+ALPHA
      F2=A3+T
      F3=A1+T
      F5=T-ALPHA
      F6=A2+B1
      G1=F1*F2-A5
      G2=(F2+2.0*F1)*BETA
      H1=G1*F3-G2*BETA
      H2=G2*F3+G1*BETA
      P1=F5*F6+A4
      P2=(F5-F6)*BETA
      P3=P1**2+P2**2
      CRE=((H1*P1+H2*P2)/P3)/T
      CIM=((H2*P1-H1*P2)/P3)/T
```

```
      TEMP=-(CRE*ROLDRE-CIM*ROLDIM)
      RNEWIM=-(CIM*ROLDRE+CRE*ROLDIM)
      RNEWRE=TEMP
      RES1=(ROLDRE-RNEWRE)/2.0
      VMS1=(ROLDIM-RNEWIM)/2.0
      RES2=(RNEWRE*STORE-RNEWIM*STOIM)
      VMS2=(RNEWRE*STOIM+RNEWIM*STORE)
      BSUMR=RES1*BJRE(I+1)-VMS1*BJIM(I+1)+ASUMR
      BSUMI=VMS1*BJRE(I+1)+RES1*BJIM(I+1)+ASUMI
      BSUMR=RES2*BJRE(I+2)-VMS2*BJIM(I+2)+BSUMR
      BSUMI=VMS2*BJRE(I+2)+RES2*BJIM(I+2)+BSUMI
      IF(ABS((BSUMR/ASUMR)-1.0)-.00000005)521,521,510
521   IF(ASUMI)520,511,520
520   IF(ABS((BSUMI/ASUMI)-1.0)-.00000005)511,511,510
510   ASUMR=BSUMR
      ASUMI=BSUMI
      ROLDIM=RNEWIM
500   ROLDRE=RNEWRE
511   RETURN
       END
      SUBROUTINE LOGGAM(X,Y,U,V)
CLOGGAM  LOG OF THE GAMMA FUNCTION OF COMPLEX ARGUMENTS  FORTRAN II
C THIS SUBROUTINE COMPUTES THE NATURAL LOG OF THE GAMMA FUNCTION FOR
C COMPLEX ARGUMENTS.  THE ROUTINE IS ENTERED BY THE STATEMENT
C      CALL LOGGAM(X,Y,U,V)
C WHERE   X IS THE REAL PART OF THE ARGUMENT
C         Y IS THE IMAGINARY PART OF THE ARGUMENT
C         U IS THE REAL PART OF THE RESULT
C         V IS THE IMAGINARY PART OF THE RESULT
      DIMENSION H(7)
      H(1)=2.269488974
      H(2)=1.517473649
      H(3)=1.011523068
      H(4)=5.256064690E-1
      H(5)=2.523809524E-1
      H(6)=3.333333333E-2
      H(7)=8.333333333E-2
      E2=1.57079632679
      E8=3.14159265359
      B1=0.0
      B2=0.0
      J=2
      X2=X
    4 IF(X)1,2,3
    3 B6=ATAN(Y/X)
      T=X**2
    5 B7=Y**2+T
C   REAL PART OF LOG
      T1=.5*ALOG(B7)
      IF(X-2.0)7,7,6
    7 B1=B1+B6
      B2=B2+T1
      X=X+1.0
      J=1
      GO TO 4
    6 T3=-Y*B6+(T1*(X-.5)-X+9.189385332E-1)
      T2=B6*(X-.5)+Y*T1-Y
      T4=X
      T5=-Y
      T1=B7
      DO 8 I=1,7
```

```
      T=H(I)/T1
      T4=T*T4+X
      T5=-(T*T5+Y)
    8 T1=T4**2+T5**2
      T3=T4-X+T3
      T2=-T5-Y+T2
      GO TO (9,10),J
    9 T3=T3-B2
      T2=T2-B1
   10 IF(X2)11,12,12
   12 U=T3
      V=T2
      X=X2
      RETURN
   11 U=T3-E4
      V=T2-E5
      X=X2
      RETURN
C   X IS ZERO
    2 T=0.0
      IF(Y)13,14,15
   13 B6=-E2
      GO TO 5
   15 B6=E2
      GO TO 5
C     X IS NEGATIVE
    1 E4=0.0
      E5=0.0
      IE6=0
   16 E4=E4+.5*(ALOG(X**2+Y**2))
      E5=E5+ATAN(Y/X)
      IE6=IE6+1
      X=X+1.0
      IF(X)16,17,17
   17 IF(MOD(IE6,2))18,4,18
   18 E5=E5+E8
      GO TO 4
   14 PRINT 19,X2,Y
   19 FORMAT(29H ATTEMPTED TO TAKE LOGGAM OF 2HX=F6.0,1X2HY8F6.0)
      CALL EXIT
      END
 .015     .045
 0.0   2.25
 1.11  76.7
 .00043  .00043  .00096
600000000.0
```

```
ZIGD=  0.00   EPRD=  2.25

A1=  .00043  A2=  .00043  A3=  .00096

FREQUENCY=  600000000.0

K1=  .36992E+06  -.36992E+06  K2=  .11251E+03  -.23370E+02

J0=  .49863E+70  .52113E+70  J1=  52113E+70  -.49863E+70

H02=  .86464E+00  .14723E+01  H12= -.11067E+01  .57375E+01

CHARACTERISTIC IMPEDANCE=   64.54555    -13.05870

I= 1   ALPHA+    7.66206   BETA=   37.87144

TETA1= 0.00  1.57   TETA2= 0.00  1.57  ZIN=   176.549     -56.234

TETA1= 0.00  0.00   TETA2= 0.00  1.57  ZIN=   163.186    -196.332

TETA1= 0.00  0.00   TETA2= 0,00  0.00  ZIN=    28.471     -98.405
```

CHAPTER VIII

SUMMARY

In this thesis we present some theoretical and experimental results on the study of a bare microprobe and an insulated microprobe in a conducting (biological) medium. The dimensions of the probe are set to be very small so that it can be imbedded easily in a biological body.

Since the current on the bare probe in a conducting medium is decaying rapidly, the probe can be truncated and treated as an asymmetric dipole in the analysis. For increasing the decay of the probe current, the probe can be coated with material with higher surface impedance. The current distribution along the probe, and the effect of the surface impedance on the current and the input impedance of the bare probe are found based on Hallen's integral equation and electric field integral equation. These equations are solved numerically by moment method. The driving source is modeled as a magnetic ring or as a delta gap generator.

A series of experiments were conducted, and the input impedances of bare probes in various conducting media were measured with vector voltmeter and E-H probe. The agreement between the theory and the experiment was found to be satisfactory.

An investigation on the applicaton of a bare probe for measuring electrical properties of a conducting medium, and for heating a tumor imbedded in a biological body for the purpose of hyperthermia cancer therapy is conducted.

The theory of lossy transmission line is used to solve the problem of an insulated microprobe in a conducting medium. The current on the insulated probe does not decay rapidly, therefore, equivalent terminal impedances are introduced. The current distributions along the probe for various terminal impedances are given. The input impedance of the probe is discussed and the input impedances of symmetric insulated probes with various terminal impedances are presented graphically.

The heat patterns of insulated probes with various terminal impedances are shown, and the effect of the terminal impedance on the heat pattern is discussed. It is concluded that the heat pattern can be altered by changing the terminal impedance of the probe.

Finally, the computer programs used for finding the current distribution and the input impedance of bare and insulated probes with examples are given.

In conclusion, the input impedance of the bare probe is more sensitive to the surrounding medium, therefore, it is suitable for measuring the electrical properties of biological bodies. On the other hand, the insulated probe can transfer more power in a biological body in comparison with the bare probe so that an insulated probe is a better device for local heating.

BIBLIOGRAPHY

BIBLIOGRAPHY

1. J.E. Robinson, M.J. Wizenberg, and W.A. McGready, "Radiation and hyperthermal response of normal tissue in situ," Radiology, 113, 1, 195-198, 1974.

2. H.H. Leveen, S. Wapnick, V. Piccone, G. Falk, and N. Ahmed, "Tumor eradication by radiofrequency therapy," JAMA, 230, 29, 2198-2200, May 17, 1976.

3. C.C. Johnson, H. Plenk, and C.H. Durney, "A 915 MHz exposure system for hyperthermia treatment of cancer," Presented at 1977 International Symposium on Biological Effects of Electromagnetic Waves, Airlie, Virginia, October 30-November 4, 1977.

4. A. Cheung, D. McCulloch, J. Robinson, and G. Samaras, "Bolusing techniques for batch microwave irradiation of tumors in far field," Presented at 1977 International Microwave Symposium, San Diego, California, June 21-23, 1977.

5. E.C. Burdette, F.L. Cain, and J. Seals, "In vivo probe measurement technique for determining dielectric properties at VHF through microwave frequencies," IEEE Trans. on Microwave Theory and Techniques, Vol. MTT-28, No. 4, pp. 414-427, April 1980.

6. T.W. Athey, M.A. Stuchly, and S.S. Stuchly, "Measurement of radio frequency permittivity of biological tissues with an open-ended coaxial line: part I," IEEE Trans. on Microwave Theory and Techniques, Vol. MTT-30, No. 1, pp. 82-86, January 1982.

7. M.A. Stuchly, T.W. Athey, G.M. Samaras, and G.E. Taylor, "Measurement of radio frequency permittivity of biological tissues with an open-ended coaxial line: part II," IEEE Trans. on Microwave Theory and Techniques, Vol. MTT-30, No. 1, pp. 87-90, January 1982.

8. G.B. Gajda, and S.S. Stuchly, "Numerical analysis of open-ended coaxial lines," IEEE Trans. on Microwave Theory and Techniques, Vol. MTT-31, No. 5, pp. 380-384, May 1983.

9. R.W.P. King, B.S. Trembly, and J.W. Strohbehn, "The electromagnetic field of an insulated antenna in a conducting or dielectric medium," IEEE Trans. on Microwave Theory and Techniques, Vol. MTT-31, No. 7, pp. 574-583, July 1983.

10. R.F. Harrington, "Field Computation by Moment Methods," Macmillan, New York, 1968.

11. G.S. Smith, "A comparison of electrically short bare and insulated probes for measuring the local radio frequency electric field in biological systems," IEEE Trans. on Biomedical Engineering, Vol. BME-22, No. 6, pp. 477-483, November 1975.

12. M.K. Hessary, "Local heating of biological bodies with HF electric and magnetic fields," Ph.D. Dissertation, Michigan State University, East Lansing, MI 1982.

13. J.A. Saxton and J.A. Lane, "Electrical properties of sea water," Wireless Engineering, October 1952.

14. L.K. Lepley and W.A. Adams, "Electromagnetic dispersion curves for natural waters," Water Resources Research, Vol. 7, No. 6, pp. 1538-1547, December 1971.

15. K. Karimullah, "Theoretical and experimental study of the proximity effects of thin wire antenna in presence of biological bodies," Ph.D. Dissertation, Michigan State University, East Lansing, MI 1979.

16. S.H. Mousavinezhad, "Implantable electromagnetic field probes in finite biological bodies," Ph.D. Dissertation, Michigan State University, East Lansing, MI 1977.

17. R.W.P. King, "Transmission Line Theory," Dover Publication, Inc., New York, 1965.

18. R.W.P. King, C.W. Harrison, "Antennas and Waves: A Modern Approach," The MIT Press, 1969.

19. R.W.P. King, "Theory of the terminated insulated antenna in a conducting medium," IEEE Trans. on Antenna and Propagation, Vol. AP-12, No. 3, pp. 305-318, May 1964.

20. N. Marcuvitz, "Waveguide Handbook," MIT Radiation Laboratories Series, No. 10, September 1950.

MICHIGAN STATE UNIVERSITY LIBRARIES
3 1293 03061 3073